GIANNINI SCIENTIFIC CORPORATION
SPECIAL PROJECTS GROUP

STUDY OF THE FACTORS AFFECTING THE EFFICIENCY IN THERMAL ACCELERATION OF PROPELLANTS

Final Technical Report
Covering 1 May 1962 to 30 April 1965
Contract AF 49(638)-1161

For
AIR FORCE OFFICE OF SCIENTIFIC RESEARCH
WASHINGTON, D. C.

Adriano C. Ducati
Principal Investigator

31 August 1965

GIANNINI SCIENTIFIC CORPORATION
Special Projects Group
3839 South Main Street
Santa Ana, California

GIANNINI SCIENTIFIC CORPORATION
SPECIAL PROJECTS GROUP

ABSTRACT

This report describes the experimental and analytical work conducted to study the various influences affecting the operating characteristics of electrothermal accelerators. A summary of the initial state-of-the-art is given together with the basic results obtained. A survey of the testing facilities, including vacuum systems, resistance heaters, and liquid metal heaters is given. Arc heaters are discussed with and without the application of external magnetic fields, and with gradually reduced propellant injection. Instruments for the measurement of thrust, mass flow, power, pressure, temperature, magnetic field, etc., are illustrated, together with suggestions for future developments. The experimental work conducted with hydrogen, helium, ammonia, nitrogen, oxygen, and argon at temperatures ranging from 300°K to 3000°K is described. Conical and annular nozzles are compared with simple cylindrical throats, and the experimental and analytical expressions relative to their behavior are included. Outlined are the development of low pressure arc heaters and the experiments which led, for the first time, to the attainment of specific impulse levels of over 10,000 seconds using hydrogen. Performance comparisons between resistance and arc heating and associated anomalies using ammonia are also discussed. The behavior of self-magnetic fields in the arc heater is explained, together with the effects of externally applied magnetic fields ranging from 500 to 12,000 gauss. Included are operation at low mass flow rates and the development of arc heaters working without propellant throughput using electrode vapors or residual ambient gas as the working fluid. Anomalies discovered during experimentation with extremely low mass flow rates are postulated and methods for their identification are suggested. An outline of future experimental and analytical work is presented.

GIANNINI SCIENTIFIC CORPORATION

SPECIAL PROJECTS GROUP

TABLE OF CONTENTS

TABLE OF CONTENTS (Cont.)

ILLUSTRATIONS

ILLUSTRATIONS (Cont.)

ILLUSTRATIONS (Cont.)

TABLES

1.0 DEVELOPMENT OF THE WORK

1.1 Time Schedule of Contract AF 49(638)-1161

This contract was started on May 1, 1962 for a period of 12 months. A 12-month extension was granted on May 1, 1963. Another 12-month extension was granted on May 1, 1964. The work was terminated on April 30, 1965.

1.2 Status at the Beginning of the Work

Reference 1 describes progress on a related program that preceded this work. For convenience, the status of work at that time is summarized below. Although the test facilities were fairly well developed at that time, some modifications were required to meet special needs in the present program. The vacuum pumping system had a capacity of 2000 liters/sec. This was adequate to provide a vacuum level from one to a few Torr with normal propellant flow. The propellant mass flow rate was measured using a gravimetric system. The system provided for offsetting the weight of the gas bottle with a carefully controlled buoyancy force so that the change in mass could be measured with a high precision analytical balance. Power to the gas was measured using a calorimeter consisting of a cooled reflector close to the thrustor, and a heat exchanger downstream of the thrustor to cool the exhaust gas to the same temperature as that of the incoming propellant. Power in the gas was determined from the cooling water flow rate and temperature rise, and checked by measurements of electrical power input and cooling water loss in the thrustor itself. All of the readout equipment involved in the tests were grouped on a panel so data could be recorded photographically by an automatic camera operating at any desired time interval.

Most of the testing done during the preceding program was accomplished using the modular plasma generator. The unit had a housing consisting of a series of connecting sleeves which could be provided with various inserts

to form variations in the anode, plenum chamber, and nozzle shape. This arrangement greatly increased the speed with which a series of thrustor geometries could be tested.

At the beginning of the present program the maximum specific impulse which had been obtained with hydrogen, helium, and ammonia was 2100, 1000, and 1400 seconds, respectively; and the overall efficiency was 17, 16, and 10 percent, respectively. Work had also been initiated using lithium hydride as a propellant, and mixtures of propellants such as hydrogen and helium or impurities in a single propellant. However, work had not progressed far enough in either area to show conclusive results.

Although no measurements were made separating the thermal losses in different parts of the arc chamber and nozzle configuration during the preceding program, thermal losses and overall efficiencies were determined for a large number of geometries. This permitted some conclusions to be drawn. Briefly, the results indicated that the advantages to be gained from long mixing chambers and nozzles (better mixing to provide a more uniform gas temperature, better guidance of the exit flow to provide a uniform jet direction, and increased opportunity for recombination) are more than offset by increased thermal losses. Relatively short electrodes and nozzles consistently showed better overall performance. Some tests were also made using hot nozzles. However, these tests were all for relatively long nozzles with the result that thermal losses remained high. No conclusions were drawn with regard to the merits of hot nozzles.

Approaches suggested for decreasing the losses associated with short nozzles without increasing the thermal losses excessively included electromagnetic or accoustic mixing of the flow upstream of the nozzle to obtain a more uniform energy distribution in the jet. A multiple array of gas generators to supply hot gas to a single nozzle and control the distribution of energy in the nozzle was also suggested together with recirculation of the layer of cool gas near the nozzle wall thereby avoiding the expansion of the cooler gas in the nozzle, while maintaining a layer of cool gas along the wall to prevent excessive thermal losses. Improvements in existing approaches (for example, improved short nozzle designs and improved regenerative-cooling technique) had also been considered.

During the last part of this period a long series of measurements was conducted using hydrogen as a propellant and a mass flow between 0.500 and 0.025 gm/sec with a range of specific impulse between 500 and 2000 seconds. Operating at constant specific impulse and changing the mass flow and the power input, it was found that the gas to kinetic efficiency increased consistently in all the tests with decreasing mass flow. For the same testing conditions the efficiency of transfer between electric input and gas decreased, compensating partially the gas to kinetic efficiency increase. This characteristic behavior was considered interesting, but its real importance was realized only years later with the continuation of this work, as will be reported in the following pages. It is interesting to remember that at the beginning of this work the hydrogen specific impulse of 2100 seconds was considered a limited value practically not improvable. The length of operation at this level was at the best not over 60 seconds.

1.3 Developments in Testing Methods and Facilities

During the program performance was measured over a very broad range of operating conditions, including some conditions which represent large incremental advances in the state-of-the-art. To obtain this data and assure accurate results, it was necessary to develop some new testing methods. These are summarized below and also described in detail in later sections of the report.

A large number of tests were run with thrustors having a short orifice in place of a supersonic nozzle. Since viscous losses and thermal losses are greatly reduced, the measured performance is very close to theoretically predicted values for a thrustor with this type of nozzle. Results are useful, for example, for exploring the effect of dissociation on performance as operating conditions change (since this effect is not masked by a large variation in thermal losses).

In the process of performing these tests, some methods were developed for measuring propellant stagnation temperatures at values near the limit of resisto-jet operation. These included measuring the resistance of hot elements, observation of a probe in the gas flow with an optical pyrometer, and observation of the hot chamber walls with an optical pyrometer using a mirror.

To facilitate the comparison of test results, the same series of values for mass flow rate were used for all tests run.

Some of the most interesting test results were obtained at low mass flow rates. Although both the thrust balance and the gravimetric mass flow measuring system are sensitive enough to provide good accuracy for these conditions, the very high arc currents used suggested that errors due to secondary interaction effects might be important. Several steps were taken to minimize this possibility.

The thrust killer was developed to attach to nozzle exits. This device collects and cools the gases in the jet and directs them at low velocity radially outward (normal to the thrust direction). This eliminates the jet thrust accurately enough that apparent thrust forces due to such things as electromagnetic interactions can be detected under actual operating conditions.

A spectroscopic investigation was made of the plume to assist in defining the arc path by locating the region of high excitation and ionization, and to search for evidence of gas entrainment in the jet by looking for evidence of nitrogen or oxygen gas in the inner high temperature region of the plume.

For many tests, the electrodes were carefully weighed before and after running to determine the amount of mass flow added by electrode erosion. This measurement was of particular interest when performance was measured with the propellant mass flow reduced to zero.

Although the gravimetric mass flow measuring system has an accuracy better than one percent, a design was made of an improved gravimetric system to have an error no greater than 0.1 percent for a one-hour operating period. When completed, this system will provide a continuous weight

measurement during operation, and permit recharging of the gas container without shutdown.

Another novel testing method which was introduced for this portion of the program involved the use of a cathode heater. This was an aid in starting the arc and permitted some control of the cathode emission as propellant flow and power were varied over a wide range.

Although the work in this program was done with direct current arcs, the electrical power has an alternating current component (due to power supply ripple and high frequency cycles that occur naturally in many arc configurations). The usual measurements made with direct current meters give average values of voltage and current which yield the direct current component of power only.

Magnetic fields were found to have a number of interesting and unexpected effects on arc behavior. The study of these effects required a different emphasis in the testing methods used.

The self-magnetic effect or pinch effect in the arc was found to have an important influence on performance in an operating regime with lower chamber pressures and higher arc currents than have previously been used. It was found that as the arc current increases, an operating condition is reached in which increasing current results in decreasing (rather than increasing) arc chamber pressure. This is apparently a result of high magnetic pressure in the arc permitting the flow to pass through the constricted throat in spite of a low surrounding pressure. This effect was not evident

in previous tests which used higher arc chamber pressures and lower arc currents (and consequently lower electrical conductivity in the gas). In observing the effect, special attention was paid to the accurate measurement of arc chamber pressure. In addition, pressure was measured at one location inside the arc using a small orifice opening at the centerline of the cathode.

When a separate coil is used to produce a magnetic field, the field lines tend to follow the flow direction and help to guide the flow of ionized gas acting in effect like a nozzle wall. This flow phenomenon helps separate the hot gas from the cooler anode wall, and may also behave as a divergent nozzle section, thereby decreasing thermal losses and increasing thrust. Testing methods that have been used to study the effect include visual observation of the jet shape, visual observation of the location of regions of anode bombardment, spectrographic measurements of the ionization in the jet at various positions, observation of anode erosion patterns, measurements of pressure at various locations in the arc chamber, measurements of overall performance, and measurements of heat losses to the walls; all as a function of magnetic field strength.

Need for understanding of the behavior of the jet in the presence of a magnetic field points out the desirability of a test facility that more closely simulates conditions in space. Ideally, this would include a vacuum system capable of continuous operation at absolute pressures less than 10^{-6} Torr, a very large vacuum chamber to permit full development of the jet and electrical discharge pattern, and vacuum chamber walls made of

nonmagnetic and nonconducting material. As a first step, the vacuum system at Giannini Scientific Corporation has been more than doubled in size and now has a capacity of 4200 liters/sec. System leakage has also been reduced so that continuous operation is now possible at absolute pressures of 100 microns and under.

It may be impractical to simulate conditions in space well enough to investigate such things as the interference of ionized gases with communication and possible bombardment of the vehicle body by charged particles. A more reasonable goal would be the close simulation of space conditions in the region of the magnetic nozzle. If the flow patterns and field patterns could be reasonably well duplicated in this region, the performance measurements obtained should be valid. Notice that the attainment of a good vacuum is considerably less difficult if the propellant is readily condensable (as is the case, for example, with alkali metal). The suggestion has been made that to avoid wall interference effects it may ultimately be desirable to construct a vacuum chamber that is essentially surrounded by diffusion pump inlets.

Motion pictures have been used to study the behavior of the jet during starting with some surprising results. The initial flow of ionized gas leaving the nozzle appears to be contained (perhaps by electromagnetic forces) and moves out slowly as a body. A fraction of a second is required for steady flow conditions to be established. This relatively slow adjustment of conditions during start is verified by measurements of the arc voltage which also requires a fraction of a second to stabilize.

1.4 Basic Results Obtained During the Program

The following guidelines were adopted in evaluating factors affecting the efficiency of thermal propulsion devices. Care was taken to measure performance with the greatest accuracy feasible to assure that small changes in performance would be detected. Measurements were made to separate thermal losses from the losses in the nozzle to help in separating effects and identifying reasons for changes in performance. Tests were made over the broadest feasible range of operating conditions (variable specific impulse, propellant flow rate, arc chamber pressure, electrode geometry, and nozzle geometry) which proved to be particularly valuable in that operating conditions were found which resulted in unexpectedly good performance at very high value for specific impulse.

The first set of tests conducted were at low and moderate gas temperatures obtained by resistive heating of the incoming propellant. A large fraction of these tests were run using a short orifice for a nozzle (no divergent section). Since thermal and viscous losses were very small, results from these tests agree very closely with predicted values for orifice type nozzles. The results are useful in verifying the accuracy of test measurements, and also in evaluating the importance of secondary effects. For example, tests with ammonia show the effect of dissociation on performance over a range of temperatures. These results appear to indicate that a significant portion of the dissociated gas is in atomic form as it passes through the nozzle (rather than molecular hydrogen and nitrogen) even at temperatures low enough that the equilibrium condition would be primarily molecular.

The remainder of the low temperature tests were conducted using divergent nozzles of various designs including a family of conical nozzles with half angles varying from 3.75° to 30° and an experimental annular nozzle. At the low gas temperature used, the optimum nozzle angle was found to be in the 7.5° to 15° range. The data also shows a trend indicating the desirability of larger angles at higher gas temperatures (when the thermal losses are a larger percentage of the energy in the jet). Other tests were conducted using catalytic materials upstream of the nozzle. However, test difficulties were encountered and results were inconclusive. Propellants used for the low temperature tests included hydrogen, helium, nitrogen, oxygen, argon, ammonia, and various mixtures of hydrogen with nitrogen and hydrogen with argon. The maximum gas temperature obtained with resistive heating was 3000°K using ammonia (a specific impulse of 425 seconds).

The most interesting results of the program were obtained at the opposite end of the range of conditions. Extremely high gas enthalpies were obtained using hydrogen in an arc jet. Arc chamber pressures were reduced to keep heat fluxes into the wall at low enough values to permit reasonable operating life with conventional water cooling. The surprising result was that the thermal losses, which were expected to be very extreme at these conditions (because of the high gas temperatures and low Reynolds numbers), were not particularly large. The following factors appear to contribute to the good performance obtained at these conditions.

At very high specific impulses, the losses associated with complete dissociation and ionization of hydrogen are not large compared to the total energy in the gas.

Thermal and viscous losses are markedly reduced by using a simple orifice type nozzle (with practically no divergent section). Notice that, in the absence of recombination, about 80 percent of the maximum jet velocity possible can be obtained in a simple orifice followed by a free expansion. This results from the fact that the hydrogen is fully dissociated and so has the properties of a monatomic gas.

At low gas pressures, the arc tends to be diffuse, and therefore heats the gas more uniformly. At the same time, the heat flow associated with the electrode drop loss is distributed over a larger area on the electrode surfaces thereby increasing electrode life.

At low gas pressures, the arc current is high (2000 to 3000 amperes). The self-magnetic or "pinch" effect is therefore important. This effect appears to contain the hot gas in the center of the passage thereby reducing thermal losses to the wall.

With the gas strongly ionized, the containment of the hot gas flow (by separate magnetic fields as well as self-induced fields) becomes an important influence for reducing thermal losses.

Performance was measured for a range of specific impulses from 3000 to 10,000 seconds. The efficiency with which electrical energy was converted

to energy in the gas (η^{eg}) remained between 60 and 70 percent over the entire range, while the efficiency of conversion from enthalpy to kinetic energy in the gas (η^{gk}) increased steadily with increasing specific impulse. Average values of performance with an external magnetic field applied are shown below.

DC Electric Power	255 kw
Arc Voltage	98 volts
Arc Current	2600 amps
Total Thrust (measured)	0.55 lbs
Specific Impulse (vacuum)	10,000 secs
Overall Thrustor Efficiency	47%
Arc Chamber Pressure	25 mm Hg a
Test Chamber Pressure	0.2 mm Hg a
Hydrogen Mass Flow	25 mg/sec

The data obtained during this program is believed to have given the first indication that operation in this regime with an arc engine could provide high specific impulse and reasonable efficiencies. Its announcement has stimulated the initiation of several new programs for the development of thrustors of the thermo-ionic type.

The use of an external magnetic field was found to improve the efficiency of conversion from enthalpy to kinetic energy in the nozzle by a significant amount. This is presumably due to the nozzle effect that the diverging field lines have on the ionized gas in the jet. The influence of the external magnetic field on the plume is clearly visible if the plume is watched while

the field strength is changed. However, this gain in performance was found to be partially offset by an increase in the thermal losses to the wall. Apparently the rotation of the arc at the anode results in an increase in thermal losses which is not entirely offset by the added containment of the ionized gas stream. Although the external field results in a small increase in overall efficiency, the primary advantage of its use appears to be an improvement in electrode life. The presence of the field seems to have two effects which increase anode life; the arc is rapidly rotated which reduces localized heating of the anode surface, and the path of the electron stream returning to the anode is contained at a smaller diameter. The higher gas density in this region appears to reduce bombardment effects.

However, uniform rapid rotation of the arc depends on other things besides the external field strength. For example, the connection of the power lead to the anode can tend to make the arc remain in one position (since the current flow tends to follow the shortest path available). This condition can be alleviated by the use of multiple leads symmetrically arranged about the axis of the anode. Actually, rotation of the arc may not be the best solution for improving anode life because at any instant the power density is very high in a single spot and zero in the others. Some initial tests have been made of an anode subdivided into many parts with power fed through separate stabilizing circuits to each segment. Some problems may arise with this technique, but the results to date are promising.

An interesting effect which has been observed in the operation of thermoionic thrustors is the variation of arc voltage with magnetic field strength

and throat diameter. It was found that the arc voltage increases much more rapidly with magnetic field strength when the throat diameter is large. This means that high values of the arc voltage can be obtained by the use of a strong external field. This has the advantage that the electrode drop losses become a smaller percentage of the total power. However, this is offset by the fact that the arc current is reduced and some of the desirable effects of high arc current (containment and uniform energy addition) are lost. As noted previously, the net effect of increasing the external field strength is to increase the thermal losses to the wall.

A second interesting effect worth noting is that when operating in the low pressure high current regime, the cathode spot becomes diffuse spreading over a wide enough area on the cathode surface that no melting is observed. When this occurs, material is actually deposited on the cathode so that it builds up rather than eroding away. Presumably, tungsten ions from the anode find their way through the arc to the cathode resulting in the deposit.

Although the results of tests on thermo-ionic thrustors are so far very encouraging, their validity is still open to some question. For example, it was found that when the mass flow was reduced to zero, a thrust force was still measured. The amount of measured thrust could not be completely explained by the loss of mass from the electrodes. It is therefore believed that external effects exist which result in an apparent change in the thrust measurement. These may include entrainment (and ionization) of ambient gas into the jet in the magnetic nozzle region, or electromagnetic interactions due to interaction of fields with magnetic material in the chamber,

interaction of fields with currents induced in the chamber walls, or discharges of currents to the chamber walls.

The "thrust killer" described in the preceding section has been used to detect such interactions, and they have been eliminated insofar as they can be detected with this device. However, the presence of the thrust killer modifies the geometry of the plume and the arc discharge which may be a source of interaction effects. A second technique that has been used is examination of the plume spectrographically. This type of investigation can indicate the path taken by the arc, and also show if surrounding "tracer" gases are entrained in the jet. Some preliminary investigations of this type were made during the program. One interesting result was that at low and zero propellant flows, no nitrogen was observed entrained in the jet. Also observed was a sheath of highly ionized gas surrounding the center core of the jet indicating an annular arc current flow in this region. This technique appears to offer promise of answering a number of questions regarding the behavior of thermo-ionic thrustors. It is believed that more detailed measurements covering a wide range of operating conditions and traversing radially as well as axially would be very enlightening.

To finally resolve the question it may be necessary to use very large volume chambers of nonmagnetic and possibly of nonconducting materials as suggested in the preceding section. The size of the chamber and the capacity of the vacuum pumping system should both be large enough to closely simulate space conditions for the flow pattern in the magnetic nozzle region.

The program has suggested a number of areas in which further work appears to be desirable. Methods should be studied for further reducing the wall surface area exposed to the high temperature gas (at high specific impulses, the thermal loss is the highest single loss with present designs). A better understanding is needed of the performance measured with condensable propellants such as alkali metals. It is necessary to determine whether the good performance measured is a result of an as yet undiscovered interaction force, or if these propellants have an unexplained advantage as propellants. In the latter case, it seems appropriate to investigate the possibility that the condensable propellants are capable of a significant amount of recombination in the magnetic nozzle region. A better understanding of behavior in the region external to the thrustor appears to be essential for understanding the performance of thermo-ionic thrustors. Promising approaches include more detailed spectrographic investigation of the plume and tests in vacuum chambers which closely simulate conditions in space (at least in the magnetic nozzle region).

2.0 TESTING FACILITIES

2.1 Vacuum Pumps and Vacuum Tanks

2.1.1 Production of High Vacuum

During our first experiments in plasma acceleration, atmospheric exhaust pressure was used. The problem of creating a low pressure environment did not exist. Later, when an exhaust pressure lower than atmospheric was considered necessary, the problem of high vacuum environment became an important factor both technically and economically. During this early period hydrogen was used as the principal propellant. The pumping system was based on a mechanical blower with a capacity of about 2000 liters/sec followed by a group of forepumps with a capacity of about 550 liters/sec. With a mass flow of hydrogen of 1 gm/sec the best vacuum attainable was about 5 Torr. All the initial low temperature experiments (under 2000°K) were conducted in a range of pressures of this order of magnitude applying the usual "perfect vacuum" corrections to the measured values. For subsequent higher temperature tests, the mass flow was decreased from 1 gm/sec to a fraction of a gram. When this was done, the operating pressure level in the vacuum tank was reduced accordingly (to under 1 Torr). With the improvement of the vacuum various advantages in the testing procedure were realized. To obtain further improvement, the pumping capacity was (for the present program) increased to 4000 liters/sec using a second group of mechanical pumps in parallel with the first. During the second part of the resistive heating tests (without an arc and operating at a gas temperature of about 3000°K) all the tests were made with both groups of pumps in

operation in a range of pressure between 300 and 800 μ. When the high temperature series of tests was started the need to improve the vacuum level was continuously arising but for economic reasons it was impossible to improve it in the most obvious manner, i. e., increasing the pumping capacity. The only alternative available was to decrease the mass flow. A level of 25 mg/sec was adopted during most of the high temperature tests. This permitted operation in a range of pressure between 50 and 100 μ. Before the end of the program further reduction of the mass flow and continuous improvements in the vacuum system (tanks and connections to pumps) permitted vacuum levels of the order of 10 μ to be attained. It was evident at that time that further reductions would be very difficult to obtain with the existing pumping facility. Reducing the mass flow to zero and operating with electrode vapors condensable before reaching the pumps, pressures no lower than a few microns have been obtained. The limit of the mechanical vacuum system (around 1 μ of mercury) was reached and further improvements could be obtained only with the introduction of different vacuum systems (diffusion and ionic pumps). At the end of the period the need for a pressure (vacuum) environment many orders of magnitude lower than the best so far obtained has been strongly evidenced. A tentative design of such a system has been made. It consists essentially of a vacuum chamber cryogenically cooled and directly connected through a cryogenic trap to a huge diffusion pump. Condensable propellants are to be used in this system. The ultimate pressure (vacuum level is estimated in the order of 10^{-8} mm (Torr). It is believed that a pressure level this low is needed to answer some of the questions that have been postulated during this work.

2.1.2 Containment of High Vacuum

One of the most significant developments during this program was the gradual definition of the technical importance of the vacuum chamber containing the plasma accelerators. Dimensions, materials, and degree of vacuum necessary to obtain good measurements were not only completely unknown at the beginning of this work, but their importance was not even suspected. The first vacuum chambers were relatively small, made of common steel with a degree of vacuum ranging from semi-atmospheric conditions to a few inches of mercury. These environmental conditions were adequate as long as long nozzles and relatively low ionization (low level of specific impulse) were experimented with. In these cases the exhaust jet was neutral and well directed and the characteristic of the space surrounding it had a very small influence on the measured results. However, when the mass flow was reduced (with an attendant reduction in the absolute value of the vacuum and increase in the power per unit mass flow, specific impulse, ionization level, and arc potential) the behavior of the arc jet changed abruptly. The environmental conditions started to play a more important role than had been imagined possible during earlier development work. The principal reason of this new secondary effect is now becoming clear. The effect of the arc is no longer confined in the so-called arc chamber or plenum chamber as occurs during operation at low power and low specific impulse. The high specific impulse type of operation developed during this program involves mechanisms which take place primarily outside the arc chamber or, in a sense, in free space. The simulation of free space conditions in the vicinity of a test engine with the exactness now required

is very difficult. During this program a number of vacuum chambers were developed and tested. All of them were provided with accessories to measure the thrust and to recover the total power of the plasma jet. Complete water cooling was used. For a low temperature work carbon steel tanks 2 to 3 feet in diameter and 10 to 15 feet long were used. However, during a long series of tests involving increased temperature and specific impulse and the use of auxiliary magnetic fields the necessity of vacuum chambers of different characteristics became evident. The principal requirement for future experimentation is avoidance of any influence of the chamber. The presence of the vacuum chamber is suspected of affecting the operation of the plasma jet and introducing errors in the measurements.

The first elementary suggestion for avoiding the influence of the vacuum tank is to make it as large as possible. To explore this possibility, a design of a tank 60 feet in diameter was made. Nonmagnetic material was used throughout and the tank was coated internally with plastic insulation. To avoid long delays in the experiments a small pre-vacuum chamber was designed to permit fast and efficient substitution of the instrumentation without disturbing the main chamber that remained permanently under vacuum. The cost of this huge tank was too high to permit its procurement under the present contract but this solution still remains the most promising for any serious future work. Using chambers of these dimensions or larger it may be possible to use magnetic materials in the construction of the tank because the distance of the walls is relatively great.

2.2 Thermal Thrustors and Components

2.2.1 Pure Resistance Heaters

The low temperature resistance type accelerators used during the first part of the experimental program were of simple design and rugged construction. Special design features included fast and easy interchangeability of the heating elements and of the plenum chamber and sonic throat configuration. Also, the entire accelerator assembly could be easily disconnected from the mounting base in the thrust stand. The design has allowed rapid performance of tests with a great variety of setups. Figure 1 presents a detailed drawing of this low temperature experimental accelerator. The housing (1) is fabricated of 303 stainless steel. A riser tube (2) is welded to the top of the housing and serves as the container for the temperature sensing instruments such as thermometers, thermocouples, etc., which are placed inside the riser tube in such a manner so as to expose the sensing elements to the gas stream in the plenum chamber. A quartz viewing window is mounted to the riser tube for the observation of the mercury column of the various thermometers used. High temperature metallic seals are used for both quartz window and end cap to ensure vacuum tight enclosure. A typical interchangeable plug (6) containing the sonic throat configuration plus extended plenum chamber is threaded into the housing. A high temperature metallic seal assures a gastight connection of the two metallic interfaces. The plug is provided with an external hexagon shape to fit a standard one-inch socket wrench. Since both housing

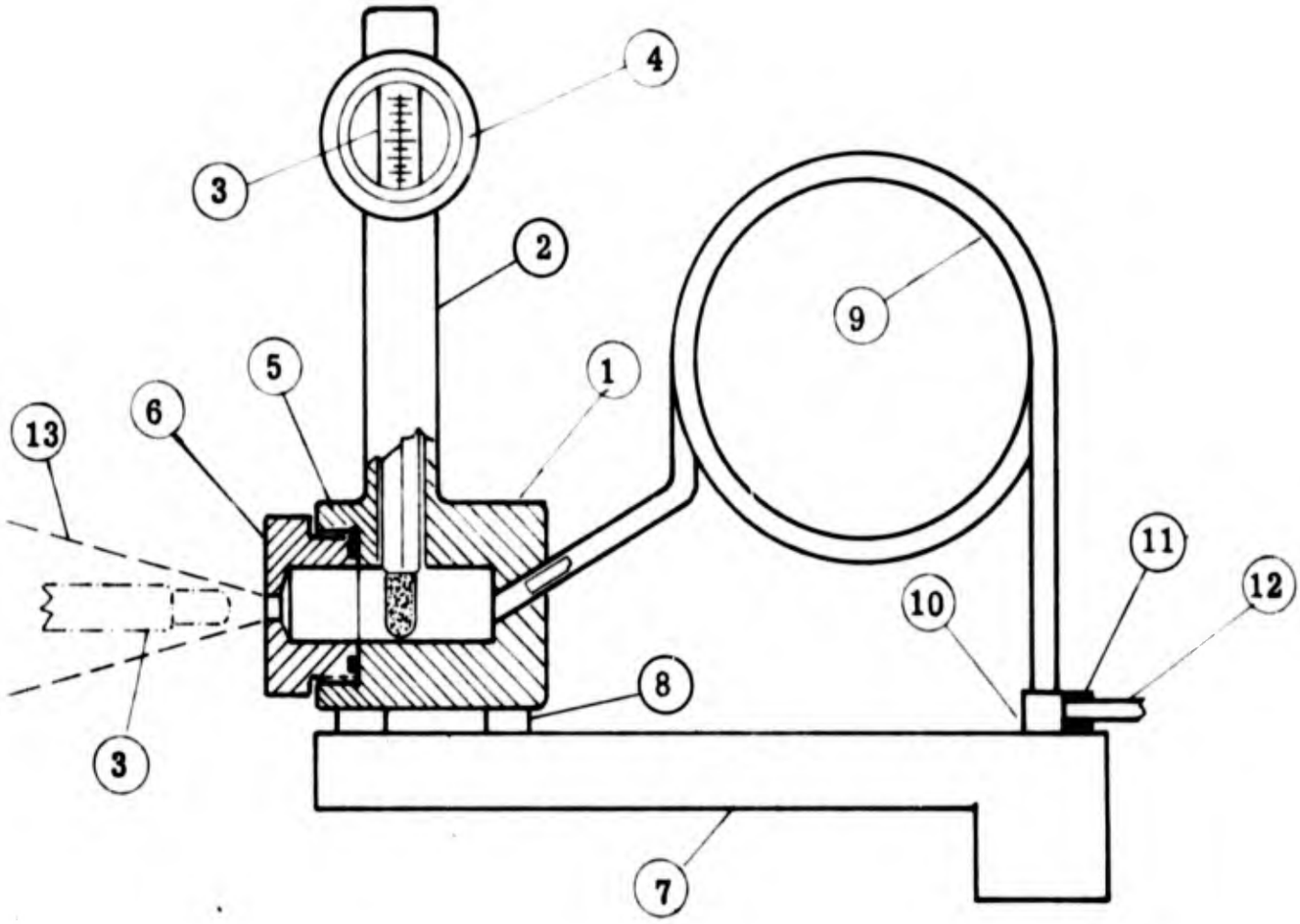

1. Housing
2. Riser Tube
3. Glass Thermometer
4. Quartz Viewing Window
5. Metal Seal
6. Interchangeable Plug
7. Mounting Platform
8. Fastener
9. Heating Element
10. Current Connector
11. Gas Connector
12. Gas Feedline
13. Gas Exhaust

Figure 1. Schematic of Low Temperature Resistance Heater

and plug are manufactured of the same material (303 stainless steel) the thread connection does not tend to loosen during thermal cycling while the accelerator is in operation. The housing is rigidly connected to the mounting platform (7) of the thrust balance by two 1/4-inch socket head stainless steel cap screws (8). The heating elements (9) consist of two 1/4-inch diameter thin wall stainless steel tubes. One end of each element is connected to the end of the housing by means of a standard AN swivel type stainless steel fitting which forms a gastight conical metal to metal seal between tubing and fitting to assure good electrical connection. The other ends of the heating element are connected to separate current connectors by means of identical fittings. These connectors are part of the mounting platform on the thrust stand and form the terminals of the power supplies which are located outside the test chamber. Separate fittings (11) on the connectors serve as receptacles for the gas feeding lines (12) which are an integral part of the thrust balance. During operation the propellant flows through the stainless steel tubular heating elements where energy is added by thermal heat transfer from the metal walls to the gas. From the heating elements the propellant enters the plenum chamber from which it is exhausted into the vacuum tank through the sonic throat. Stagnation temperature and pressure is measured in the plenum chamber. The sonic orifice plug (6) is interchangeable with inserts having fully expanding divergent nozzles. Figures 2, 3, and Table 1 show typical plug dimensions and nozzle configurations used during the early part of the experimental investigations. In addition to conventional nozzles, some annular nozzles were tried.

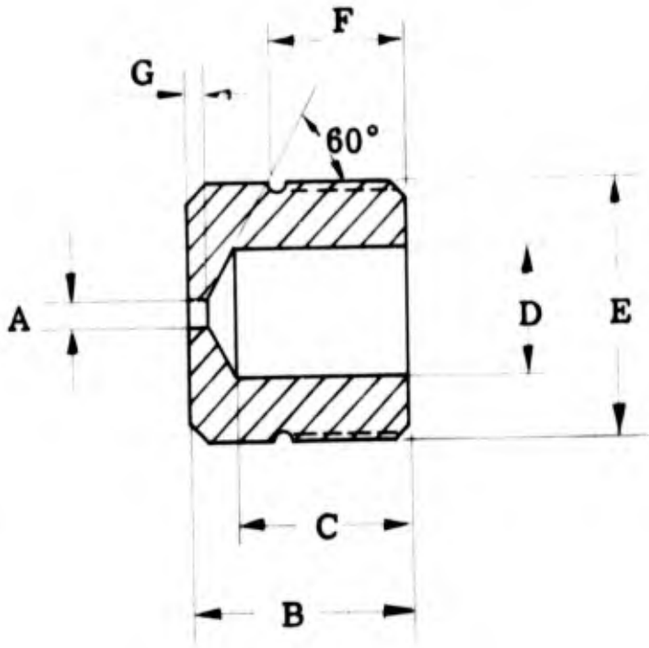

Figure 2. Dimensions of Interchangeable Throat Configurations (see Table 1)

TABLE 1

DIMENSIONS OF INTERCHANGEABLE THROAT CONFIGURATIONS

Nozzle No.	A	B	C	D	E	F	G
1	0.020	0.625	0.525	0.406	1.000	0.343	0.000
2	0.040	0.625	0.532	0.406	1.000	0.343	0.000
3	0.080	0.625	0.535	0.406	1.000	0.343	0.000
4	0.160	0.625	0.562	0.406	1.000	0.343	0.000
5	0.320	0.625	0.595	0.406	1.000	0.343	0.000
6	0.020	0.645	0.525	0.406	1.000	0.343	0.020
7	0.020	0.665	0.525	0.406	1.000	0.343	0.040
8	0.020	0.705	0.525	0.406	1.000	0.343	0.080
9	0.020	0.785	0.525	0.406	1.000	0.343	0.160
10	0.040	0.665	0.532	0.406	1.000	0.343	0.040
11	0.040	0.705	0.532	0.406	1.000	0.343	0.080
12	0.040	0.785	0.532	0.406	1.000	0.343	0.160
13	0.040	0.945	0.532	0.406	1.000	0.343	0.320
14	0.080	0.705	0.535	0.406	1.000	0.343	0.080
15	0.080	0.785	0.535	0.406	1.000	0.343	0.160
16	0.080	0.945	0.535	0.406	1.000	0.343	0.320
17	0.080	1.265	0.535	0.406	1.000	0.343	0.640
18	0.160	0.785	0.562	0.406	1.000	0.343	0.160
19	0.160	0.945	0.562	0.406	1.000	0.343	0.320
20	0.160	1.265	0.562	0.406	1.000	0.343	0.640
21	0.160	1.905	0.562	0.406	1.000	0.343	1.280
22	0.320	0.945	0.595	0.406	1.000	0.343	0.320
23	0.320	1.265	0.595	0.406	1.000	0.343	0.640
24	0.320	1.905	0.595	0.406	1.000	0.343	1.280
25	0.320	3.185	0.595	0.406	1.000	0.343	2.560

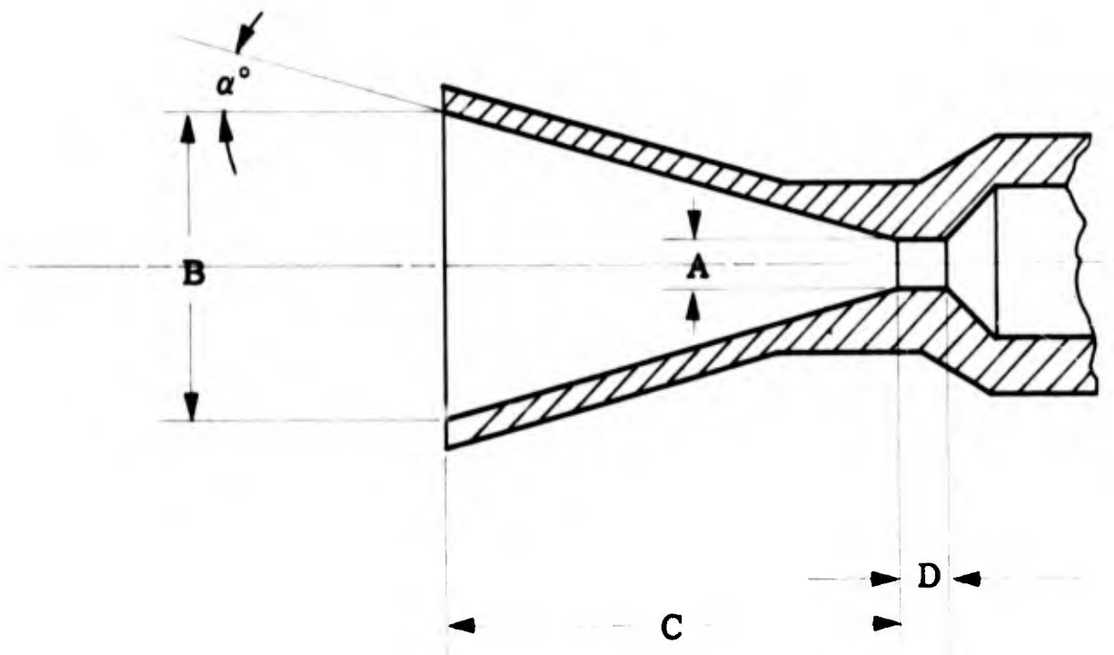

Nozzle No.	A	B	C	D	α°	$\frac{A}{A^*}$
1	0.080	0.800	0.623	0.080	30.00	100
2	0.080	0.800	1.343	0.080	15.00	100
3	0.080	0.800	2.617	0.080	7.50	100
4	0.080	0.800	5.496	0.080	3.75	100

Figure 3. Dimensions of Interchangeable Nozzle Configurations

Figure 4 shows the dimensions of the plug insert used and of the various annular nozzles investigated. The experimental results obtained using this type of pure resistance heater with the three different kinds of nozzles shown are discussed in Section 3.0.

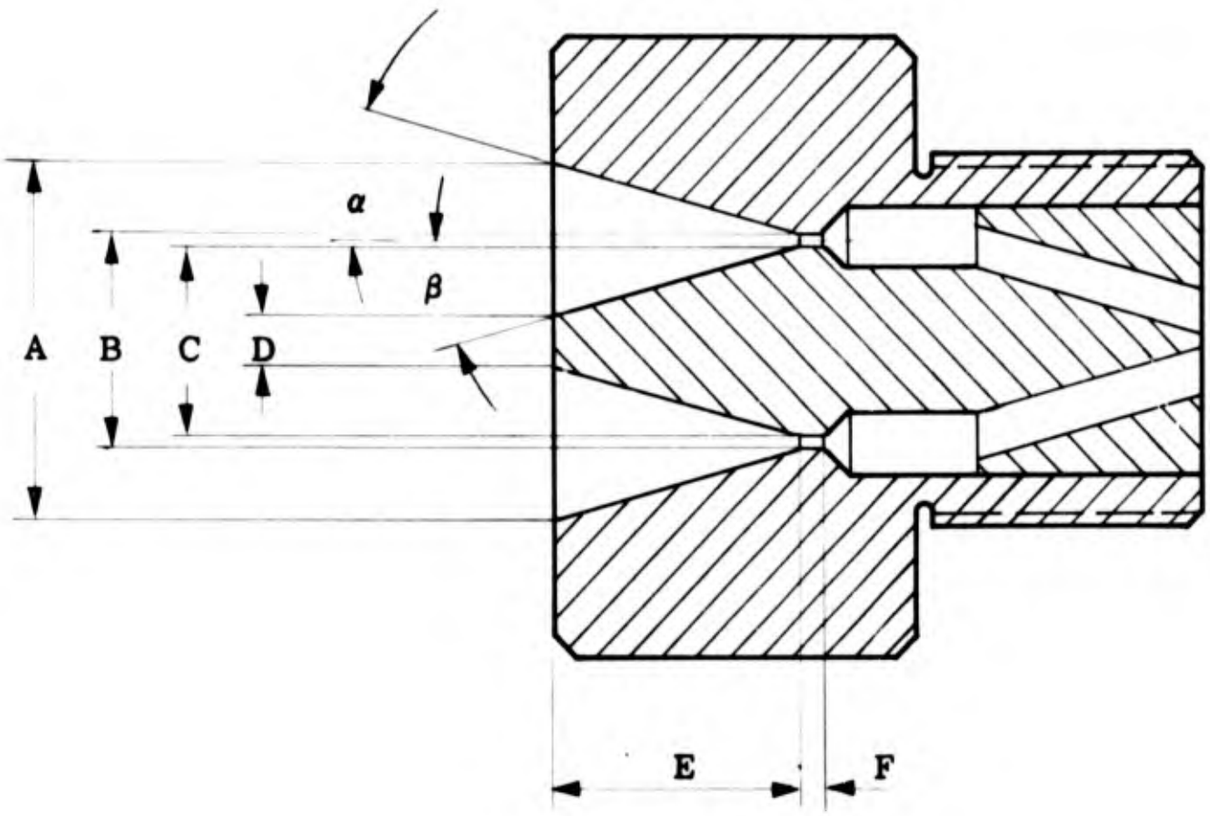

No.	α	β	A	B	C	D	E	F
1	15°	15°	0.800	0.17000	0.15000	0	1.156	0.01000
2	15°	15°	0.800	0.33000	0.32000	0	0.889	0.00500
3	15°	15°	0.890	0.64250	0.63750	0.390	0.466	0.00250
4	15°	15°	1.405	1.28075	1.27825	1.155	0.233	0.00125
5	7°30'	7°30'	0.890	0.64250	0.63750	0.390	0.466	0.00250
6	6°5'	8°33'	0.755	0.64250	0.63750	0.500	0.466	0.00250

Figure 4. Dimensions of Interchangeable Annular Nozzle Configurations

2.2.2 Contact and Hybrid Heaters

In order to achieve propellant temperatures in the range of 1500 to 3000°K it was necessary to design and manufacture special accelerators which would allow continuous operation at this severe condition. The designs combined techniques used for the simple resistance type and the contact resistance type of heater. Figure 5 shows a typical design of this type. The basic concept of this heater involves the use of outer and inner electrodes (1) and (2) arranged coaxially. The electrodes make electrical contact in the plenum chamber near the nozzle throat through slight diametrical interference. The total impedence of the accelerator consists therefore of the sum of the resistance of the inner electrode, the contact region, and the outer electrode. Both electrodes are attached by threaded connections on a water-cooled base (3) which is mounted to the platform of the thrust balance. The water-cooled mounting base was chosen for this initial design to insure that the insulators (5) which in this case were fabricated from teflon and linen based phenolics, would not be overheated. The sonic exhaust throat, or if used, the diverging nozzle are both an inherent part of the outer electrode. Both electrodes are designed to extend well out of the water-cooled mounting base (10 inches approximately). In this way thermal drain of the input power due to conduction through the electrodes themselves into the water-cooled mounting base is kept low since temperature along the axis of both inner and outer electrodes is at minimum at the mounting base and increases gradually to a maximum in the contact region. The propellant flow is injected at the mounting base

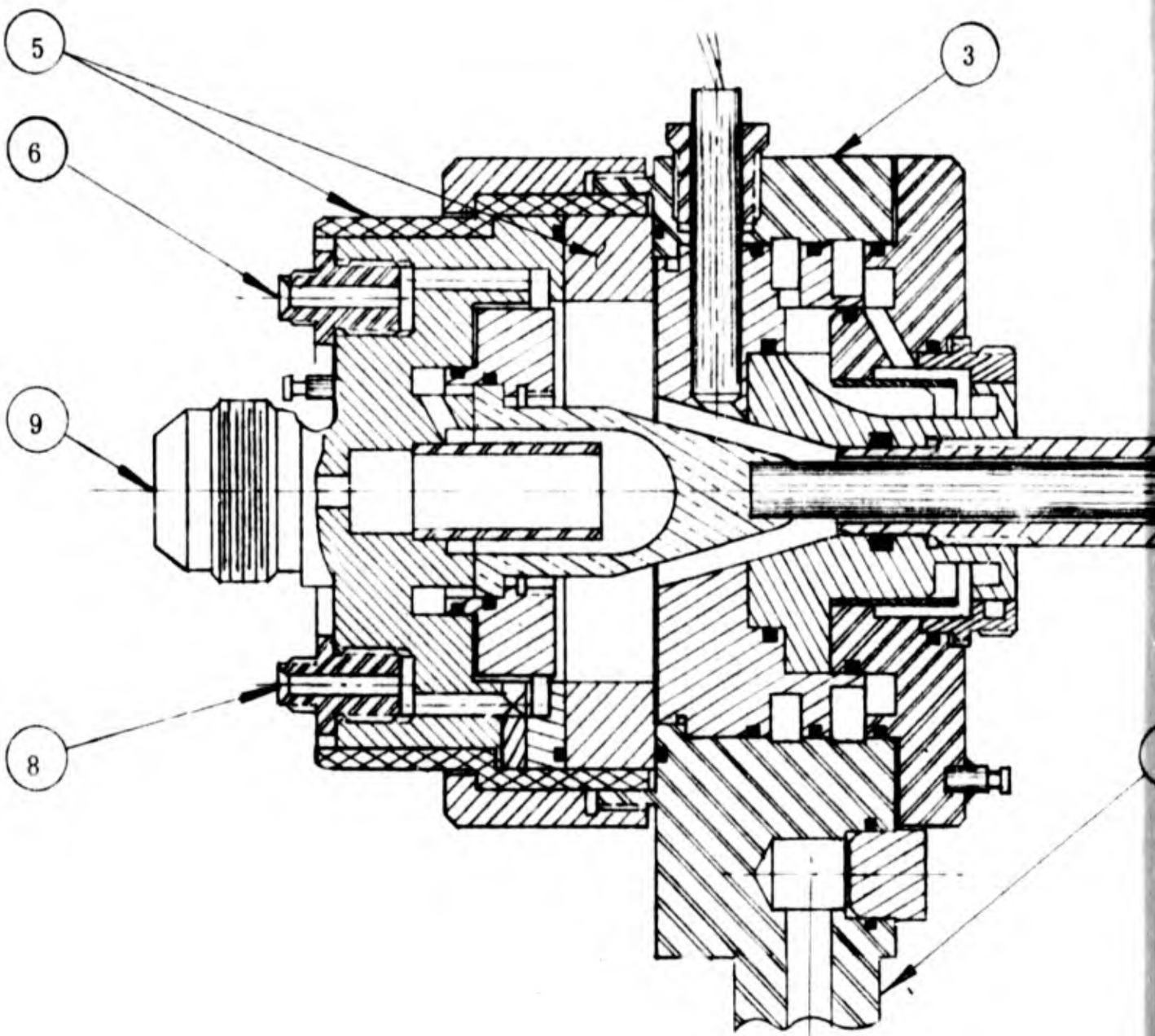

Figure 5. Design of H

A

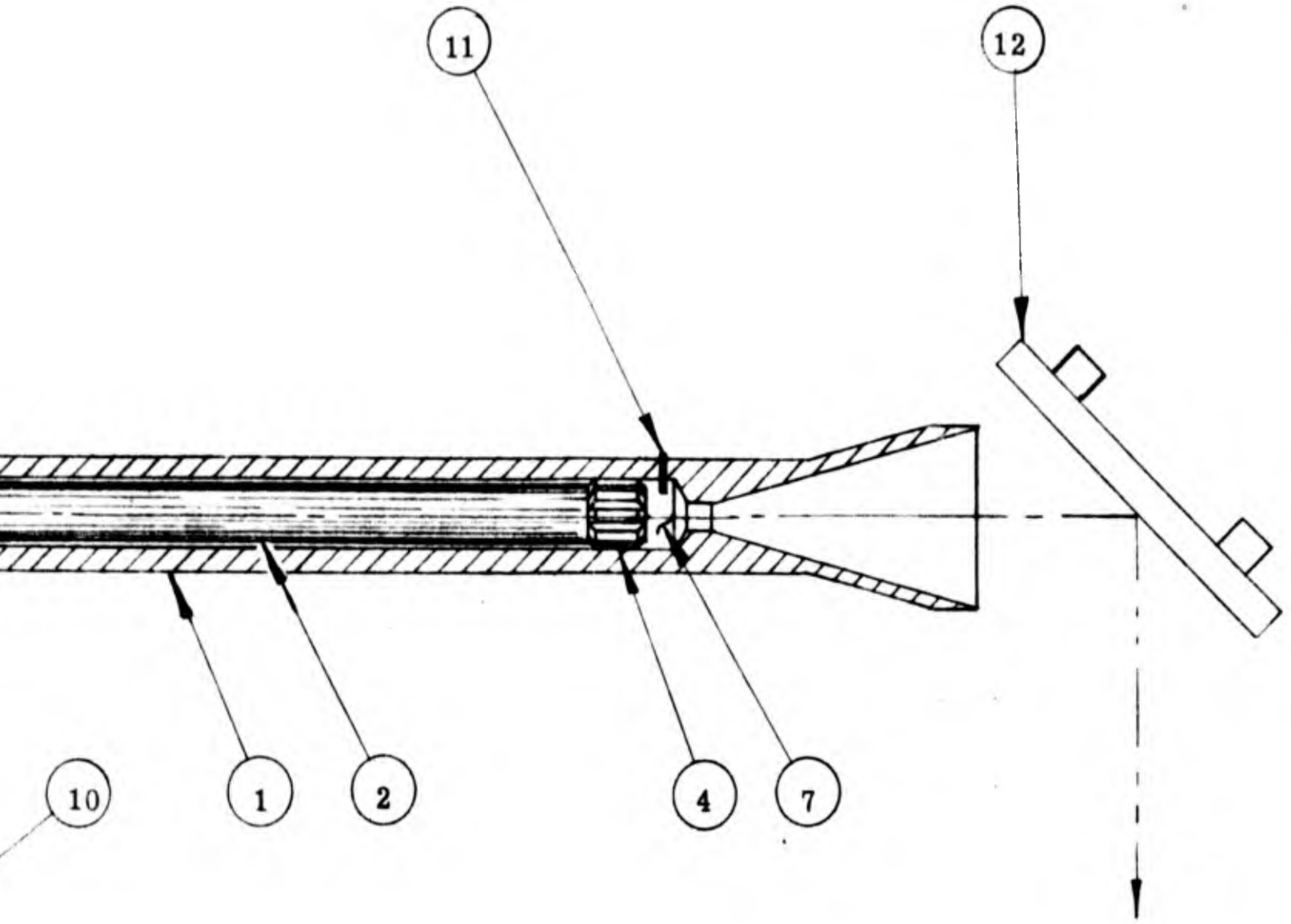

1. Outer Electrode
2. Inner Electrode
3. Water-Cooled Mounting Base
4. Contact Region
5. Electrical Insulators
6. Propellant Inlet
7. Plenum Chamber
8. Pressure Sensor
9. Current and Water Connector
10. Current and Water Connector
11. Temperature Sensor
12. Water-Cooled Mirror

of Hybrid Resistance Heater

B

from where it is allowed to flow through an annular passage formed between the electrodes into the plenum chamber region (7) and on through the nozzle. The designs are of rugged construction ahd have been found to give quite reliable service.

Total pressure measurements of the flow are made at the base of the outer electrode (8). A special fitting is provided to allow connection to various kinds of pressure sensors. Electrical terminals (9) and (10) are provided on the water-cooled mounting base for both inner and outer electrodes. Propellant stagnation temperatures can be obtained by inserting thermocouples (11) through the outer electrode near the contact region or by insertion of special carbon stagnation probes into the flow region in the plenum chamber (7). These probes can be viewed with an optical pyrometer with the help of a water-cooled front surface mirror (12) placed into the exhaust region. Since heat losses were not critical for this part of the experimental studies, the propellant temperature was monitored at all times, and no specific attempt was made (with this particular heater) to reduce the power losses due to conduction into the water-cooled base and radiation from the high temperature outer electrode. Improved thermal efficiency of the thrustor itself was achieved by a later design shown in Figure 6. The water-cooled mounting base was replaced with a regeneratively-cooled thrustor housing (1) which was entirely fabricated from 303 stainless steel. Electrical insulation for this improved type of resistance-heated accelerator was obtained by using a high temperature 500°C epoxy (2) which forms an integral part of the insulated inner electrode mount (3) and the end cap (4)

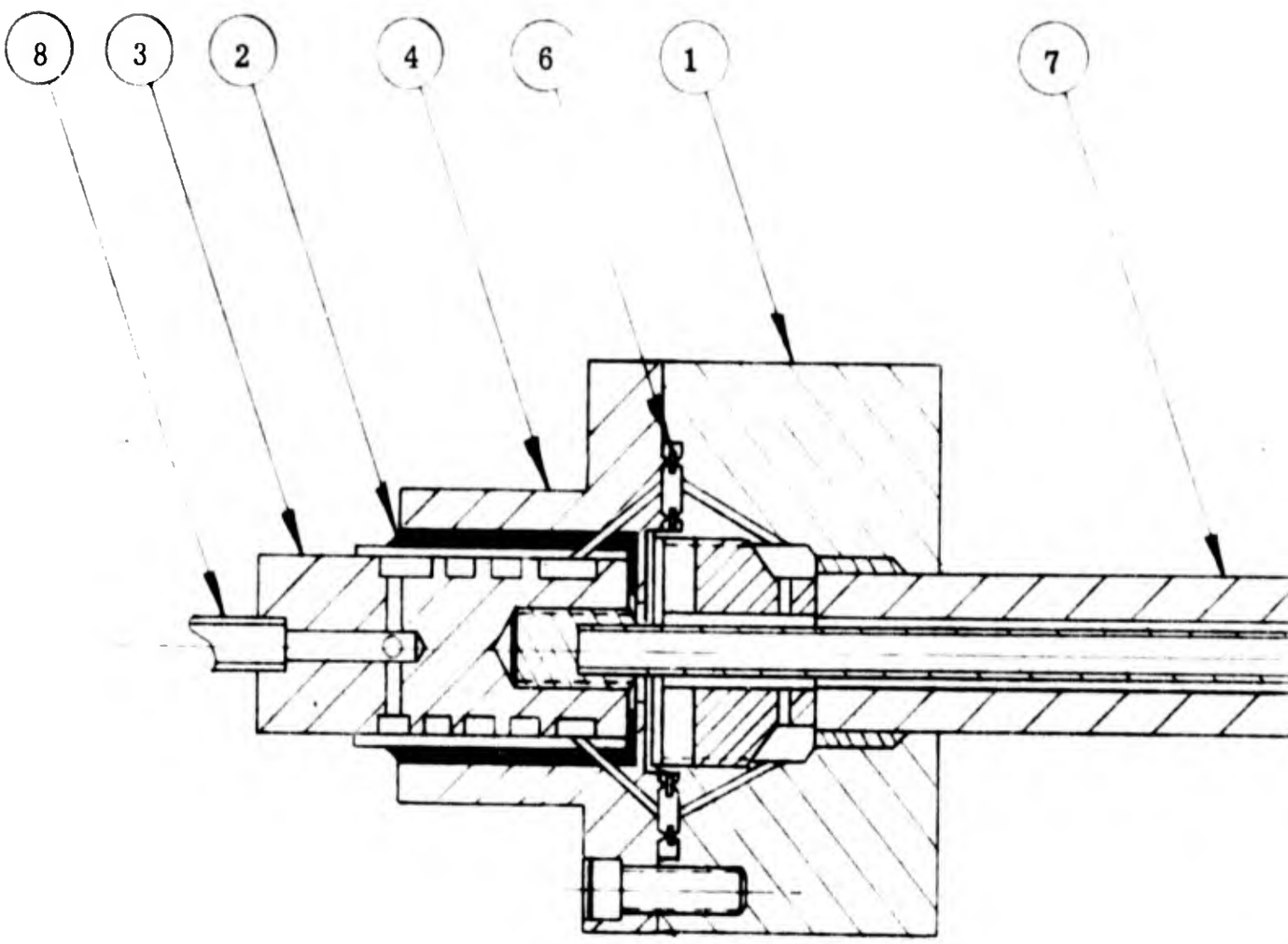

1. Thr
2. Epo
3. Inne
4. End
5. Inne

Figure 6. Design of Regeneratively-

A

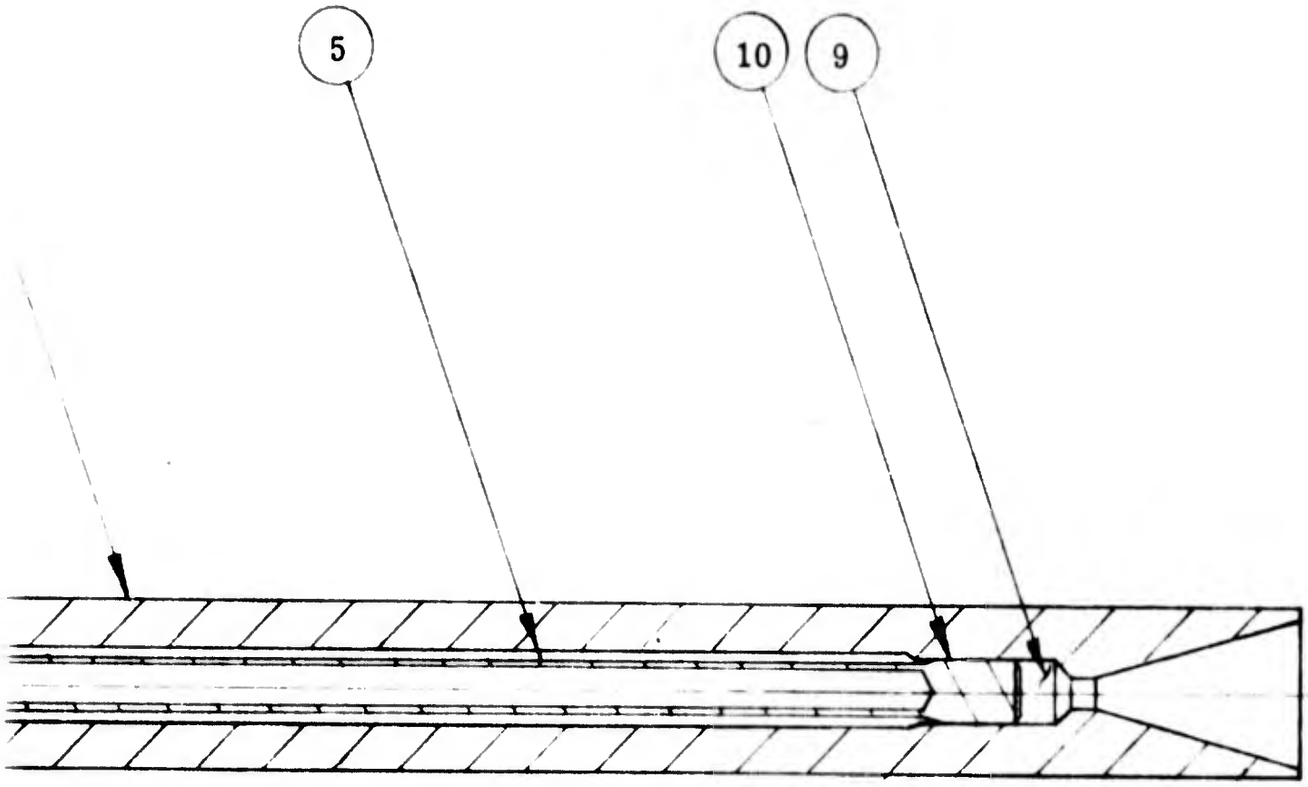

1. Thrustor Housing
2. Epoxy Seal
3. Inner Electrode Mount
4. End Cap
5. Inner Electrode
6. Metallic Seal
7. Outer Electrode
8. Propellant Gas Connection
9. Plenum Chamber
10. Contact Region

eneratively-Cooled Hybrid Resistance Heater

B

which is at the potential of the outer electrode. The inner electrode (5) is threaded into the inner electrode mount. The end cap plus inner electrode assembly are screwed to the main thrustor housing (1). A high temperature metallic seal (6) assures a gastight connection. The outer electrode (7) fabricated entirely of 2 percent thoriated tungsten is screwed into the main thrustor housing. A conical seal between outer electrode and housing assures a gastight connection at this location. This type of construction allows quick disassembling of all vital thrustor parts. The propellant flow enters the thrustor at the center connection (8) of the inner electrode mount through a threaded passage. It first regeneratively cools the inner electrode mount and then passing through radial holes through the epoxy seal it flows into passages of the thrustor housing from where it is injected into the annular heating passage formed by the inner and outer electrodes. The flow proceeds along the axis in this annular passage and enters through axial slots milled into the inner electrode into the plenum chamber from where it is exhausted through the nozzle. The unique design involving the contact resistance principle allows the inner electrode to expand within the configuration of the outer electrode without the generation of harmful stresses. This results in dependable operation at high temperatures (up to 3000°K) for a large number of test runs.

2.2.3 Liquid Metal Heaters

Continuous experimentation with very high temperature resistance-heated thrustors provided the basis for the concept of a new type of heater which would allow operation at even higher propellant temperatures. Temperatures of 5000°K and up clearly exceed the melting point of all high temperature refractory materials. The concept therefore involves the use of heaters of high temperature refractory materials in the liquid state. During experiments with heaters of the type shown in Figure 6 it was observed that when overheating occurred in the inner electrode, molten tungsten material appeared on its outer surface wherever cracking had occurred. The electrode was constructed entirely of 2 percent thoriated tungsten. Cross sections of inner electrodes in the contact region showed that the inner core was in the molten state during operation. The highest temperature of this type of heater would naturally occur in the center of the rod since the temperature gradually drops off toward the periphery where the energy is absorbed by the propellant gas. This observation led to the design of a "super heater" which is described and shown schematically in Figure 7. The inner and outer electrode in this case are combined (1) with the inner part forming a cavity in which molten metal is held by centrifugal force. The inner tubular section is rigidly connected to the rotor (10) which in turn is driven by an electrical motor (11). Current leads for both negative and positive potentials are connected to the mercury brushes (8) and (3) so that the current is allowed to flow from the heavier outer section of the electrode into the nozzle region and through the thin tubular section of the inner

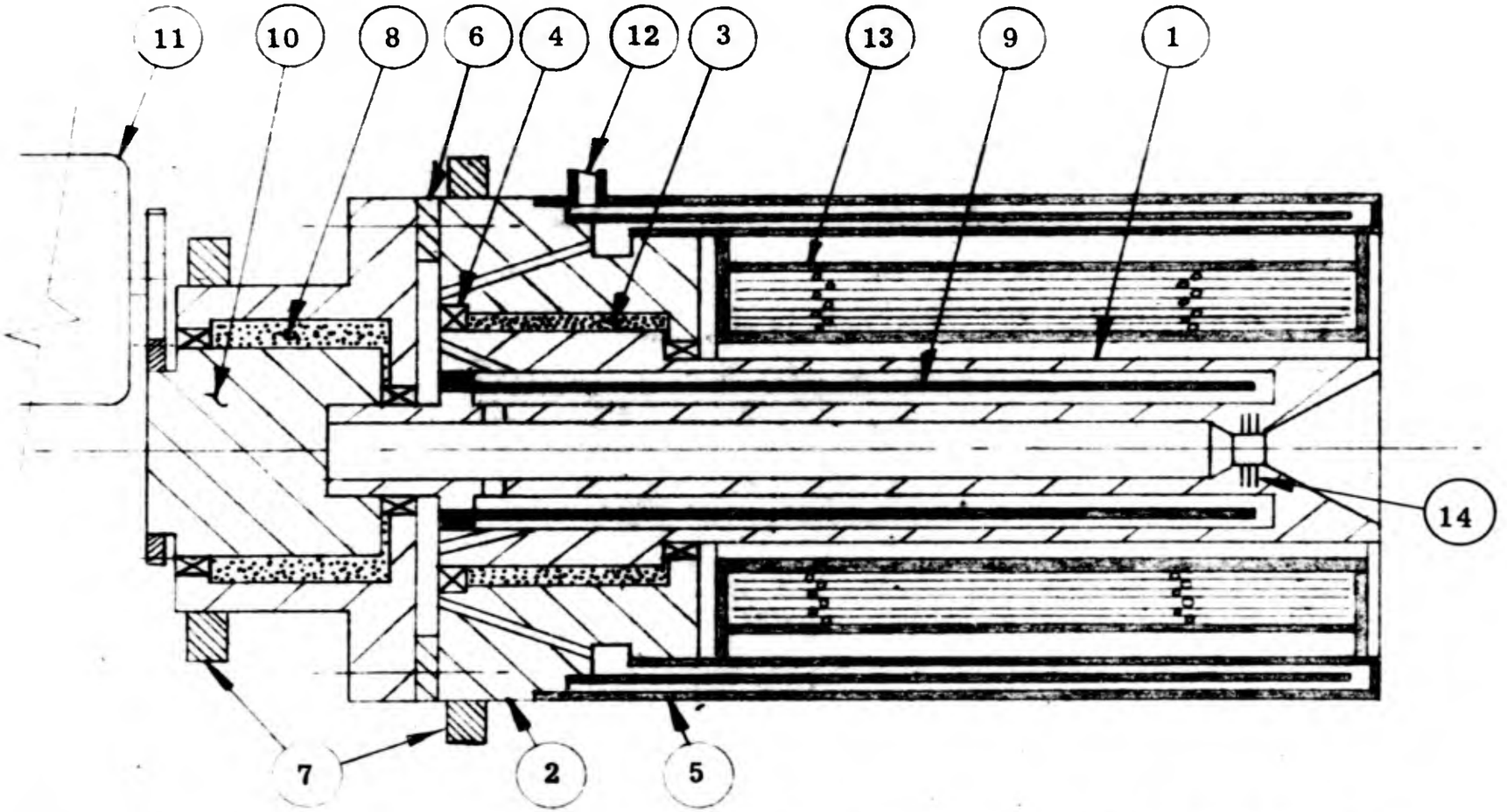

1. Electrode Assembly
2. Main Housing
3. Mercury Brush
4. High Temperature Seals
5. Thermal Radiation Shields
6. High Temperature Insulator
7. Current Connectors
8. Mercury Brush
9. Flow Divider
10. Rotor Assembly
11. Electrical Motor
12. Gas Connector
13. Multiple Radiation Shield
14. Transpiration Cooling

Figure 7. Schematic of High Temperature Liquid Metal Heater

part back to the rotor assembly. The propellant enters through the gas connector (12) of the thermal radiation shield (5). This allows regenerative cooling of the thermal heat shield and the main bearing housing (2). The propellant then flows through the insulator (6) into the heat transfer passages of the electrode and is injected through radial holes into the center tube section. The wall thicknesses of the center tube are chosen so that a temperature gradient occurs which keeps a thin layer on the inner surface of the center tube in the liquid state. The propellant passes over this surface before it escapes through the nozzle throat into the vacuum tank. The electrical motor (11) keeps the electrode assembly in rotation so that the thin layer of molten tungsten material will be kept from being swept into the nozzle section. The rate of vaporization of the tungsten at temperatures below boiling can be reduced by operating at high propellant pressures. The concept described presents a unique scheme to resistively super heat gaseous propellants under very high pressures. This heater design appears to be promising enough to warrant further development.

2.2.4 Arc Heaters Early Geometries

The arc heaters or thrustors which were used during the early part of the experimental investigation included the latest improvements in design available from the state-of-the-art at that time. The early basic design geometries illustrated in Figure 8 are typical of the arc geometries used during this period. The electrode geometry consists of two coaxially placed electrodes with the conical tip of the cathode (10) extending far into the conical cavity of the anode (9). This conical section terminates at the intersection of the anode throat and the diverging nozzle section. An annular passage is formed between cathode and anode through which the propellant is forced to flow. The arc discharge is prevented from reaching upstream of the anode cone and is swept into the throat and nozzle region by the inrushing propellant gas. The electrodes used with the early configurations were water cooled. Both electrodes were manufactured of copper, but in some cases a tungsten tip was gold soldered to the cathode and likewise a tungsten sleeve was soldered to the anode. The electrodes are firmly held in place by the anode and cathode assembly (7) and (11). The heater housing (8) is rigidly connected to the mounting platform (14) of the thrust balance. The insulators (17) which are used to separate the cathode assembly from the thrustor housing and anode assembly were generally manufactured of teflon, phenolic, or nylon based materials. Electrical power leads and propellant gas feedlines (12) and (13) are connected to the cathode assembly and to the thrustor housing. The power cables serve as the water coolant, feed, and discharge lines as well. All water cooling, electrical power,

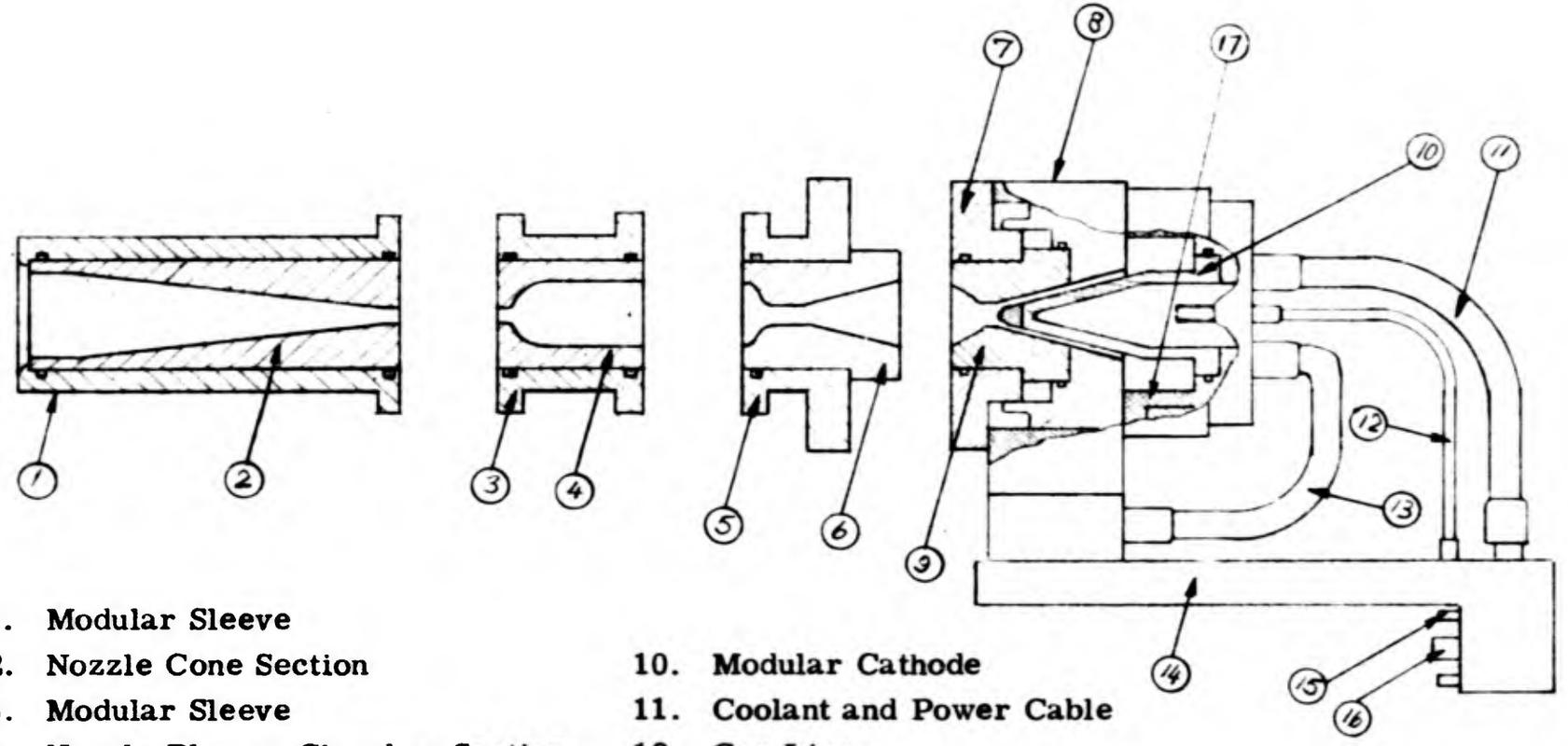

1. Modular Sleeve
2. Nozzle Cone Section
3. Modular Sleeve
4. Nozzle Plenum Chamber Section
5. Modular Connector
6. Modular Anode Section
7. Modular Connector
8. Thrustor
9. Short Nozzle and Anode
10. Modular Cathode
11. Coolant and Power Cable
12. Gas Line
13. Coolant and Power Cable
14. Mounting Platform
15. Gas and Pressure Connectors
16. Power and Water Connector
17. Insulator

Figure 8. Design of Early Arc Heater (Modular Type)

and propellant gas is received at the mounting platform which when attached to the thrust balance automatically connects to the primary feedlines which are an inherent part of the thrust balance. A modular thrustor design was chosen to allow quick interchange of the many different kinds of arc plenum chambers, sonic throats, and diverging nozzles used during the experimental investigations. The various nozzle geometries can be readily assembled using this modular design as shown in (1), (2), (3), and (4). The design concept of the early geometries provides for heating the propellant by the arc in the arc plenum chamber and expanding the hot gas through the throat and diverging nozzle section in the conventional manner. Generators and arc heaters of this type are capable of operating in the range of 1 to 300 kw power input using most of the common propellant gases. A practical limit of performance obtained with these early arc heater geometries was a specific impulse of 2000 seconds using hydrogen gas.

2.2.5 Arc Heaters Operating at Low Pressures

To achieve operation at higher power inputs and greatly increased propellant stagnation temperature in the arc heater, several design changes were made following completion of the work with early geometries. The design of a water-cooled arc heater electrode configuration capable of operating at the specific impulse range from 1000 to 10,000 seconds using hydrogen gas is shown in Figure 9. The thrustor still uses the basic coaxial arrangement; however, the plenum chamber section as well as the diverging nozzle section have been totally eliminated. As in the early configurations, the propellant flow is allowed to pass through the annular passage formed by the anode and cathode directly into the throat region. The arc discharge with this geometry originates at the cathode tip and extends through the anode throat far into the downstream exhaust region. A characteristic of this heater is that it operates at greatly reduced arc chamber pressures (100 to 1 mm Hg). Energy addition from the electrical discharge to the propellant therefore occurs partially within the heater in the throat region and partially outside the heater in regions of the exhaust where current is flowing. Due to the extended arc discharge into the exhaust region, the thermal losses to the arc heater configuration itself are considerably lower. Thus the heater can be operated at higher power input and at greatly reduced propellant mass flow rates. The thrustor also can be operated with water-cooled or radiation-cooled electrodes.

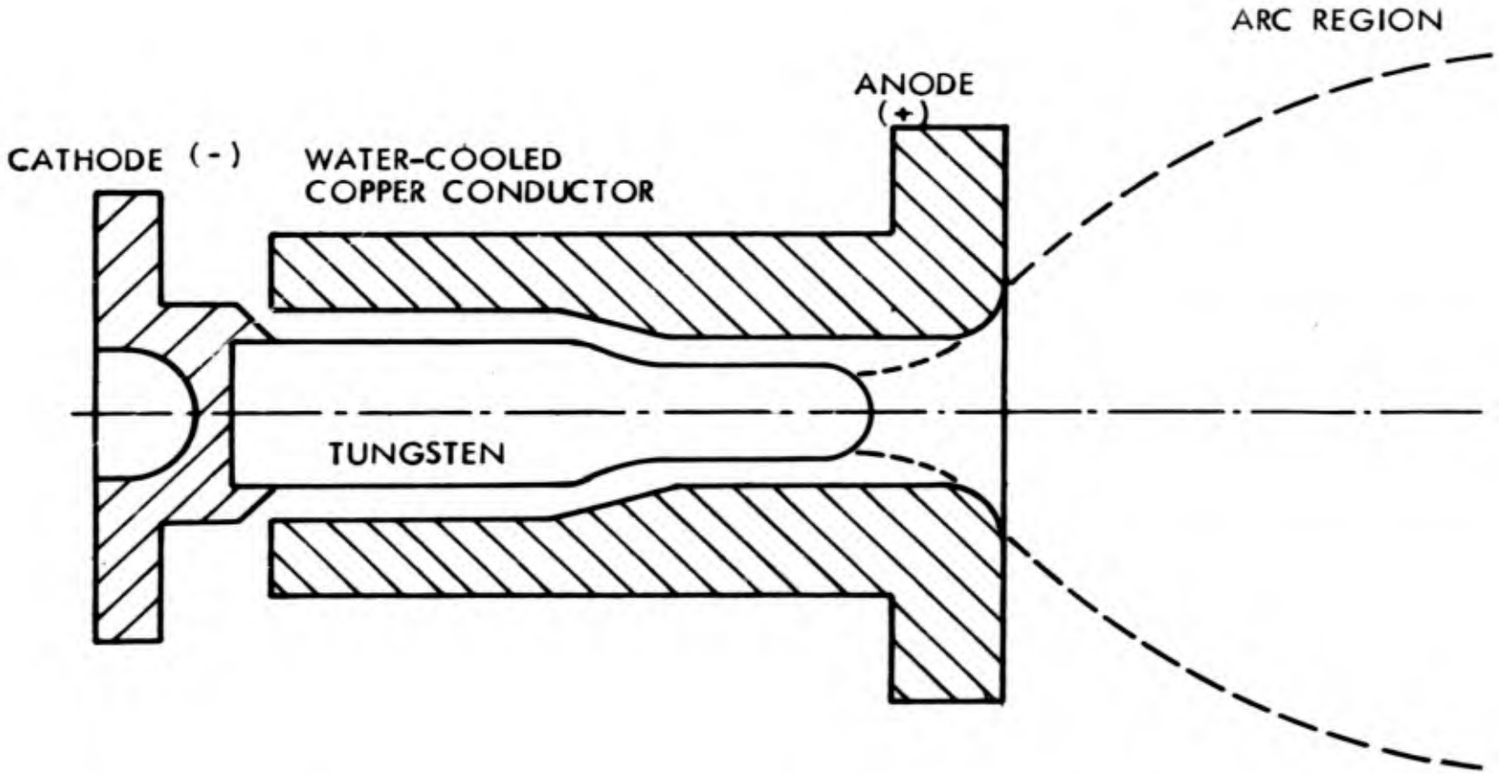

Figure 9. Electrode Configuration for Arc Heater Operating at Low Pressure

2.2.6 Arc Heaters with External Magnetic Fields

In order to reduce local anode erosion and to establish a more uniform arc discharge, an externally applied magnetic field was added to the thrustor configuration to rotate the arc attachment point. The external magnetic field consisted of a tightly wound coil manufactured of thin wall copper tubing and coaxially placed directly over the anode configuration (2). Figure 10 shows the thrustor design with the external magnetic field coil mounted in its proper position. The magnetic field coil (1) can be energized in two ways. One, it can be connected in series with the arc heater current so that the coil current is always equal to the arc current or, two, it can be entirely separated from the arc circuit and controlled independently by a different power circuit. The second method is preferable for experimental purposes because the independent control of current makes it easier to correlate test results showing arc power versus magnetic field strength. The external magnetic field coil is located around the electrode configuration in such a way that maximum field strength occurs in the center of the arc column formed between the cathode tip (3) and anode throat. The coils used allowed a variation of the magnetic field strength from 600 to 12,000 gauss. The coil is water cooled by an independent flow circuit so that power losses in the coil do not interfere with the measurement of power losses in the water-cooled arc heater itself. The external magnetic field coil is also adaptable to all of the arc geometries that were used during the experimental investigation. The coil is mounted on its own support which is rigidly connected to the mounting platform (6) of the thrust balance. Current

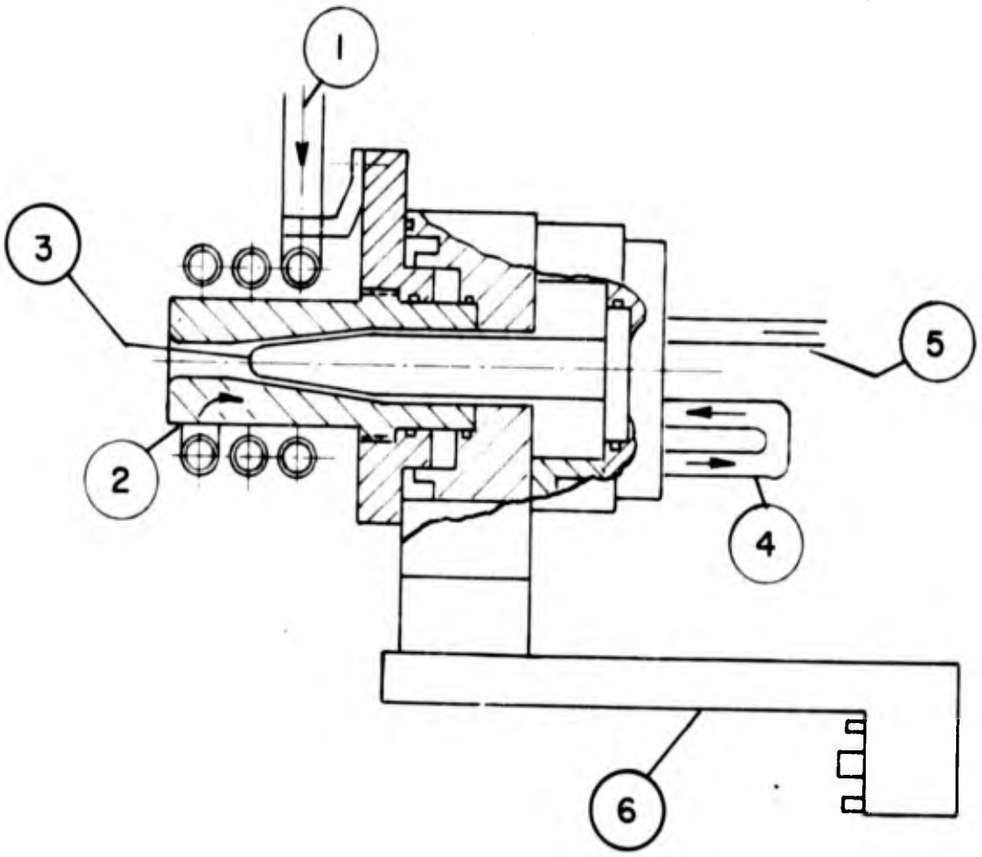

1. External Magnetic Field Coil
2. Anode Configuration
3. Cathode
4. Current and Coolant Connectors
5. Propellant Feedline
6. Mounting Platform

Figure 10. Design of Arc Heater With External Magnetic Field

and water lines to the coil are part of the thrust balance system and are arranged in such a manner that the rather large currents for high fields do not influence the thrust produced by the heater itself. Figures 11 and 12 show the dimensions of a typical magnetic field coil, and the relationship between magnetic field strength and coil current.

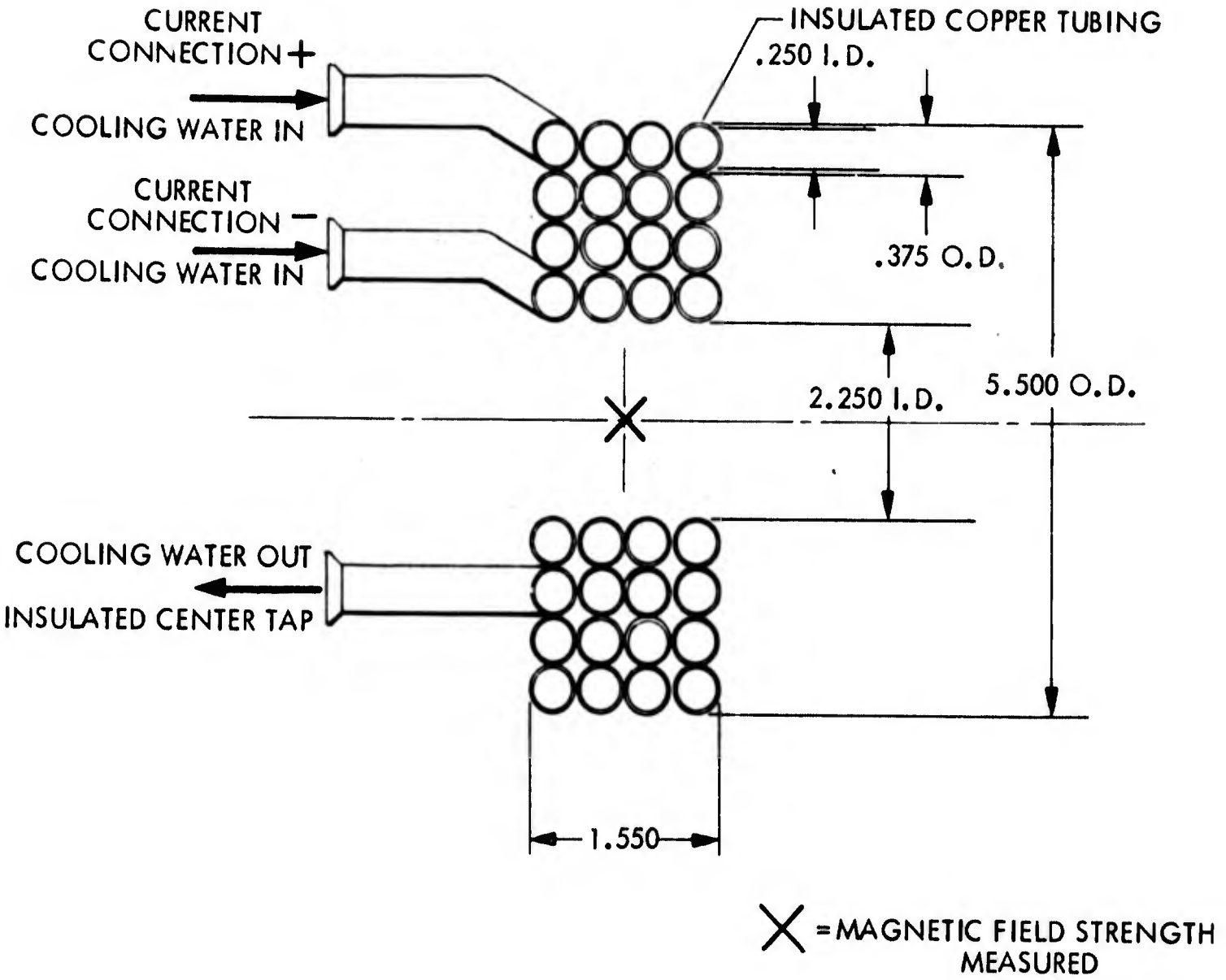

Figure 11. Dimensions of External Magnetic Field Coil

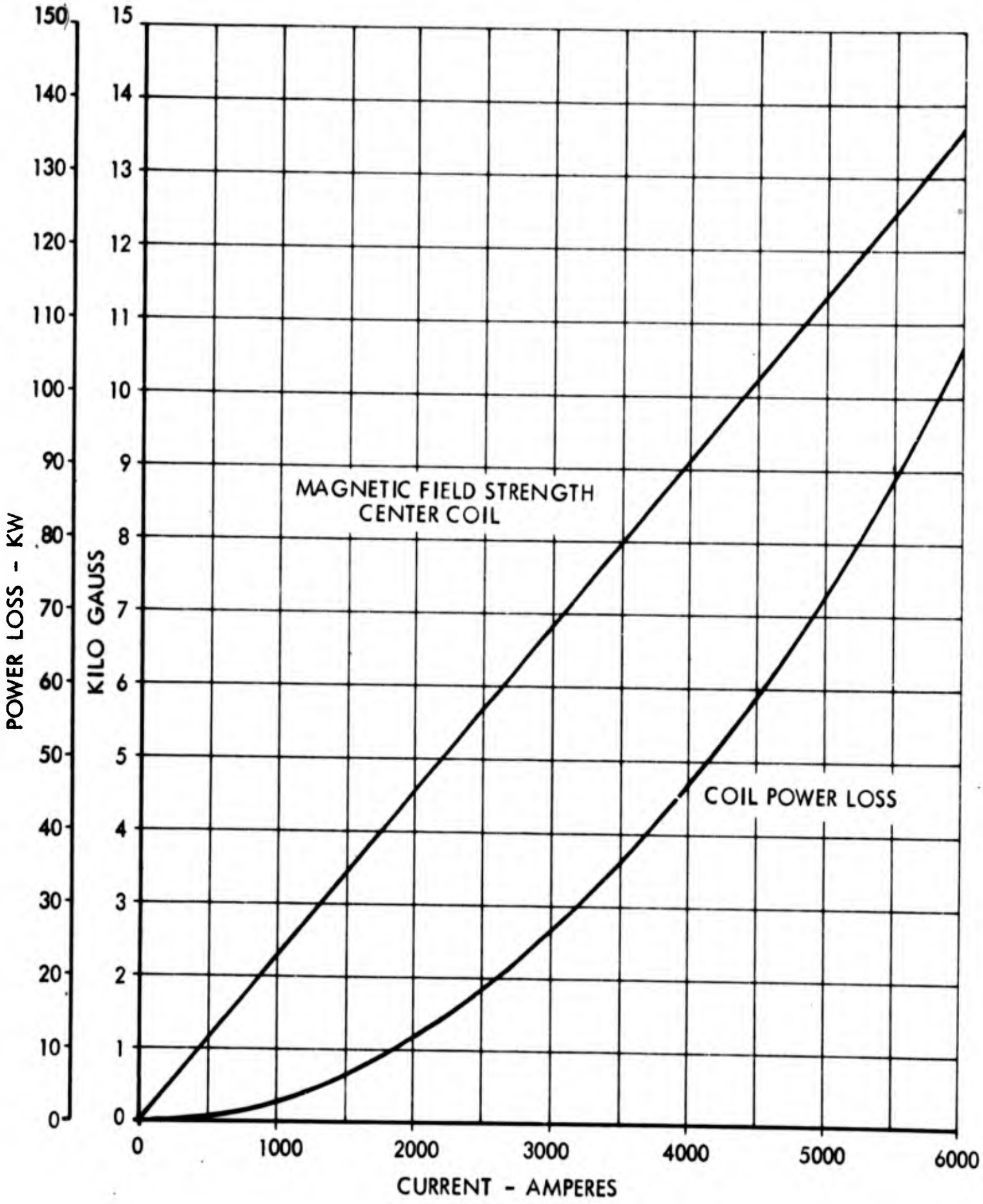

Figure 12. Magnetic and Electrical Parameters of External Magnetic Field Coil

2.2.7 Arc Accelerators Without Propellant Throughput

During the final phases of the investigation, arc heaters were designed and developed which allowed operation at very low propellant mass flow rates and with totally eliminated injected propellant mass flow. The arc discharge in the latter case is fed by vaporized electrode material and by the ambient gas which surrounds the thrustor configuration. Figure 13 shows the design of an arc heater capable of operating with no propellant throughput. The cathode (1) and anode (2) are entirely fabricated of tungsten. Although the electrodes are of the usual coaxial design, the annular passage between them is very wide so that a boron nitride insulator sleeve (5) can be placed between them extending down to the conical section of the electrode configuration. To obtain high enough operating temperatures, the thrustor is radiation cooled. It is required that one or both of the electrodes operate at near melting temperature so that in a vacuum environment sufficient material will be vaporized to act as the working fluid. The thrustor housing to which both anode and cathode assembly are mounted is either radiation or water cooled. The electrode assemblies protrude well out of the thrustor housing so that little energy is drained into the thrustor housing through the electrodes themselves. A water-cooled copper heat shield (3) surrounds the anode so that thermal losses from the thrustor can be accurately measured. The boron nitride insulator surrounding the cathode prevents the arc discharge from striking upstream of the conical sections of the electrodes. The magnetic field coil (4) is located directly over the arc discharge region in the anode assembly. It was necessary to use a magnetic field coil with

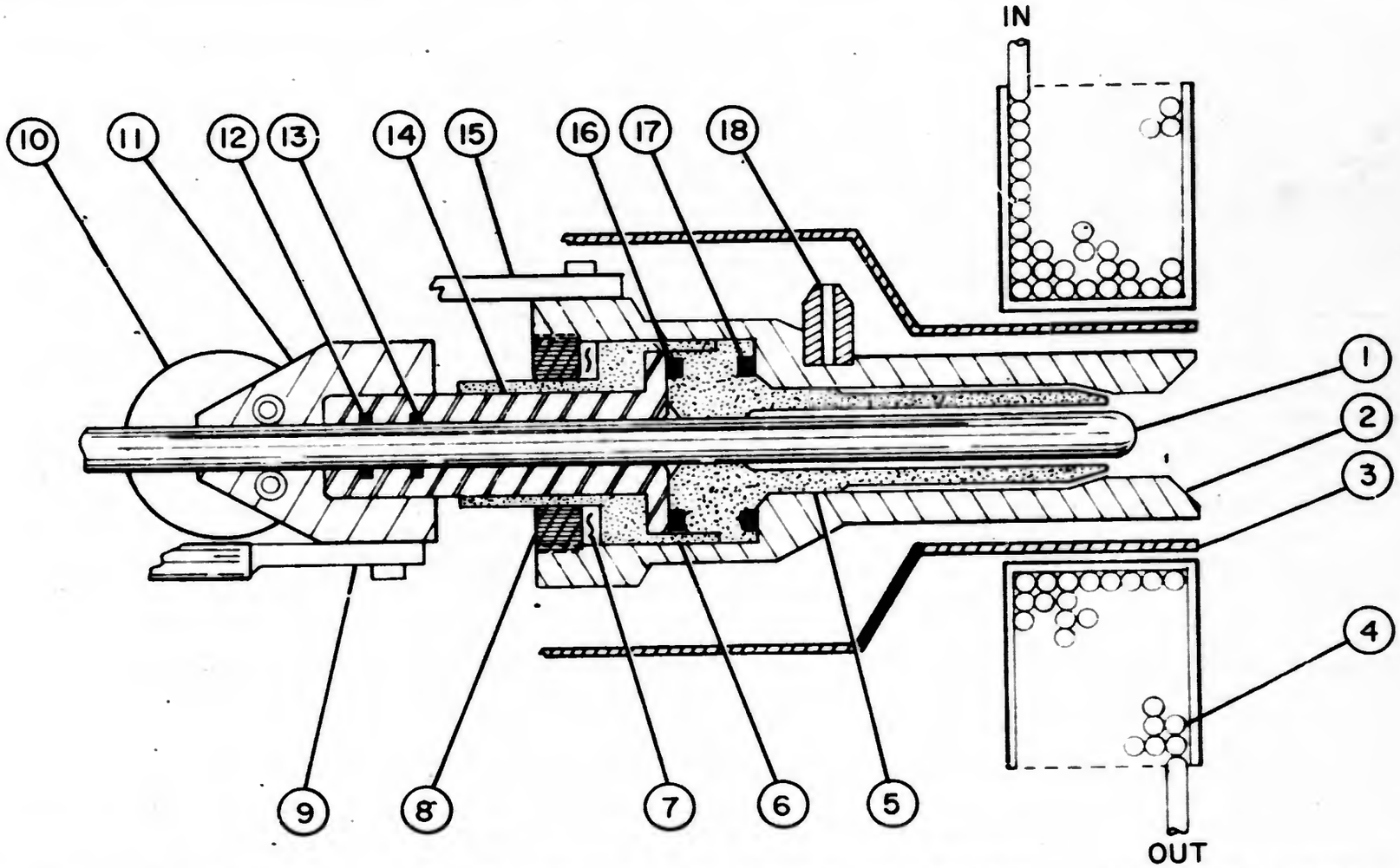

1. Inner Electrode (feedable)
2. Outer Electrode
3. Radiation Shield
4. External Magnetic Field Coil
5. High Temperature Insulator
6. High Temperature Insulator
7. High Temperature Spring Washer
8. Lock Ring
9. Power Connector
10. Drive Motor
11. Center Electrode Feeding Mechanism
12. Metal O-Ring
13. Metal O-ring
14. Inner Electrode Holder
15. Power Connector
16. High Temperature Metal Seal
17. High Temperature Metal Seal
18. Starter Gas Connector

Figure 13. Design of Arc Accelerator Without Propellant Throughput

this type of heater since uniform erosion of both anode and cathode was essential for satisfactory operation. Thrustors of this type have been operated during numerous test runs extending through several hours of duration. Operation in the power range from 1 to 50 kw have been obtained. Due to the coaxial design of the electrodes it is desirable to have the main mass flow contribution furnished by the central electrode since it can be easily fed into the arc chamber should operation of long duration be desired. To precisely determine the contribution of mass flow, both electrodes were weighed before and after each test run. Operating characteristics and thrustor performance using this design are discussed in detail in other sections of this report.

2.3 Measuring Instruments

The measurements made during the program may be considered in two categories; measurements needed for determining overall performance (efficiency and specific impulse), and measurements used only to determine operating conditions and to obtain a better understanding of flow phenomena in and near the thrustor. The first group (which we will call the primary measurements) include thrust, propellant mass flow, and electrical power; while the second group includes thermal losses, pressures, temperatures, and other measurements of conditions in and around the thrustor. In order to detect small changes in performance resulting from design modifications it is desirable to determine efficiency with good accuracy. Since efficiency is determined from the primary measurements, the accuracy of measurement is usually more critical for these items. For example, if thrust, mass flow, arc current, and arc voltage were all measured with errors of 1 percent, the probable error for the determination of efficiency would be $\sqrt{7}$ percent or 2.65 percent. Notice that thrust enters as the square in the equation for efficiency while the other measured quantities enter as the first power. The accuracy of the thrust measurement is therefore of greater importance than the other three. For example, an increase in the error of thrust measurement from 1 percent to 5 percent would increase the probable error for the determination of efficiency from 2.65 percent to 10.4 percent; while a corresponding increase in the error of measurement of mass flow would increase the probable error to only 5.57 percent.

The instruments used for taking the primary measurements are all capable of measurements with errors of less than 1 percent under the proper test conditions. However, in the operation of thermo-ionic thrustors extreme operating conditions are encountered which produce side effects resulting in increased error. The methods of measurement used and some of the problems encountered in obtaining the desired accuracy are described below.

2.3.1 Measurement of Thrust

Thrust is measured by determining the deflection of a cantilever beam on which the thrustor is mounted. The amount of deflection (which is large compared to thermal distortion effects in the vacuum chamber) is sensed by a differential transformer. The beam itself is constructed of tubing and maintained at constant temperature by water circulating through the tubing and by radiation shielding around the tubing. Cooling water lines and propellant lines are arranged to avoid Bourdon tube effects in the thrust direction, while electrical power cables are arranged in a twisted pattern to avoid electromagnetic effects acting in the thrust direction. A more complete description of the thrust stand is given in FR041-766.*

There may be additional electromagnetic interaction forces due to the presence of the thrustor with its magnetic coil. In the past, it has been possible to cancel these effects using an adjustable steel plate to generate symmetrical interaction forces. However, in the present program while testing thermo-ionic thrustors the arc currents are so high (in comparison to the thrust level) that the presence of significant unbalanced interaction forces is suspected. These devices often operate with arc currents up to 5000 amperes and with external magnetic fields in the order from 3000 to 12,000 gauss. In many cases high pressure cooling water or gas circuits are needed. It is reasonable that currents and magnetic fields of this magnitude, as well as exhaust plumes carrying a jet power of hundreds of kw and consisting of a highly ionized gas filling the entire exhaust region, can produce parasitic effects on the thrust sensing mechanisms. This is

*Contract AF 49(638)-766 final report

especially true when the total thrust values are not very large, i.e., 10 to 100 grams. In order to accurately balance or allow for these forces the "thrust killer" described in the next paragraph was developed. This device allows a tare reading and a calibration curve to be obtained with the thrustor operating in the normal manner. Since the arc is in operation, interaction forces are presumably accurately simulated. However, a small uncertainty remains because the arc (in the absence of the thrust killer) may extend some distance downstream into the plume. If this portion of the arc produces a significant interaction force, some error in the thrust measurement may remain. The accuracy of thrust measurement is believed to be better than 2 percent under normal test conditions, but the error may exceed 5 or even 10 percent under severe conditions such as occur, for example, when the thrustor is operating with no external propellant flow.

The thrust killer, which attaches directly to the thrustor, was developed under this program. Its purpose is to stagnate and cool the exhaust gas and direct it at low velocities radially outward normal to thrust direction. The thrust killer can be swung in and out of the jet region at any time while the thrustor and entire supporting mechanism are in full operation. This provides a corrected tare reading that practically eliminates many side effects that generally would either add to or subtract from actual thrust as produced by the escaping exhaust gases. Figure 14 shows schematically the design of this device which is made of solid copper metal containing cooling passages through which high pressure cooling water is forced. The device is capable of continuously absorbing jet powers in the order of

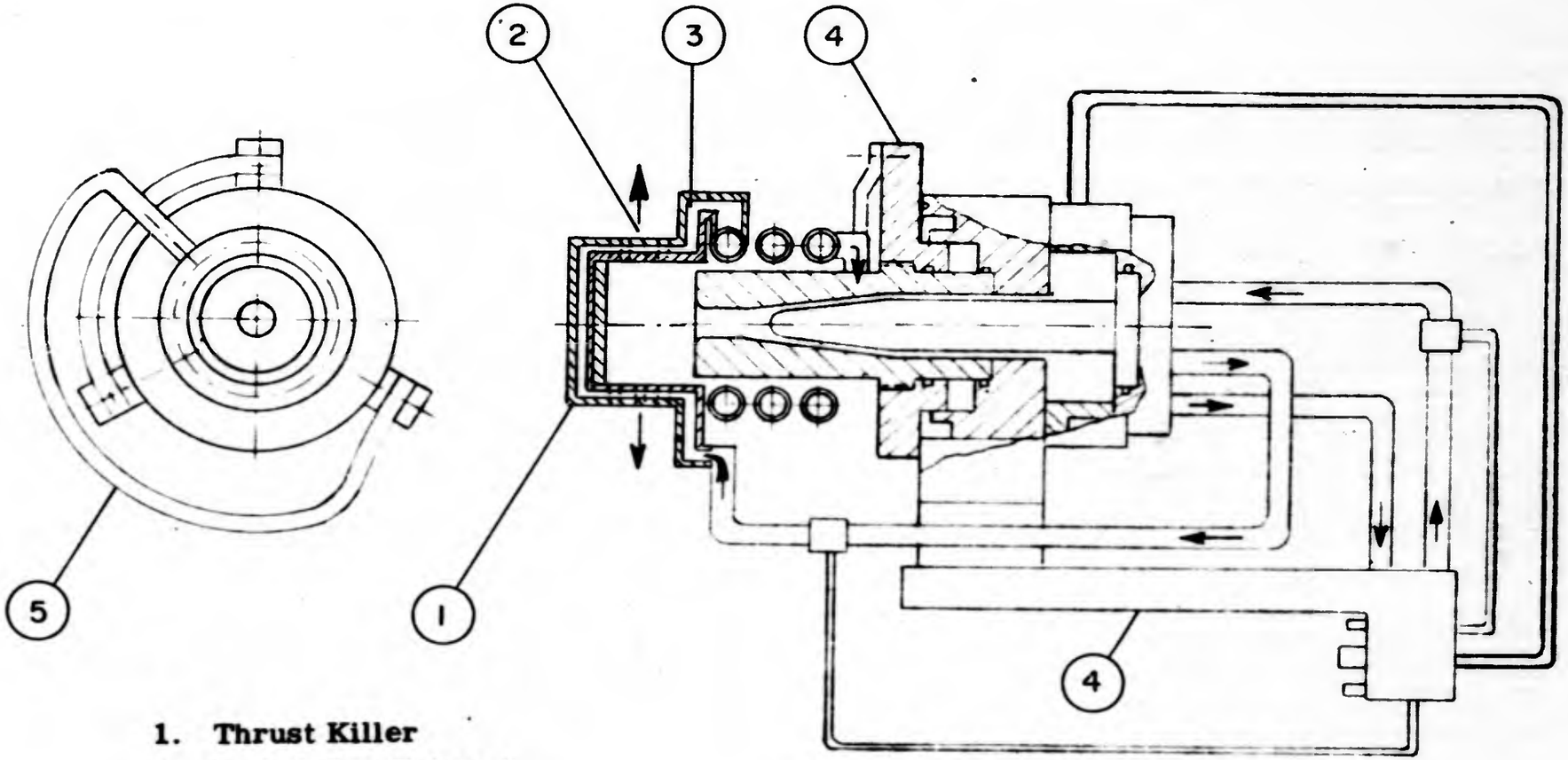

1. Thrust Killer
2. Radjal Gas Exhaust
3. Cooling Passage
4. Arc Heater
5. Cooling Circuit

Figure 14. Cutaway View of Thrust Stagnator Mounted on Arc Heater

100 kw. The thrust killer can be positioned in or out of the jet region by an electrical motor assembly which is remotely controlled from the console. The device is balanced so that the motion does not affect the thrust sensor. The difference of thrust indication from in or out positions represents the total net thrust produced by the jet exhaust proper. The effectiveness of the thrust killer has eliminated many problems which otherwise could not have been readily solved. The device can be calibrated by having a large amount of propellant gas at room temperature stagnated into the thrust killer without arc power and magnetic field coils turned on. The effective thrust in this case must indicate zero. This assures that all the exhaust gas is escaping in a radial direction with no force produced on the thrust sensing mechanism.

The use of a sonic throat (as described in Section 2.2.1) makes it possible to record thrust data which is influenced in a predictable way by changes in the ambient pressure in the test chamber, and is relatively unaffected by thermal and viscous losses in the nozzle. The system also permits the rapid interchange of various throats with a minimum of shutdown time.

The use of a sonic throat avoids the costly design and manufacturing of fully expanding supersonic nozzles which would in principle be different for each test point to yield optimum results. The results obtained show thrust values which agree closely with theory. If fully developed, a sonic throat in conjunction with a sensitive force balance could serve as a thrust standard in the propulsion field. The same artifice can be used in a completely different application as illustrated below.

An apparatus capable of analyzing the unknown materials in liquid or gaseous form could be constructed on this principle. The schematic presented in Figure 15 shows the principle of such an apparatus. A pipeline through which liquid or gaseous substances flow is interrupted by a T wherein a force balance (1) is mounted. The extension arm (2) serves as the mount for the sonic throat (3). The substance is forced to flow through the supporting arm into the sonic orifice from where it is ejected into the continuing pipeline. At known flow rates the thrust force measured by the electrical readout instrument (4) is a direct indication of the properties of the fluid flowing through the pipeline. Inversely at constant thrust the amount of flow gives the same indication. Also with known fluids the same instrument can indicate the amount of flow. The apparatus could be very useful in chemical plants where mixtures of substances must be maintained within a high degree of accuracy during a continuous process.

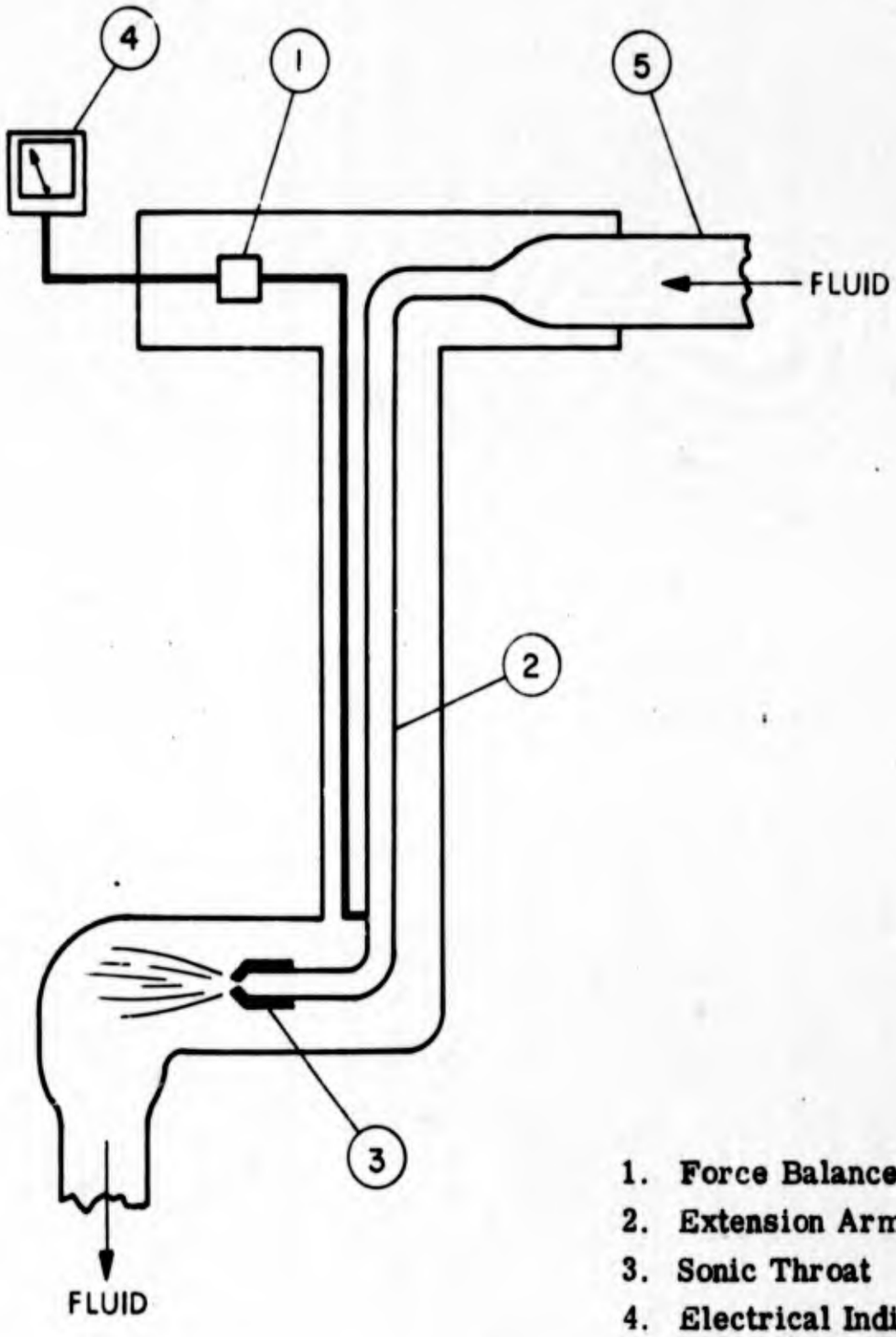

1. Force Balance
2. Extension Arm
3. Sonic Throat
4. Electrical Indicator
5. Pipeline

Figure 15. Schematic of Fluid Analyzer Using Sonic Throat

2.3.2 Measurement of Mass Flow

To assure increased accuracy of the propellant mass flow rate measurement a company developed improved conversion of the prototype gravimetric mass flow measuring system as described in earlier reports was made available for mass flow calibration. This new system is capable of measuring mass flow rates of gaseous propellants to an accuracy of better than 0.1 percent. The system is fully described in a company printed brochure (PRE-115 of May 1964). The improvements basically consist of a better thermally insulated floating sphere where the working fluid is located, and the installation of a taring fluid mechanism which allows operation within the range of a high precision electronic balance. The addition of this precision electronic balance makes possible a continuous recording of the net weight loss from the sphere. Added electronic circuits also serve to divide the elapsed exhausting time into the net weight loss as sensed by the electronic balance so that an integrated propellant mass flow rate is continually recorded by a voltage channel recorder on the control console. The system also permits operation periods of one hour using hydrogen gas at a mass flow rate of 25 mg/sec, and recharging of the floating sphere during operation. The original prototype model of this precision gravimetric mass flow metering system was developed under this program and has been used at the Giannini Scientific Corporation laboratory for some time. It has proved to be an invaluable measuring and calibration tool for mass flow rates of gaseous propellants.

For convenient correlation of test data it was decided that all environmental tests using the various propellants should be conducted at identical values of mass flow rate. This decision proved fruitful in that when all data was plotted and correlated it was easy to detect variations in performance associated with the characteristic of the propellant. It is important when comparing the performance characteristics of hydrogen and helium gas, for example, at identical stagnation temperatures, to use identical mass flow rates, then other variables could enter and substantially alter the performance making the performance more difficult. The propellant mass flow rate is closely connected to the efficiency of the thrusting mechanism because pressure differences in the plenum chamber, flow distribution in the exhaust, heat transfer through the chamber walls, and other related phenomena are affected and can easily influence the performance.

At very low (and zero) propellant flows, the primary working fluid might be electrode vapor. For these cases it has been necessary to carefully time test runs and to weigh the electrodes before and after runs to obtain a working fluid flow rate. The weight change of insulator parts has also been measured, but has been found to be nearly negligible.

2.3.3 Measurement of Power

The meters used for the measurement of arc current and arc voltage have an accuracy of 0.5 percent of full scale which, in normal use, results in an error of less than 1 percent of the reading. The direct current component of power is therefore determined with a probable error which is less than 1.42 percent. However, there is also an alternating current component (due to power supply ripple and high frequency cycles that occur naturally in many arc configurations) which is not detected when direct current meters are used. To determine the importance of this error, separate measurements of arc voltage and current fluctuations using a cathode ray oscillograph were made for several test points. These showed the alternating current component to be less than 2 percent of the direct current component. Although small, this error cannot be considered negligible. It was concluded that the measurement of electrical power should, in the future, be done using a wattmeter which is accurate in the frequency range of the power supply ripple. If required, sufficient inductance should be added to the power supply circuit to iron out fluctuations in the current due to arc voltage fluctuations. This will eliminate the need for a wattmeter which is accurate in the very high frequency range since there will be no alternating current component of power if there is no current ripple. (Arc voltage fluctuations with frequencies as high as 200 kilocycles per second have been observed. This is considered to be too high for measurement with wattmeters of proven design.)

A check of the power measurement is obtained by comparing it to the sum of calorimetric measurements of the thermal power in the jet and the

thermal losses. The agreement is consistantly found to be within 1 percent. This is a useful check which can be used to detect improper operation of the instrumentation. However, the close agreement does not necessarily imply that the measurements are that accurate. Both sets of measurements are expected to be slightly low because the alternating current component of power is normally not measured, and because some of the thermal energy may be lost by thermal radiation or convection in a manner that by-passes the calorimeters.

Two separate water circuits are used for the measurement of thermal energy. The first circuit passes through a coil of copper tubing lining the vacuum chamber walls and through a cooling baffle at the exit end of the chamber. This circuit is used to measure the thermal power in the jet. The coils are considerably larger in diameter than those that were previously used in the water-cooled exhaust pipe (the chamber is nominally 4 feet in diameter and 17 feet long). The increase in size reduces interaction effects between the jet and the cooled wall surfaces.

The second circuit passes through cooling passages in the plasma generator and in the thrust killer (in series). When the thrust killer is rotated out of the jet stream, this circuit measures losses to the cooling water in the plasma generator. Since the gas passages in the thrust killer are designed to remove nearly all of the thermal energy from the gas, the circuit measures total thermal energy when the thrust killer is in operation. Although not intended for use as a precise calorimeter, reasonably good

results have been obtained using the thrust killer in this manner. Total thermal power was found to agree with electrical power input within 2 or 3 percent. Also, the thermal power absorbed by the coils lining the vacuum chamber was found to be negligible with the thrust killer in operation.

The water flow in the two circuits is measured for each test condition by weighing containers which have been filled for a measured time interval from the cooling circuit. The weight change is measured very accurately, so the accuracy with which the water flow rate is measured depends primarily on the accuracy with which the filling interval is timed. This is done using a stop watch for a filling time of 30 seconds. The resulting accuracy for the flow rate measurement is about 1 percent. The temperature rise is measured using both precision thermometers and thermocouples at the inlet and exit of each circuit. The temperature rise varies from 10°C minimum to about 40°C depending on the operating condition. Since the error of temperature measurement is no greater than 0.1°C, the temperature rise is determined with a probable error no greater than about 1.4 percent. The corresponding probable error in thermal power measurement is about 1.7 percent.

For some of the tests, thermocouples were added between sections of the cooling passages in the plasma generator. This permitted thermal losses to the two electrodes to be separated. The thermal power measurements have the purpose of separating thermal losses from other losses, and of providing a check of the electrical power input.

2.3.4 Measurement of Pressure

In the thermo-ionic type of thrustor, a significant portion of the energy addition and gas expansion seems to take place in the plume region outside of the thrustor body. So, to obtain an understanding of the operation of this type of thrustor, it is important to make measurement surveys in the plume region. Steps were initiated for the development of suitable instrumentation and a limited number of measurements were made during this program. The work included the design and partial fabrication of a three-dimensional survey mechanism capable of accurately locating a probe in the plume region. The survey mechanism which is shown in Figure 16 is water cooled and moves in cylindrical coordinants centered about the jet axis. Movement in all three coordinants is remotely controlled. The device has been used in incomplete form to make a few surveys of pressure and temperature. Some of the measurements made are discussed in the paragraphs that follow, after which some suggestions are made regarding measurements which appear to be desirable for future programs.

Pressure measurements in the vicinity of the plume are useful for studying flow patterns around the jet and evaluating magnetic containment effects. Measurements in the subsonic region are easier to use since they require less interpretation than stagnation pressure measurements in the supersonic jet.

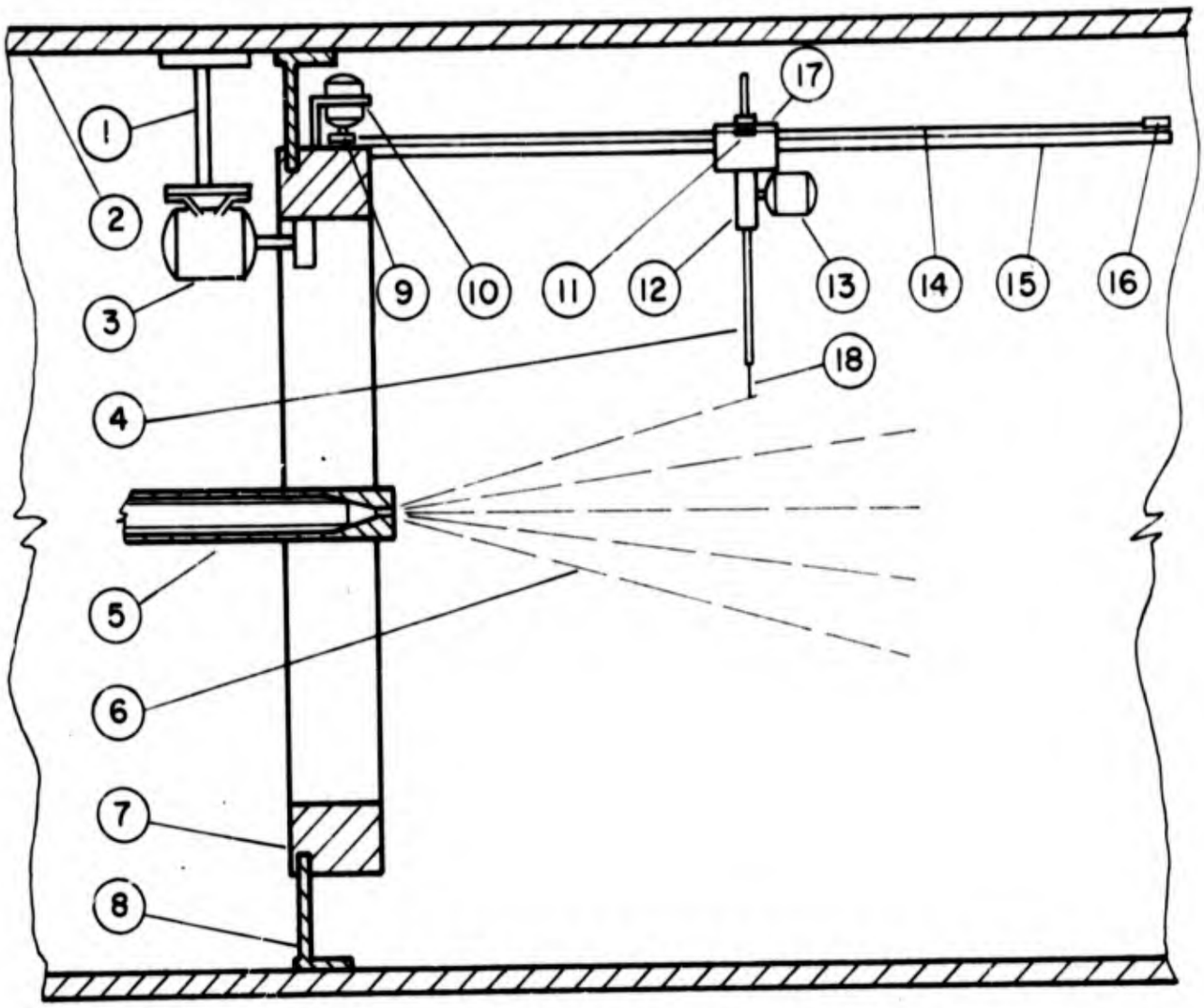

1. Motor support
2. Tank wall
3. Main motor for rotation
4. Vertical probe shaft
5. Thermal heater
6. Gas jet
7. Gear assembly
8. Bearing
9. Pulley
10. Motor for longitudinal motion
11. Wire connection
12. Bearing for vertical shaft
13. Motor for radial motion
14. Wire
15. Horizontal column
16. Pulley
17. Bearing housing
18. Pressure and temperature sensor

Figure 16. Design of Three-Dimensional Survey Mechanism

For much of the earlier work the pressure environment was higher than 1 mm (Torr) absolute and secondary standards were easily available. An accuracy of at least 1 percent can be obtained in this range, so no special development was necessary. Standard mercury and oil manometers have been used together with precision mechanical pressure gauges with good reproducibility. However, when the pressure is reduced to around 1 mm (Torr) or lower it becomes a difficult task to obtain accuracies of the order of 1 percent. Differences of many hundreds percent have been found between various commercial gauges operating at pressures in this low range. The difficulty of calibration is increased by the fact that most of the vacuum gauges available on the market show different indications for the same pressure if different gases are used. Also, if any condensable components are present, different indications are given for the same pressure. This last fact is particularly evidenced in the universally used McLeod gauge (keeping the gas at constant pressure condenses the components showing a pressure much lower than the real). Using manometers with extremely wide diameters and special micrometers to detect their level, pressures as low as a tenth of a micron have been measured reproducibly. The National Bureau of Standards suggested the use of the oil manometer illustrated in Figure 17 that can give absolute readings of pressure two or three orders of magnitude under the millimeter. We believe that a manometer of this type can be a reliable instrument to calibrate secondary standards in the range of 1 to 0.01 mm (Torr). In exceptional cases the range can be extended to 0.001 mm (Torr) but special precautions must be taken.. As said before, this instrument is primarily used

1. Precision Micrometer
2. Housing
3. Standard High Vacuum Source
4. Glass Tube
5. Oil Column
6. Test Pressure Source
7. Glass Tube

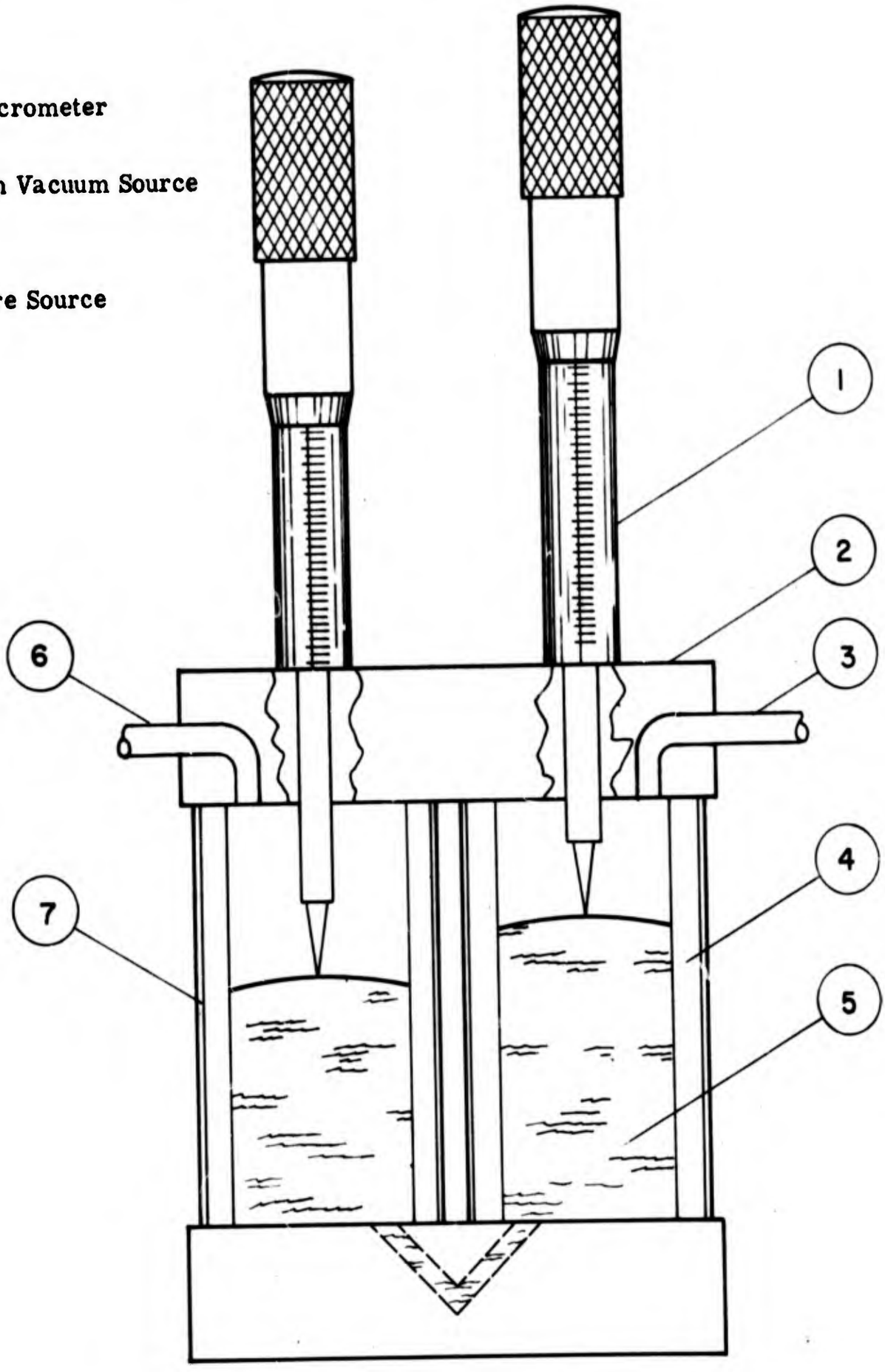

Figure 17. Design of a Precision Oil Manometer

for calibration purposes; so for the test measurement, secondary standards are necessary. The so-called thermocouple vacuum gauge measures the value of vacuum between 1 mm (Torr) and 0.001 mm (Torr) by indicating the temperature of a hot wire cooled by environmental gas. This type of instrument is very sensitive to the type of gas, requires an extremely stable power supply, and must be constantly recalibrated to give reproducible results. A precision of 1 percent is very difficult to achieve with this instrument, especially in some parts of the scale. During our tests the vacuum thermocouple instrument has been extensively used, and good reproducibility has been maintained through continuous recalibration. For this purpose the calibration unit illustrated schematically in Figure 18 has been constructed. The basic principle of this calibrator is to produce the desired pressure using the desired gas and to use this pressure as a standard to calibrate the unknown gauge. Practically, several containers are used with volumes less than that of a master container by ratio of 10, 100, 1000, 10,000, etc. One or more of the small containers are filled with the working gas at a pressure higher than 1 mm (Torr) (which is easily measurable with high precision using a standard instrument). The gas is successively expanded in the large container (highly evacuated beforehand) and its new pressure is computed using the pressure in the small container and the volume ratio. With this system the various gauges can be periodically calibrated and the precision of the vacuum measurements can be kept between limited tolerances.

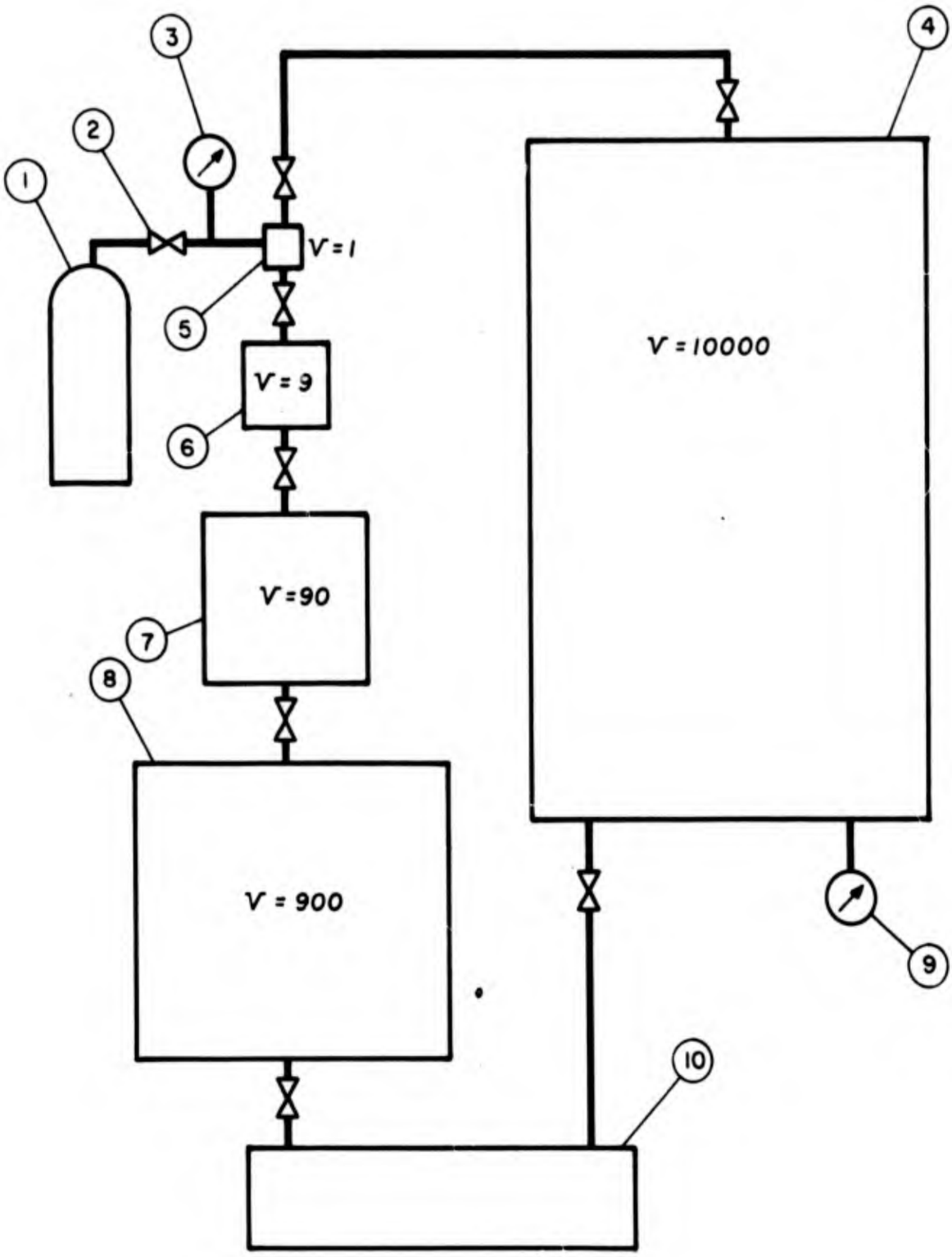

1. Test Gas Supply
2. Precision Valves
3. Precision Test Pressure Gauge
4. Large Test Volume
5. Small Test Volume
6. Intermediate Test Volumes
7. Intermediate Test Volumes
8. Intermediate Test Volumes
9. Vacuum Gauge to be Calibrated
10. Standard High Vacuum Source

Figure 18. Schematic of Vacuum Gauge Calibration System

Although frequent calibration increases the confidence that can be placed in the vacuum pressure measurement, there are often times when the reading is questionable because the gas composition at the point where the reading is taken is not accurately known. This can occur if there is leakage or outgassing in the chamber, if a tracer gas is being used, or if a sizeable fraction of the working fluid is made up of electrode vapor. In an effort to avoid the problem, a study is being made of types of vacuum gauges which are less sensitive to the propellant composition. The type which senses the deflection of a diaphragm by measuring a varying capacitance appears to offer advantages and is being seriously considered. However, the problem is particularly difficult if part or all of the gas is condensable. In this case, the propellant would condense on the sensing parts of the instrument disturbing their response. Furthermore, continued condensation in the tube leading to the sensing element can drastically change the pressure at the sensing element. To avoid these difficulties, it appears to be necessary to use a carefully metered flow of purging gas or to operate the entire instrument at a temperature above the boiling point of the condensable material.

Since a survey of pressure in the region surrounding the plume would be valuable, it is in order to continue investigating possible methods for obtaining meaningful pressure measurements in the vicinity of a thermoionic thrustor, particularly for the case where a condensable propellant (or electrode vapor) is used for the working fluid.

2.3.5 Measurement of Stagnation Temperature

Efforts were made to employ techniques and apparatus which could determine propellant stagnation temperature either in the plenum chamber or the exhaust region to a high degree of accuracy. Below are listed the various methods used during the low temperature phase of the experimental investigation.

Direct readings of temperature were made with precision thermometers placed in the flow ahead of the plenum chamber (see Figure 1). These thermometers are capable of accurately determining gas temperatures in the range of 260 to 625 °K. Identical thermometers were also placed in the jet near the throat exit. Measured values of stagnation temperature in the plenum chamber and in the exhaust region agreed within a few percent. The thermometers were calibrated prior to their use with accepted standards such as the boiling point of water and the melting points of lead at one atmosphere.

Stagnation temperature measurements were also made with commercial shielded thermocouples, i.e., iron constantan, platinum-rhodium, tungsten-rhenium, etc. As in the case of the thermometers, the thermocouples were placed in the plenum chamber and in the exhaust. Close agreement between the two values was again found in this case.

Probes with elements of high temperature refractory material were inserted into the plenum chamber and in the exhaust region for observation and temperature measurement with a radiation pyrometer. Various forms of

stagnation probes were made and inserted into the hot gas flow. The temperature of these heated materials could be conveniently read by means of a precision optical radiation pyrometer viewed as shown in Figure 19. The values thus obtained were corrected for emissivity, window absorption, etc.

Measurements of stagnation temperature were made with an optical pyrometer using a mirror to view probes of refractory material exposed to the hot jet. When using stagnation probes consisting of very fine carbon needles it was observed that erroneous temperature readings resulted when probes were viewed from a direction 90° to the exhaust axis. It was found that the temperatures read from this view were generally 20 percent lower than those on the probe surface facing the throat. It was therefore necessary to employ an optical fron surface mirror which permitted observation of the heated surface of the stagnation probe facing the throat (see Figure 20). In this case the measured temperature values once again agreed closely with those obtained from the stagnation probes of identical materials placed in the plenum chamber.

A number of tests were conducted using ma terials of known melting point to determine the gas temperature. This was done with probes having wire elements made of silver, aluminum, lead, etc., and placed in the flow exhaust region near the throat. The side of the wire probe facing the throat was closely observed with a telescope. Thrust data was taken when the first indications of liquid droplets were noted on the surface of the probe,

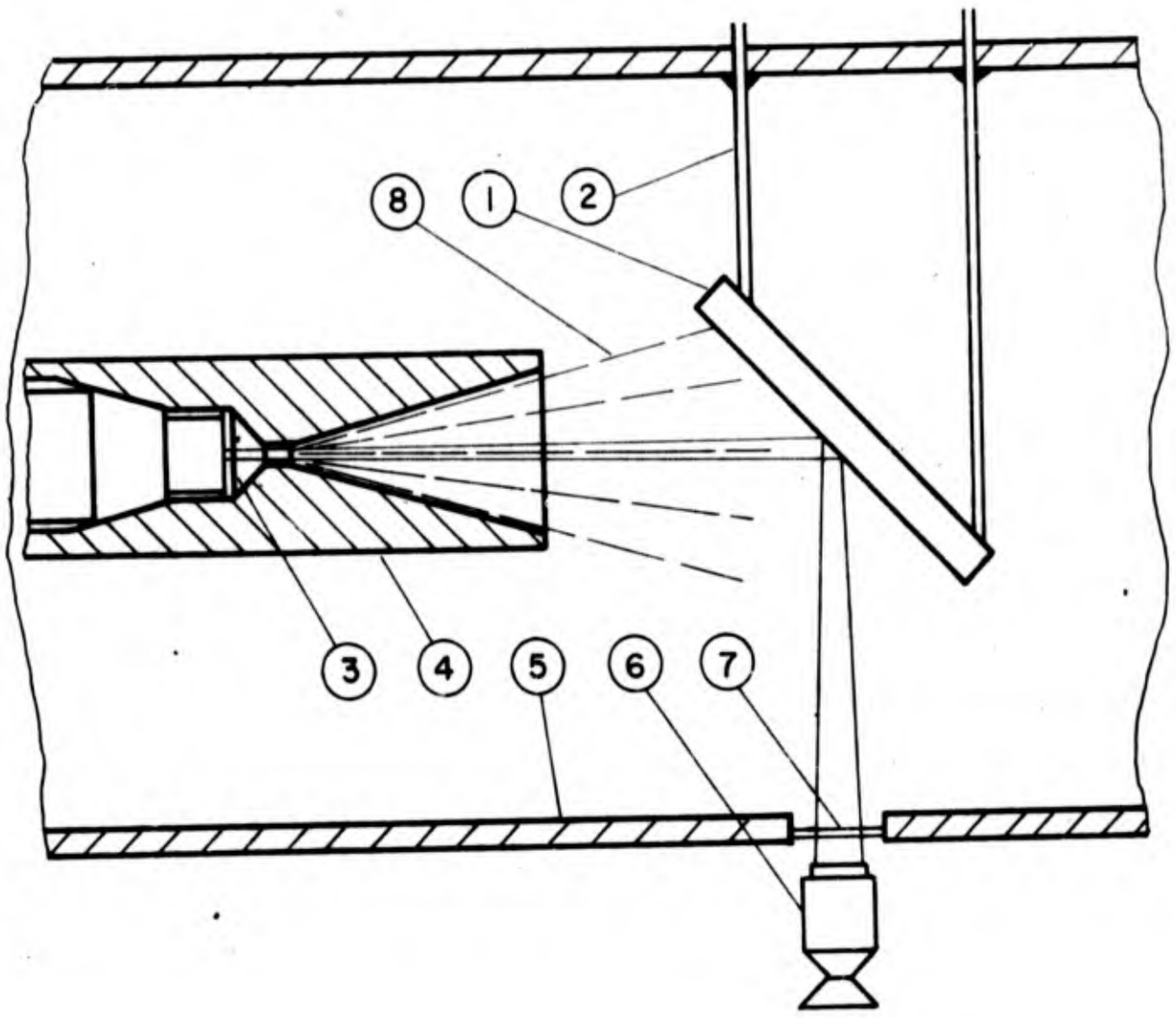

1. Water-Cooled Mirror
2. Mirror Mount
3. Stagnation Temperature Probe
4. Thermal Heater
5. Tank Wall
6. Optical Pyrometer
7. Glass Window
8. Gas Jet

Figure 19. Measurement of the Internal Temperature of Electrothermal Heaters

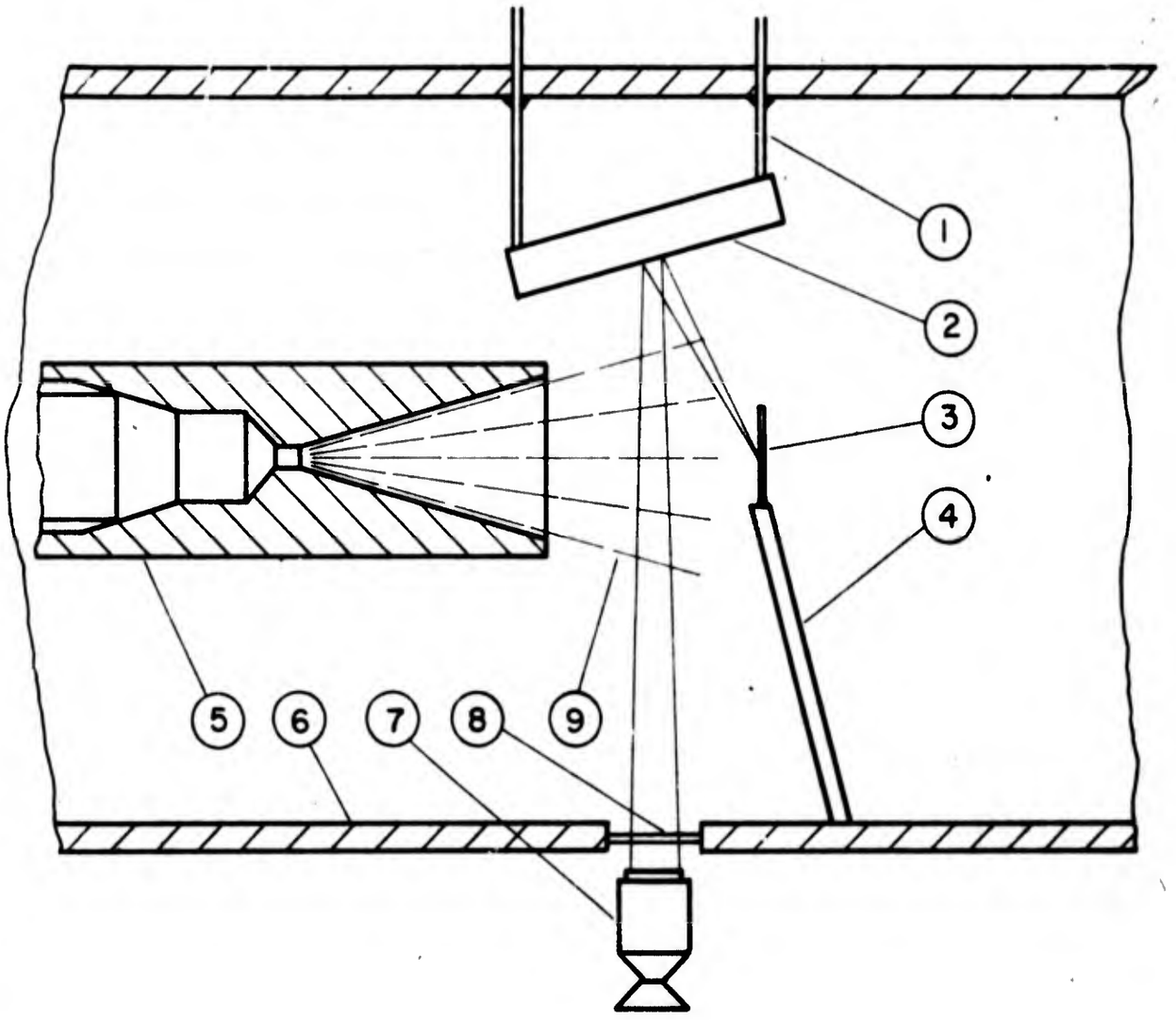

1. Mirror Support
2. Water-cooled Mirror
3. Temperature Probe
4. Probe Support
5. Thermal Heater
6. Tank Wall
7. Optical Pyrometer
8. Glass Window
9. Gas Jet

Figure 20. Measurement of the Surface Temperature of Stagnation Temperature Probes

indicating that the melting point was reached. The melting point was corrected to allow for the environmental pressure under which the test was conducted. Measured temperature values agreed closely with those obtained with the other methods discussed.

2.3.6 Measurement of Magnetic Field, Electric Field, and Optical Patterns

The determination of magnetic and electrical field patterns in the vicinity of the plume is useful because these patterns (together with the gas properties) determine the effectiveness of magnetic containment, the importance of magnetic nozzle effects, and the distribution of energy addition to the gas. Measurements of magnetic field strength obtained during this program were made with a gaussmeter without the arc in operation. Measurements of the electric field strength have not yet been attempted.

A great deal of qualitative and some quantitative information concerning gas properties in the plume can be obtained optically without the need for the tedious detailed surveys required when movable probes are used. Often magnetic and electrical field patterns can also be inferred from illumination patterns in the plume. The effectiveness of this technique can be seen by comparing photographs of the plume taken as the magnetic field strength is changed. Definite patterns appear indicating paths followed by ionized gas through the magnetic field. Methods used included black and white photographs of the plume, color photographs of the plume using different filters, and motion pictures of the plume (conventional and Fastax) taken during startup and steady operation. The photographs are useful for giving a qualitative evaluation of the influence of varying operating conditions (such as magnetic field strength) on the plume structure, while the motion pictures are used to study starting phenomena and arc oscillations during steady operation.

Two optical pyrometers have been used for measuring the temperature of exposed thrustor surfaces and refractory survey probes. Much of the work was done with a filament type pyrometer (operated manually), but a recently acquired infrared recording pyrometer is now in service and is greatly increasing the amount of temperature data obtainable.

Some spectrographic analyses have been performed of the gas in the jet region. Information of this type can be used to assist in defining the arc path by locating regions of high excitation and ionization, and to search for evidence of gas entrainment in the jet by looking for indications of ambient gas in the inner high temperature region of the plume. In the future, detailed spectrographic surveys of the plume region will be required to provide more complete information on the plume structure.

It is believed that future work should concentrate more heavily on the detailed measurement of conditions in the plume region. A study has been made of possible diagnostic type measurements that appear promising. The following suggestions have resulted.

Some improved experimental techniques are necessary for obtaining the desired information. Acquisition of such data ranges from almost trivial measurements to highly sophisticated tasks and is so indispensable to further progress in understanding the acceleration process that it would well justify a program of its own. Clearly needed is a more detailed measurement of the external magnetic field pattern which is a straightforward measurement, readily accomplished with a gaussmeter or flip coil.

The measurement of the self-magnetic field induced by the arc current pattern is also important. This requires the use of small, cooled, magnetic probes, either of the induction coil or Hall-current semi-conductor type. The former have the disadvantage of requiring a rapid rotational or vibrational motion, or of a ripple modulation of the arc; the latter tend to be highly temperature sensitive. This measurement yields not only B_θ', but by simple analysis, the arc current density distribution throughout the field.

The electric field pattern can be achieved by floating Langmuir probes, or by a double probe, and will yield both local magnitude and direction of the field. By comparing this information with the current density data, local conductivity and Hall parameters can be inferred.

The electron temperature distribution may be readily determined by high density Langmuir probe techniques, and corroborated by spectroscopic line intensity ratio methods. The primary aim here would be to establish the absolute magnitude of T_0, and the validity of the simple exponential model. The ion temperature distribution can be obtained with local calorimeter techniques that readily yield information about heavy particle temperatures. Presuming that the gas is fully ionized or that the neutral and ion temperatures are very nearly the same, this measurement defines the ion temperature.

The electron density is the essential measurement for identification of the degree of ionization as well as for establishing the available density of current carriers. In general it is difficult to perform precisely, although

several methods may be applied, depending on the absolute range of n involved. Langmuir probes are the simplest to operate but care must be taken to compensate properly for the electrical sheaths, gasdynamic boundary layer, and bow shock which form around the probe. Microwave probes do not disturb the plasma, but are sensitive only over a small range of electron densities. Spectroscopic line broadening techniques are useful only for very high electron densities. Optical interferometry will be difficult because of the cylindrical geometry and microscopic fluctuations in the flow field.

The pressure distribution can be obtained with vacuum gauges with a fast response. Relatively small dimensions are necessary to measure the pressure in various zones of the testing chamber. This measurement presents various difficulties, especially because of the small dimensions of the testing probes. Static and stagnation pressure measurements can supply important information on the circulation of the propellant in the testing area.

Measurements of the velocity and direction of the jet stream are difficult and delicate but are valuable to have as an indirect confirmation of the values of thrust obtained with other means as well as aiding in obtaining a better understanding of the acceleration process. Double probes detecting the transit of disturbances in the jet have been used, but the initial results are still unreliable. Improvements in this important measurement are necessary. The use of doppler spectrometry is also considered.

Color movies of the luminous part of the jet with the simultaneous recording of the indications of the most important instruments is a basic aid for

diagnostic studies of the dynamic behavior of the arc. Sequential photographs can also be used for the recording of single events. A continuous spectrographic record in synchronism with the photographs is also a useful diagnostic tool.

The mass flow probe is useful in the supersonic region of the jet for determining the product of density and velocity so that streamline shapes may be plotted. In large probes, this function is frequently combined with the enthalpy probe. However, in order that the flow inducted by the probe will come from a known stream tube cross section area, it is necessary to use a sharp leading edge so the shock wave will attach. This is believed to be easier to accomplish in a small size by using a separate probe.

A tracer gas having a different characteristic color when ionized can be introduced into the vacuum chamber to detect (either visually or spectroscopically) if some of the tracer gas will be entrained in the high temperature jet. If it is possible to ionize the tracer gas in a small arc heater before introducing it into the chamber, it may be possible to observe flow patterns in the vacuum chamber visually.

For many of the measurements described, it will be necessary to develop special probes which are insulated from external ground connections and are designed to eliminate, as far as practical, conducting parts and surfaces that could provide a path for electrical current flow. This would be necessary to avoid modification of the conditions in the plume which are being measured. Development of this special instrumentation will be a basic necessity of any future work.

3.0 THE EXPERIMENTAL WORK

The experimental work performed during this program was carried out in two phases. Phase 1 was concerned with the measurement of performance with resistance heated gas. The primary goal was the verification of theoretical predictions of performance and measurement techniques in an operating engine which is nearly free of dissociation and ionization. In Phase 2, arc heating was used to extend these studies to higher temperatures where dissociation and ionization become extremely important. Finally, studies were made at extremely high gas enthalpies obtained by operating an arc at low propellant mass flows and low propellant pressures. The experiments therefore cover the widest feasible range of thermal acceleration devices. Results obtained during the three phases are discussed separately below.

3.1 Tests With Resistance Heating

The effort during this phase of the work was concentrated on obtaining precise measurements of gas temperature, propellant flow rate, and thrust with resistance-heated thrustors. No direct effort was made to reduce losses unless the losses increased the difficulty of comparing experimental results with theory. For example, it was found helpful to use a short throat in place of a divergent nozzle because this reduced the thermal and viscous losses (which are difficult to predict) at the expense of an increase in the incomplete expansion loss (which is readily predictable) (see Figure 21). The resistance-heated thrustors used are described in Section 2.2.1. They

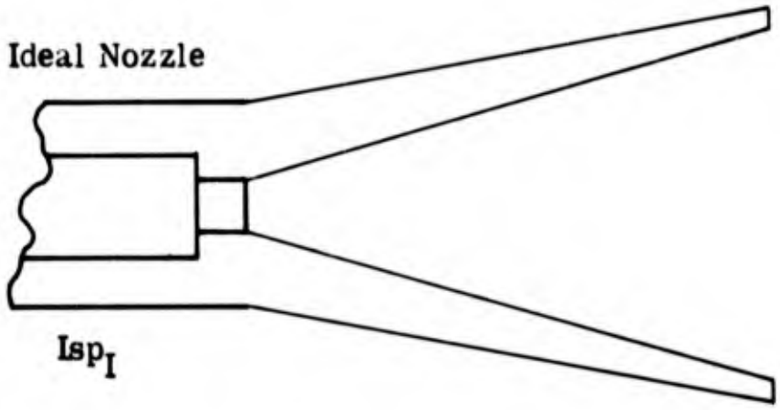

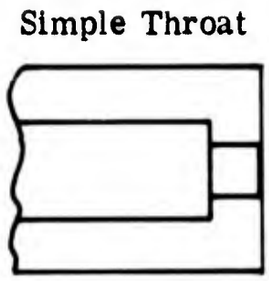

γ	1.66	1.40	1.30	1.20	1.03
$\frac{Isp}{Isp_I}$	0.80	0.70	0.65	0.54	0.23

Figure 21. Ratios of the Isp Obtained With a Simple Throat to the Isp Obtained With Ideal Fully Expanding Nozzle for Various Values of γ

are designed to permit rapid changes in geometry. The tests covered a wide range of nozzle geometries, propellants, and temperatures.

Some results obtained with hydrogen at room temperature (300°K) using a simple cylindrical throat with no divergent section are shown in Table 2 Five throat diameters (0.020, 0.040, 0.080, 0.160, and 0.320 inches) and five length to diameter ratios (0, 1, 2, 4, and 8) for each diameter were tested. The throats of zero length to diameter ratio are sharp-edged orifices. It is seen that performance is nearly independent of throat size and length.

Table 3 shows results of a similar test series at higher gas temperature (600°K). Again, no significant variations in specific impulse is evident as a result of changing the throat dimensions over a wide range. These two sets of tests indicate that the thermal and viscous losses in a simple throat are not important in this operating regime.

Having established that consistant results can be obtained using a simple throat, the remaining tests of this type concentrated on exploring the effects of operating temperature and propellant on performance, and comparing these results with theoretical predictions. Results are shown in Figures 22, 23, and 24. It is interesting to note that (for most propellants) experimental results agree very closely with theory. This indicates that the incomplete expansion loss is the only important loss associated with operations using a short orifice for a nozzle. A notable exception to this good agreement is the test series conducted with ammonia which depart from

TABLE 2

EFFECT OF CHANGING THROAT LENGTH AND DIAMETER AT 300°K

Throat Diam. inches	Throat Length inches	Gas	Mass Flow gm/sec	Chamber Pressure psia	Gas Temp. °K	Thrust grams	Isp sec	Tank Pressure mmHg
0.020	0.000	H_2	0.100	135.0	300	19.6	196	0.80
0.040	0.000	H_2	0.100	34.0	300	19.9	199	0.80
0.080	0.000	H_2	0.100	9.0	300	20.0	200	0.80
0.160	0.000	H_2	0.100	3.0	300	19.9	199	0.80
0.320	0.000	H_2	0.100	0.5	300	19.3	193	0.80
0.020	0.020	H_2	0.100	132.0	300	19.9	199	0.80
0.020	0.040	H_2	0.100	124.0	300	19.8	198	0.80
0.020	0.080	H_2	0.100	120.0	300	20.1	201	0.80
0.020	0.160	H_2	0.100	130.0	300	19.9	199	0.80
0.040	0.040	H_2	0.100	29.0	300	19.8	198	0.80
0.040	0.080	H_2	0.100	26.0	300	19.9	199	0.80
0.040	0.160	H_2	0.100	30.0	300	19.9	199	0.80
0.040	0.320	H_2	0.100	30.0	300	19.9	199	0.80
0.080	0.080	H_2	0.100	9.0	300	20.1	201	0.80
0.080	0.160	H_2	0.100	9.0	300	20.1	201	0.80
0.080	0.320	H_2	0.100	9.0	300	20.1	201	0.80
0.080	0.640	H_2	0.100	9.0	300	20.1	201	0.80
0.160	0.160	H_2	0.100	2.0	300	20.1	201	0.80
0.160	0.320	H_2	0.100	2.0	300	20.0	200	0.80
0.160	0.640	H_2	0.100	2.5	300	19.9	199	0.80
0.160	1.280	H_2	0.100	2.5	300	19.9	199	0.80
0.320	0.320	H_2	0.100	0.5	300	19.6	196	0.80
0.320	0.640	H_2	0.100	0.5	300	19.6	196	0.80
0.320	1.280	H_2	0.100	0.6	300	19.5	195	0.80
0.320	2.560	H_2	0.100	0.7	300	19.6	196	0.80

TABLE 3

EFFECT OF CHANGING THROAT LENGTH AND DIAMETER AT 600°K

Throat Diam. inches	Throat Length inches	Gas	Mass Flow gm/sec	Chamber Pressure psia	Gas Temp. °K	Thrust grams	Isp sec	Tank Pressure mmHg
0.040	0.000	H_2	0.100	46.0	600	27.8	278	0.80
0.080	0.000	H_2	0.100	12.0	600	27.8	278	0.80
0.160	0.000	H_2	0.100	3.0	600	27.9	279	0.80
0.320	0.000	H_2	0.100	1.0	600	26.7	267	0.80
0.040	0.040	H_2	0.100	42.0	600	27.9	279	0.80
0.040	0.080	H_2	0.100	37.0	600	27.9	279	0.80
0.040	0.320	H_2	0.100	43.0	600	27.9	279	0.80
0.080	0.080	H_2	0.100	12.0	600	27.9	279	0.80
0.080	0.640	H_2	0.100	12.0	600	27.9	279	0.80
0.160	0.160	H_2	0.100	3.0	600	27.7	277	0.80
0.160	1.280	H_2	0.100	3.0	600	27.6	276	0.80
0.320	0.320	H_2	0.100	1.0	600	26.5	265	0.80
0.320	2.560	H_2	0.100	1.0	600	26.5	265	0.80

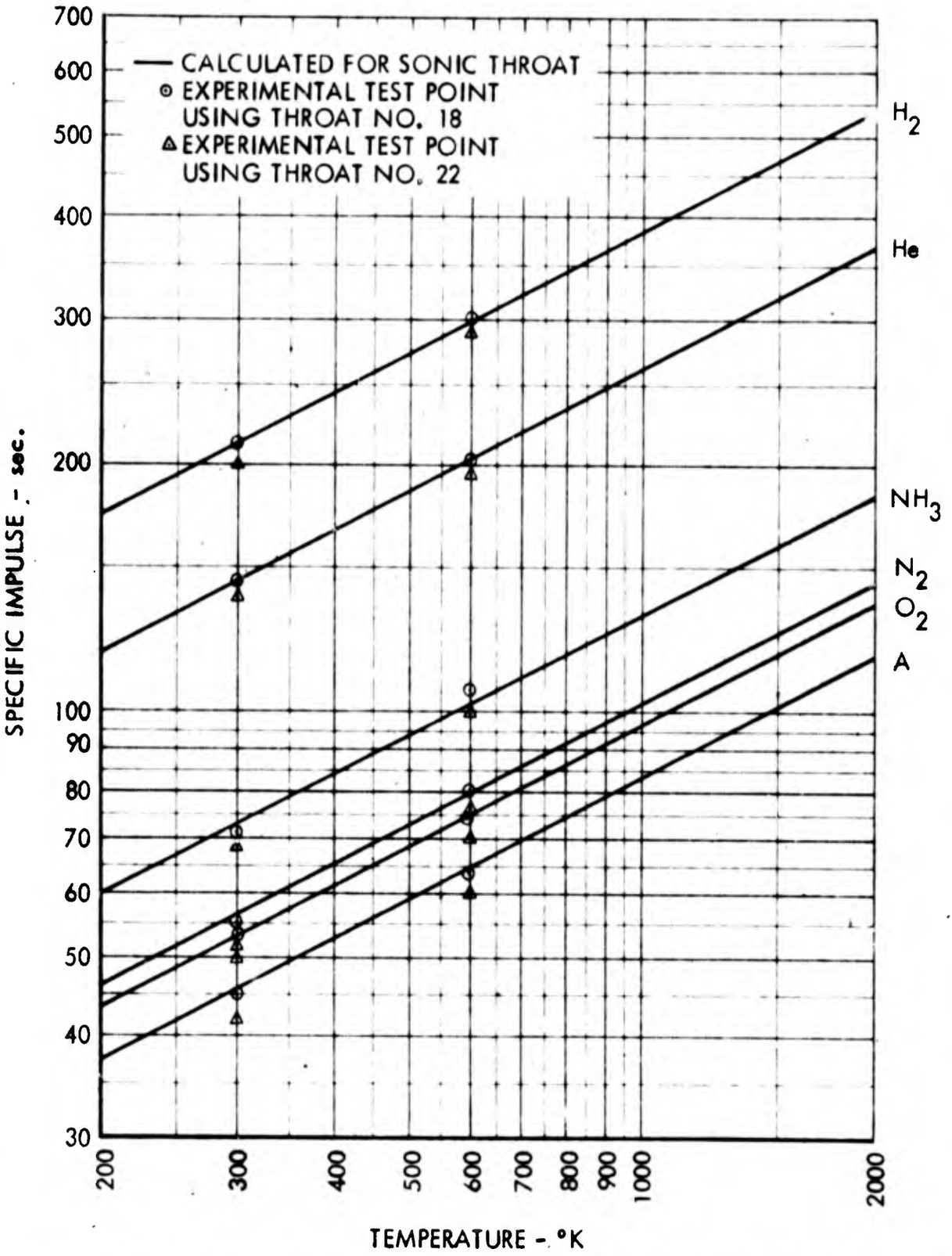

Figure 22. Experimental and Theoretical Performance for Various Propellants at 300°K and 600°K (Resistance Heating)

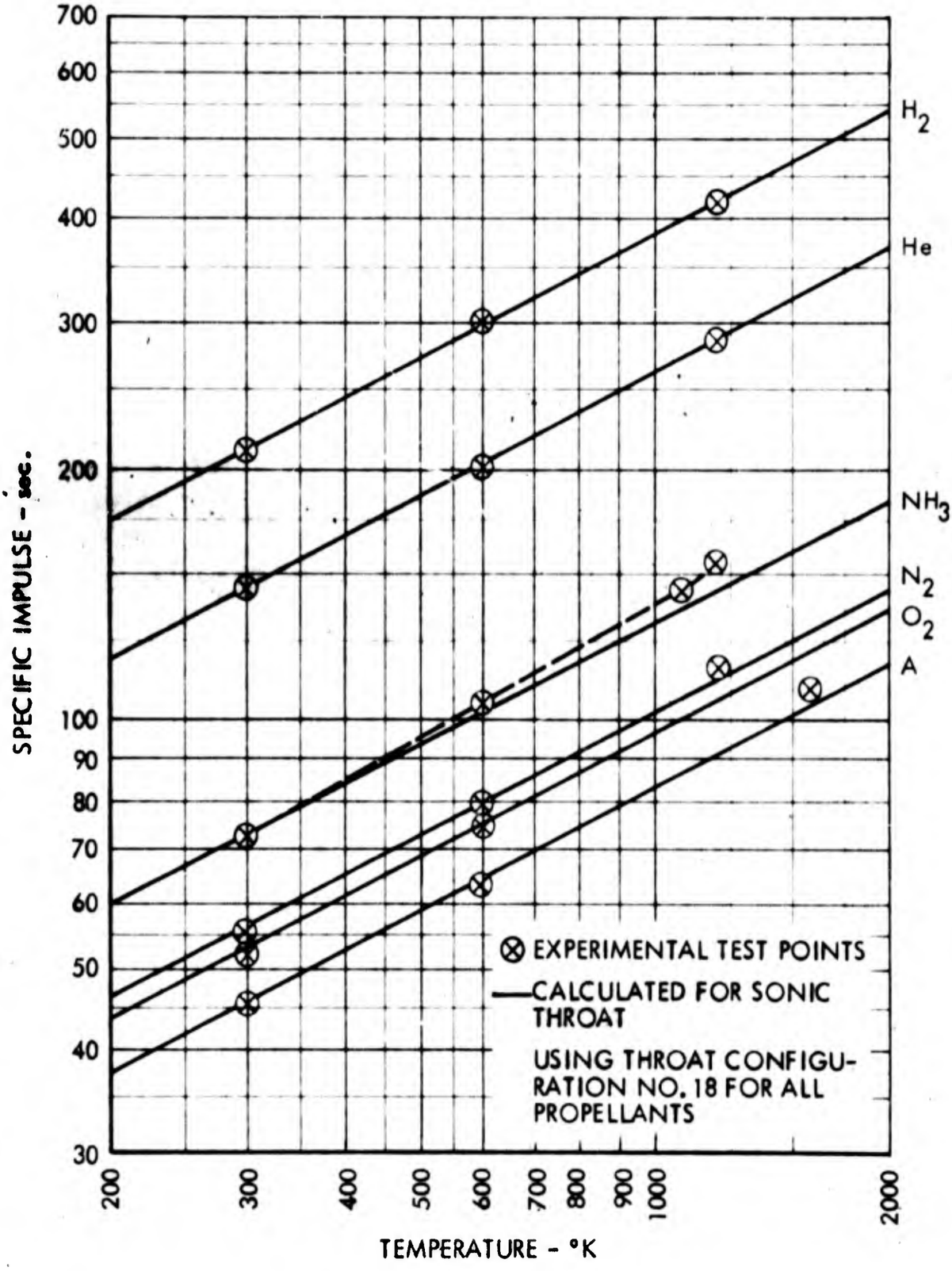

Figure 23. Experimental and Theoretical Performance for Various Propellants 300, 600, and 1200°K (Resistance Heating)

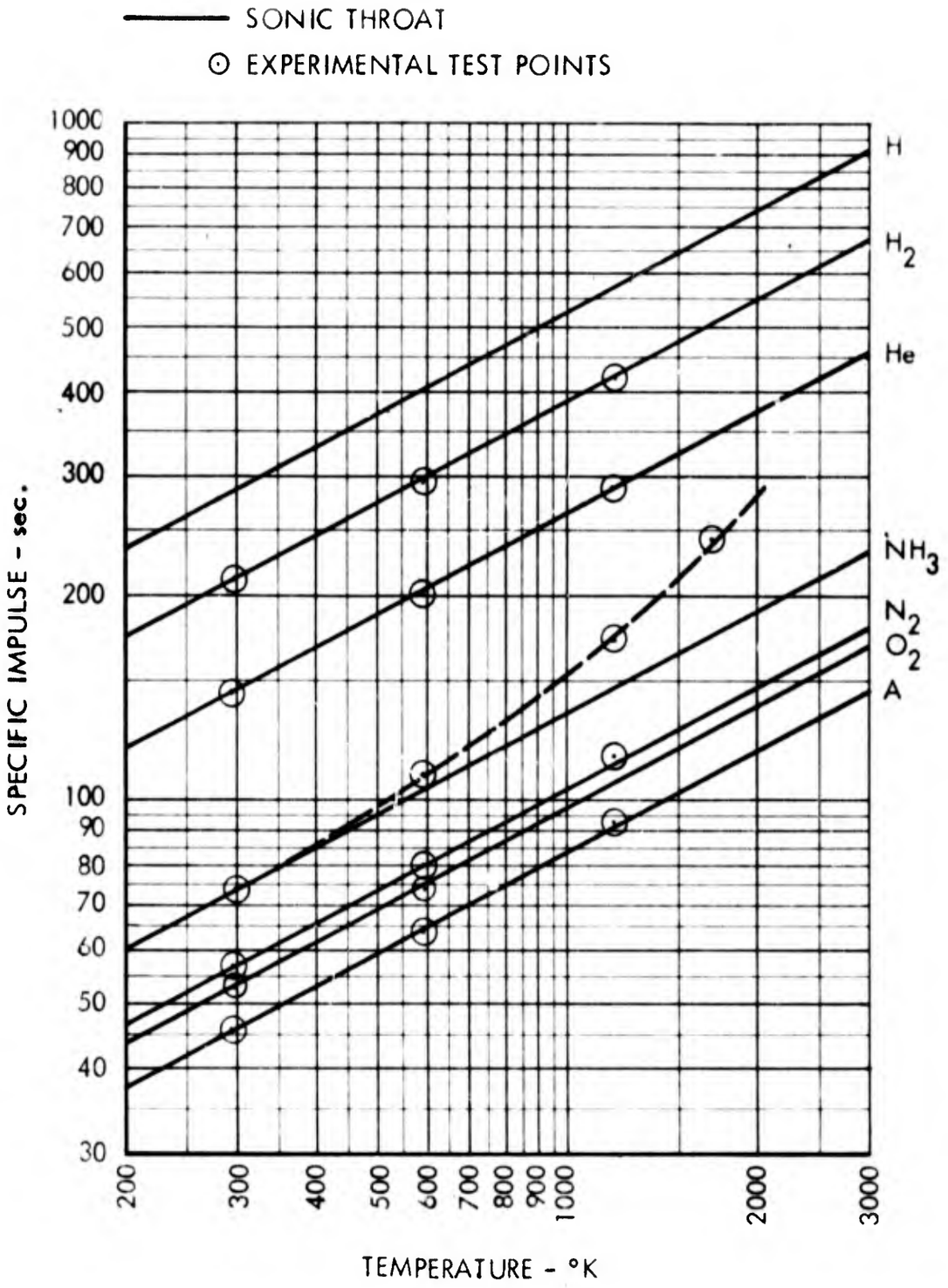

Figure 24. Experimental and Theoretical Performance for Various Propellants to 1800°K (Resistance Heating)

predictions by increasing amounts at higher temperatures (see Figure 25 A discussion of this result is given in Section 4.0. Tests at moderate temperature using a simple throat were found to serve three purposes;

1. A check is provided for the validity of the performance measurements.

2. A check is provided for the applicability of the theory used to predict performance in the moderate temperature regime, and

3. A sensitive means is provided for detecting departures from predicted performance (as for example might be caused by the beginning of dissociation effects). Such a case is evident in the results obtained with ammonia.

Further studies along these lines with increased accuracies and extension of the field covered are recommended.

In addition to the tests run using a simple throat for a nozzle, a number of tests were conducted using divergent nozzles (see Figure 1). The results obtained at the temperatures of 300° and 600°K are tabulated in Tables 4 and 5 and are shown in Figures 26 through 32. It is apparent that a residual loss of about 10 percent is very difficult to eliminate even though a correction for the imperfection of the vacuum is introduced. As expected, the monatomic gases give better efficiencies with divergent nozzles than diatomic gas. This is presumably because the nozzle area ratio required for

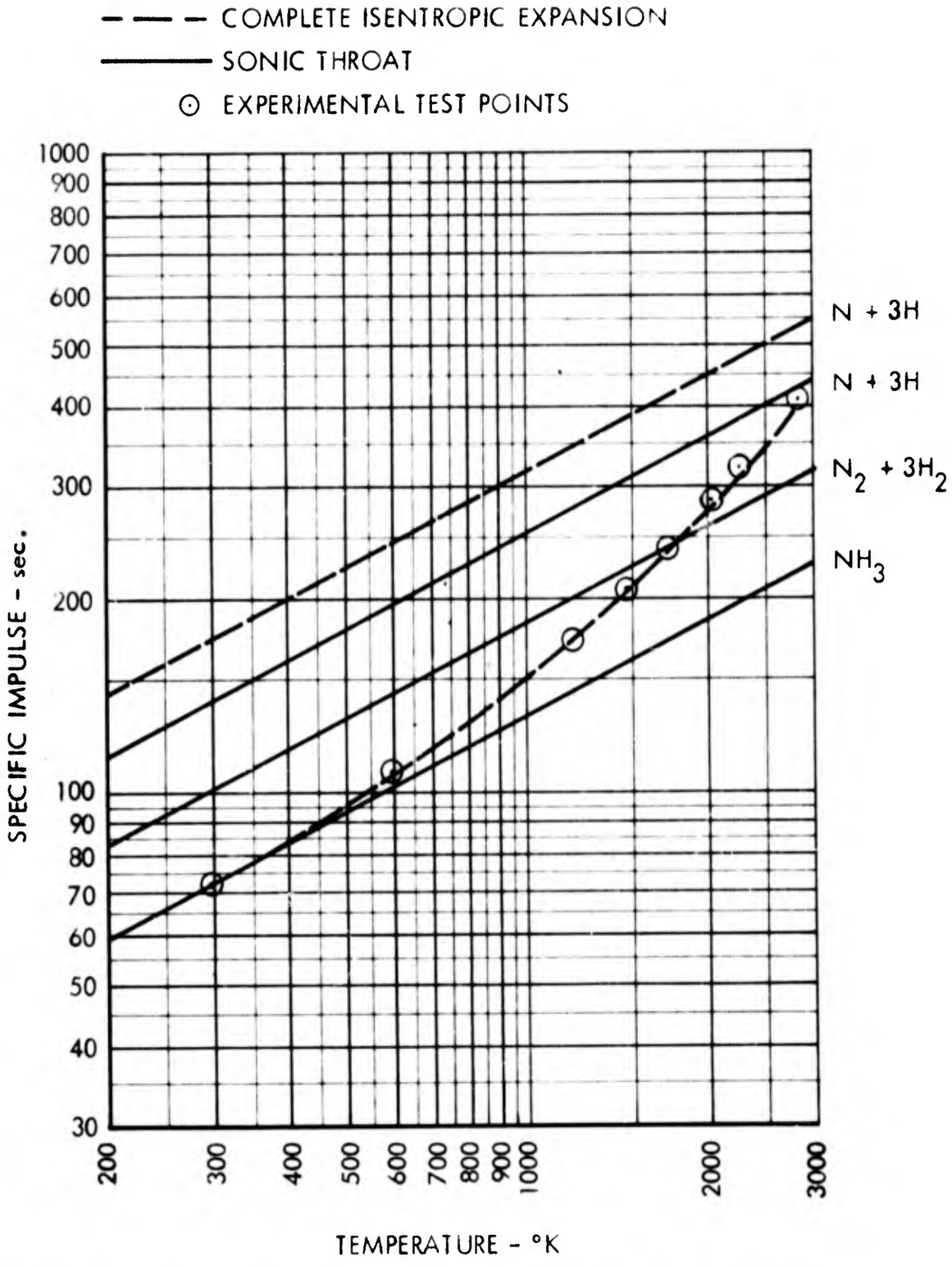

Figure 25. Experimental Test Points for Ammonia Compared to Calculated Values for Different Molecular Conditions

TABLE 4

TESTS AT 300°K WITH DIFFERENT NOZZLES AND DIFFERENT PROPELLANTS

Nozzle No.	Gas	Mass Flow gm/sec	Chamber Pressure psia	Gas Temp. °K	Thrust grams	Isp sec	Tank Pressure mmHg
1	H_2	1.000	79	300	229	229	8.0
1	He	1.000	54	300	149	149	4.5
1	NH_3	1.000	28	300	100	100	1.2
1	N_2	1.000	22	300	66	66	1.2
1	O_2	1.000	21	300	63	63	1.2
1	A	1.000	18	300	48	48	1.0
2	H_2	1.000	81	300	244	244	8.0
2	He	1.000	55	300	160	160	4.0
2	NH_3	1.000	28	300	105	105	1.0
2	N_2	1.000	22	300	69	69	1.0
2	O_2	1.000	21	300	66	66	1.0
2	A	1.000	18	300	51	51	1.0
3	H_2	1.000	82	300	244	244	8.0
3	He	1.000	55	300	160	160	4.0
3	NH_3	1.000	28	300	106	106	1.0
3	N_2	1.000	22	300	69	69	1.0
3	O_2	1.000	21	300	66	66	1.0
3	A	1.000	18	300	53	53	1.0
4	H_2	1.000	77	300	245	245	8.0
4	He	1.000	52	300	160	160	4.0
4	NH_3	1.000	27	300	103	103	1.0
4	N_2	1.000	21	300	70	70	1.0
4	O_2	1.000	20	300	66	66	1.0
4	A	1.000	17	300	52	52	1.0

TABLE 5

TESTS AT 300 AND 600°K WITH DIFFERENT NOZZLES AND DIFFERENT PROPELLANTS AND MIXTURES OF PROPELLANTS

Nozzle No.	Gas	Mass Flow gm/sec	Chamber Pressure psia	Gas Temp. °K	Thrust grams	Isp sec	Tank Pressure mmHg
3	$H_2$75$N_2$25	1.000	69	300	215	215	2.5
3	$H_2$25$N_2$75	1.000	45	300	136	136	1.5
3	$H_2$75A25	1.000	69	300	213	213	2.5
3	$H_2$25A75	1.000	43	300	131	131	1.5
2	H_2	1.000	117	600	360	360	4.0
2	He	1.000	78	600	227	227	3.0
2	NH_3	1.000	42	600	145	145	0.8
2	N_2	1.000	31	600	100	100	0.8
2	O_2	1.000	30	600	93	93	0.8
2	A	1.000	24	600	73	73	0.8
3	H_2	1.000	116	600	357	357	8.0
3	He	1.000	80	600	224	224	4.0
3	NH_3	1.000	44	600	139	139	1.0
3	N_2	1.000	30	600	95	95	1.0
3	O_2	1.000	29	600	89	89	1.0
3	A	1.000	25	600	70	70	1.0
3	$H_2$75$N_2$25	1.000	102	600	306	306	5.2
3	$H_2$25$N_2$75	1.000	65	600	200	200	2.0
3	$H_2$75A25	1.000	102	600	306	306	5.2
3	$H_2$25A75	1.000	64	600	194	194	2.2
2	$H_2$75$N_2$25	1.000	102	600	306	306	5.4
2	$H_2$25$N_2$75	1.000	65	600	200	200	5.4
2	$H_2$75A25	1.000	103	600	304	304	2.2
2	$H_2$25A75	1.000	62	600	192	192	2.2

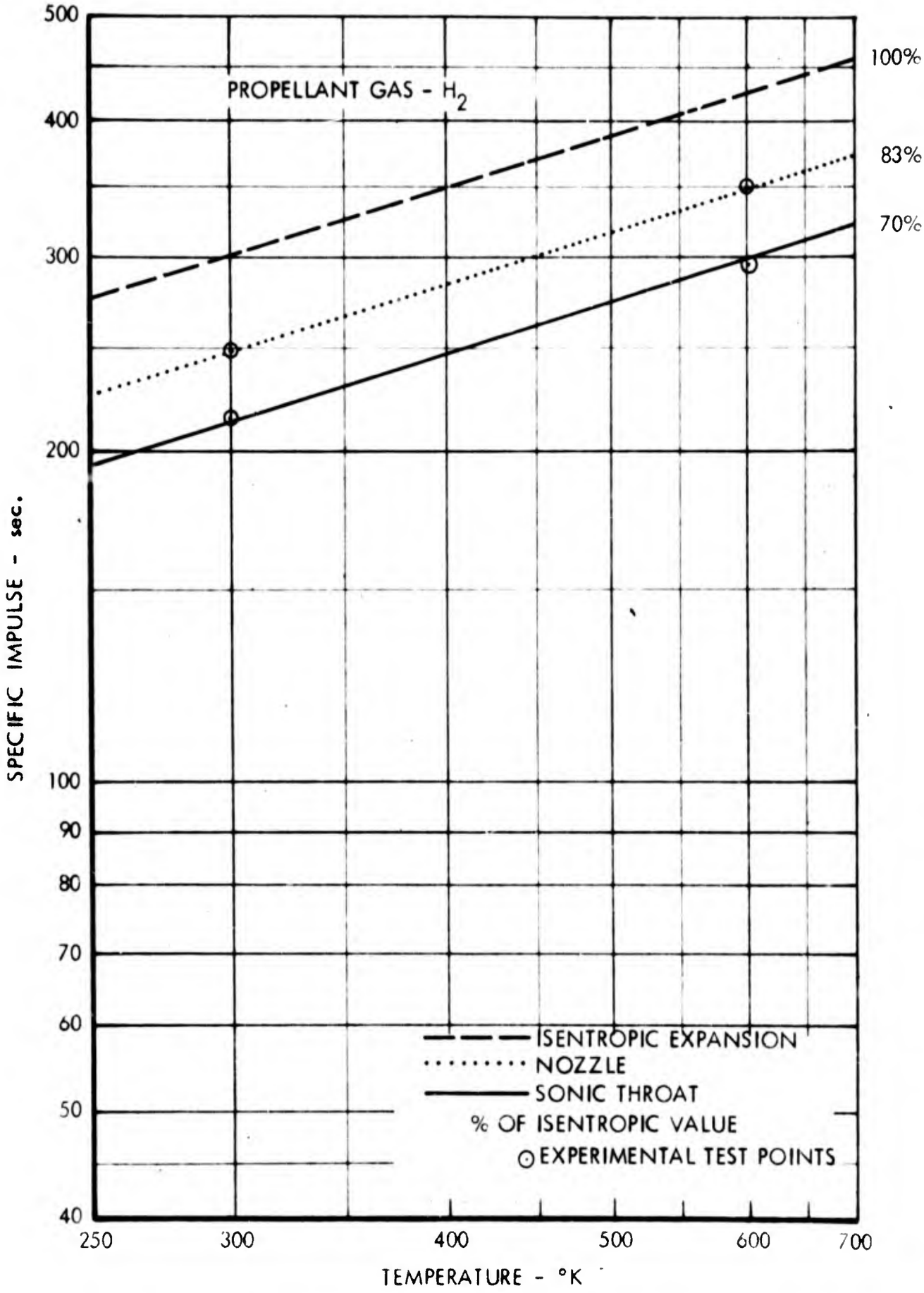

Figure 26. Experimental Results With Simple Throat and With Nozzle at 300°K and 600°K for Hydrogen

3193

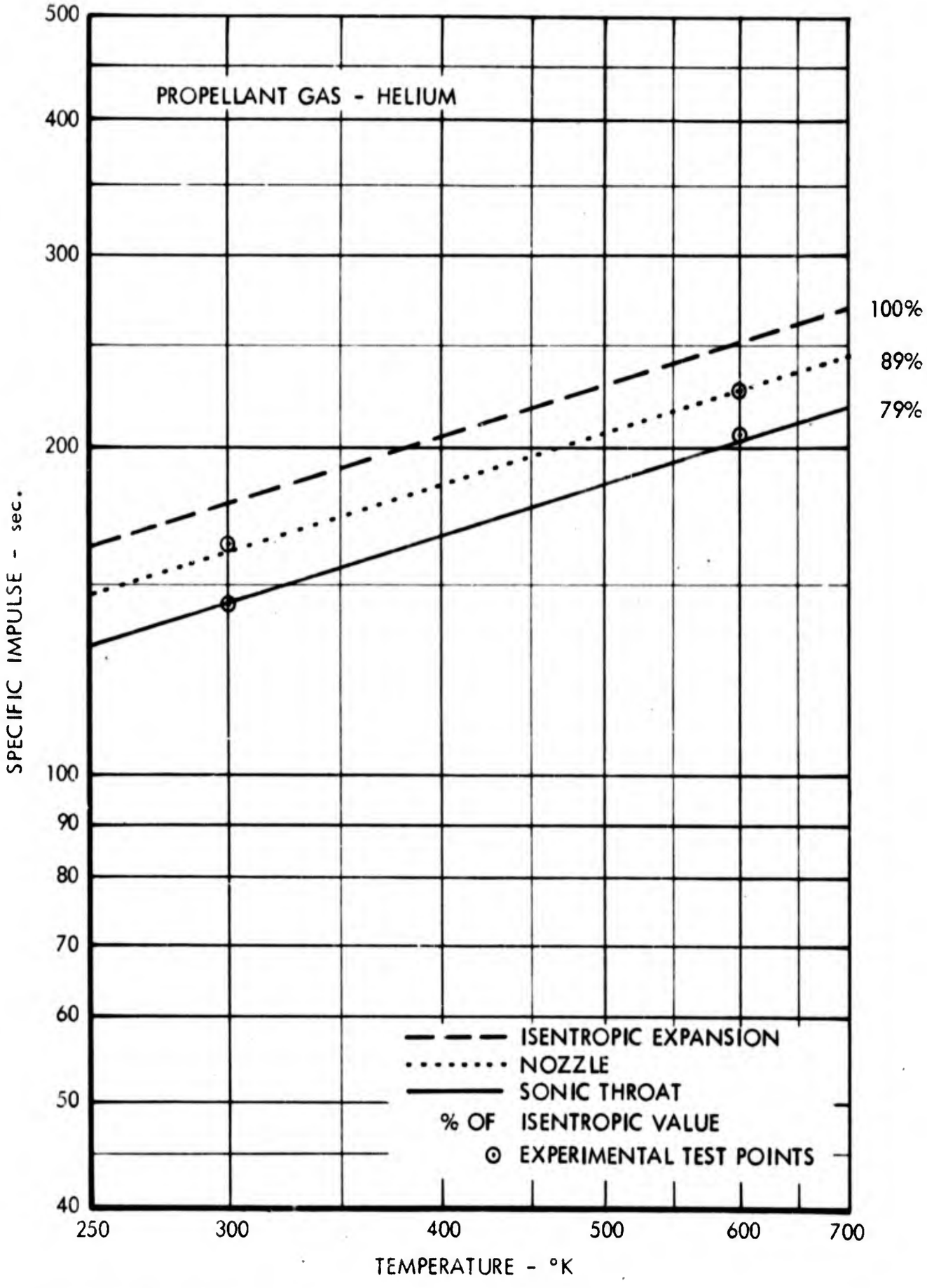

Figure 27. Experimental Results With Simple Throat and With Nozzle at 300°K and 600°K for Helium

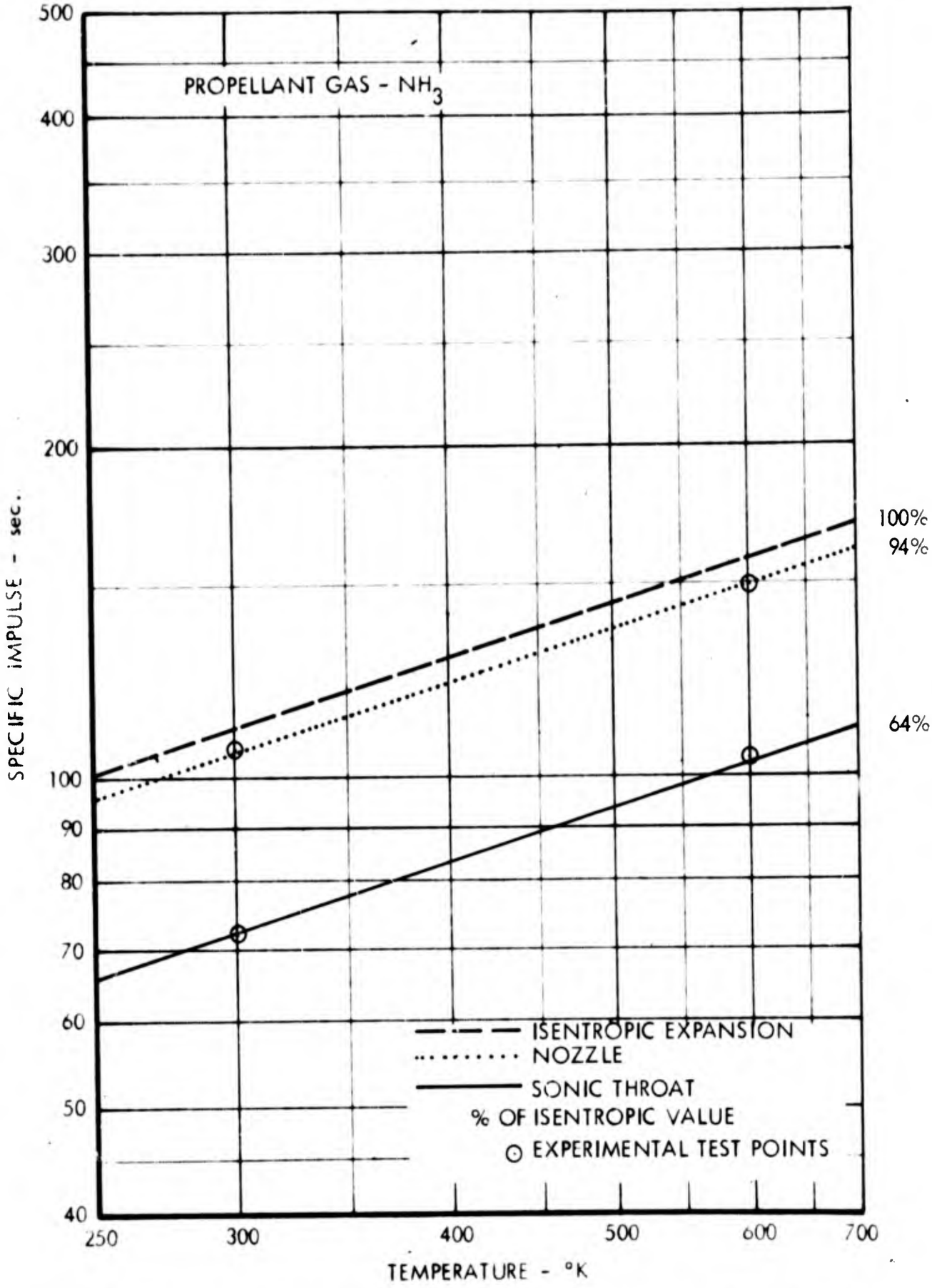

Figure 28. Experimental Results With Simple Throat and With Nozzle at 300°K and 600°K for Ammonia

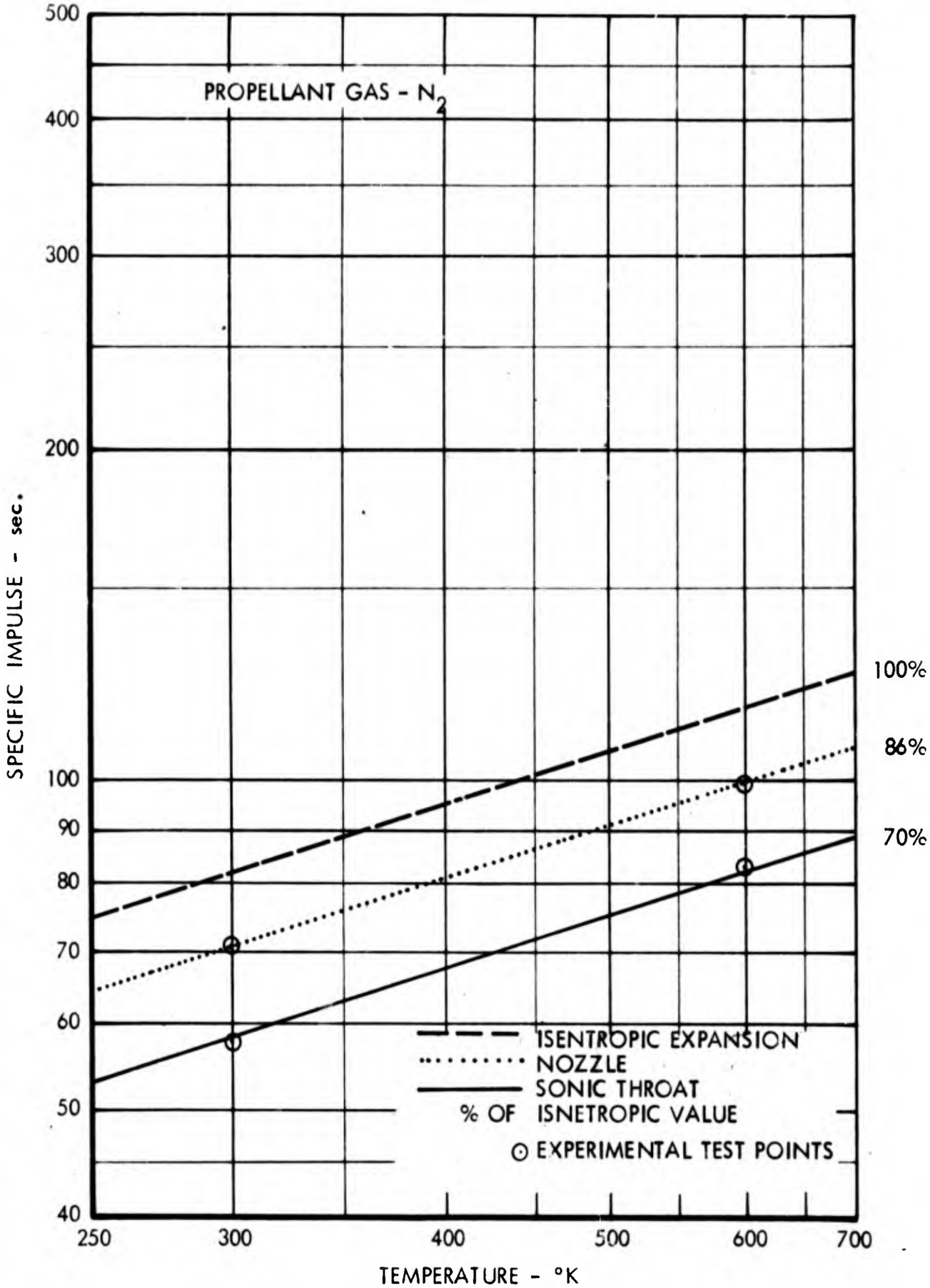

Figure 29. Experimental Results With Simple Throat and With Nozzle at 300°K and 600°K for Nitrogen

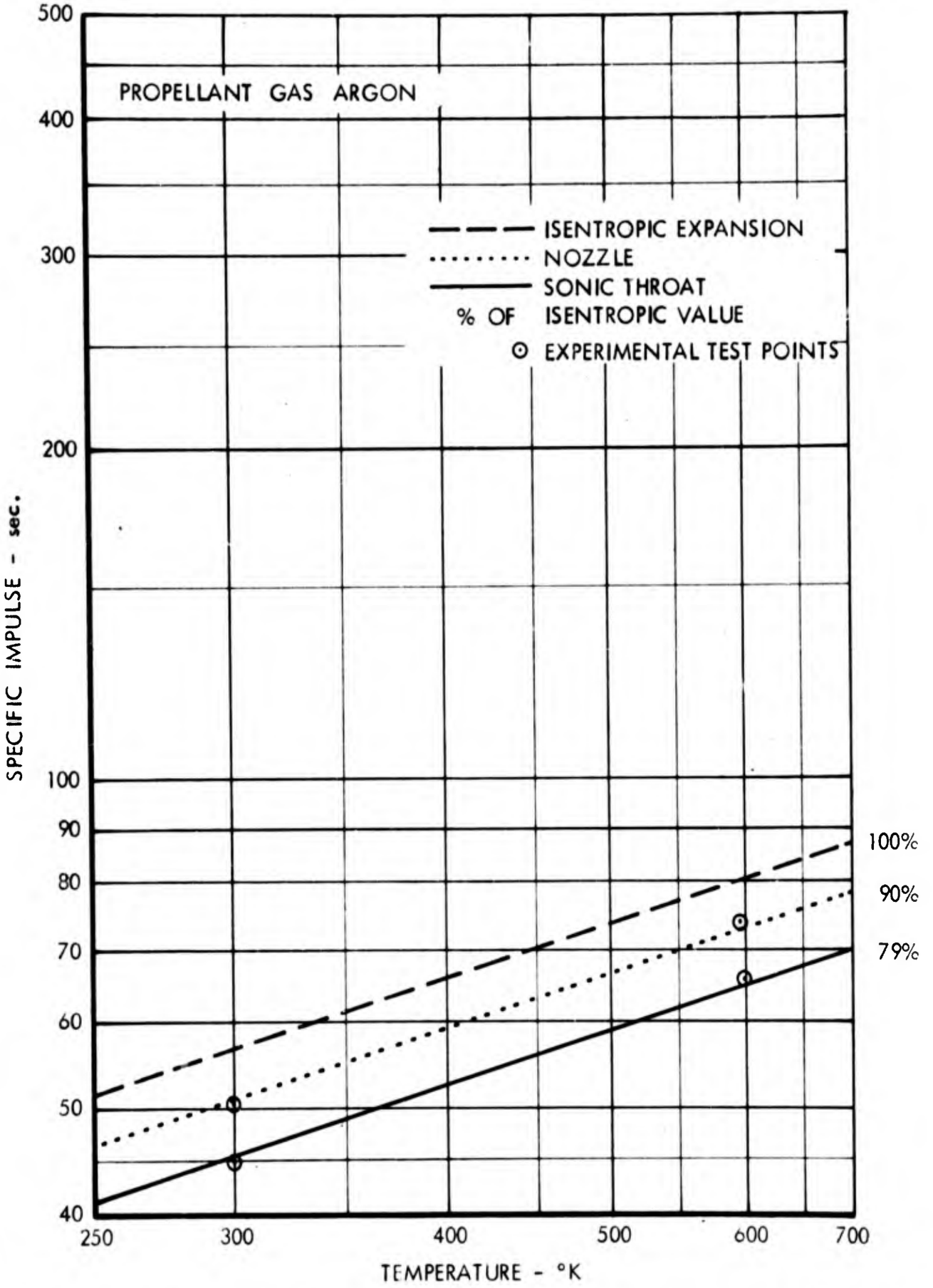

Figure 30. Experimental Results With Simple Throat and With Nozzle at 300°K and 600°K for Helium

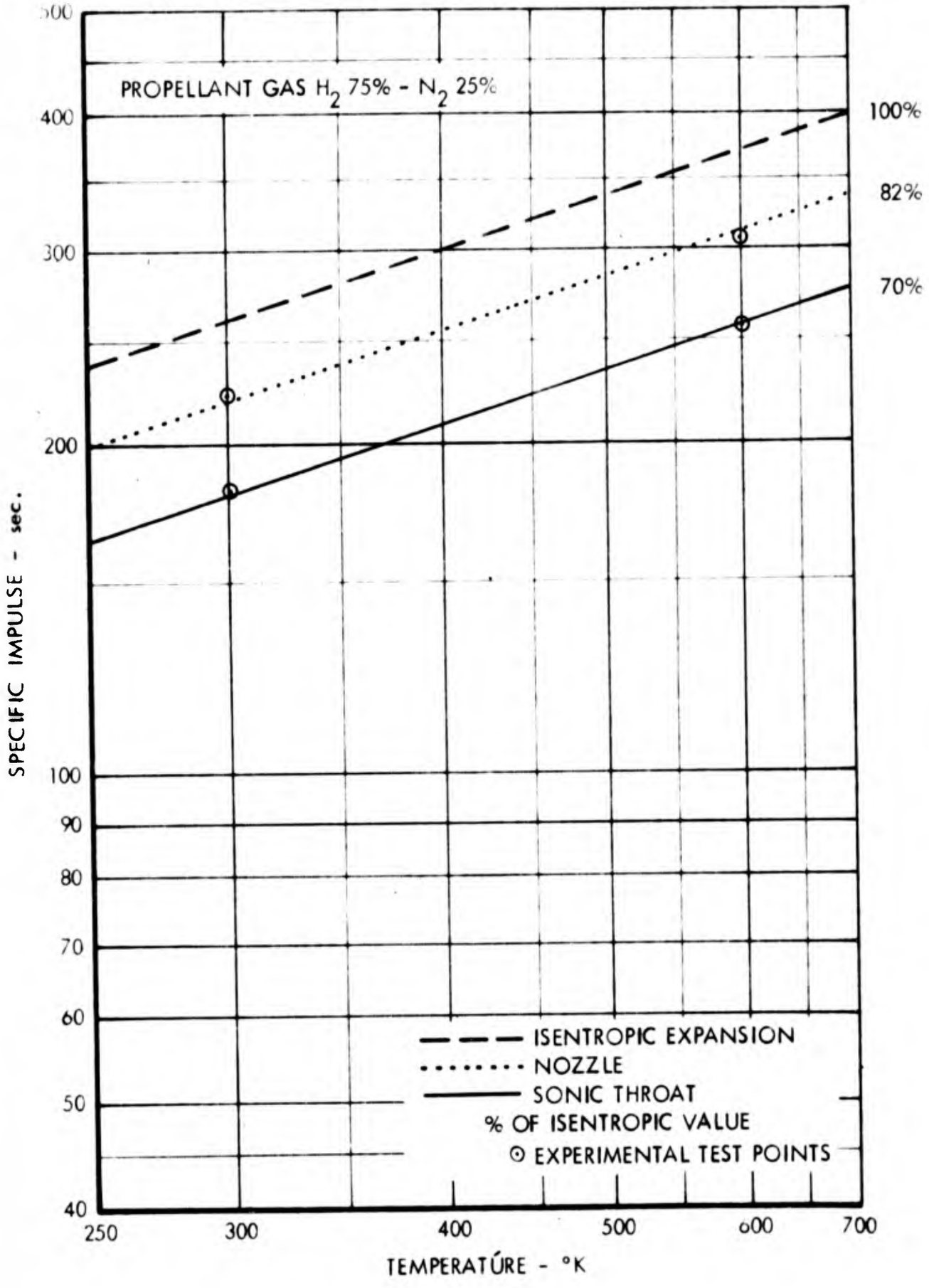

Figure 31. Experimental Results With Simple Throat and With Nozzle Using a Mixture of H_2 and N_2

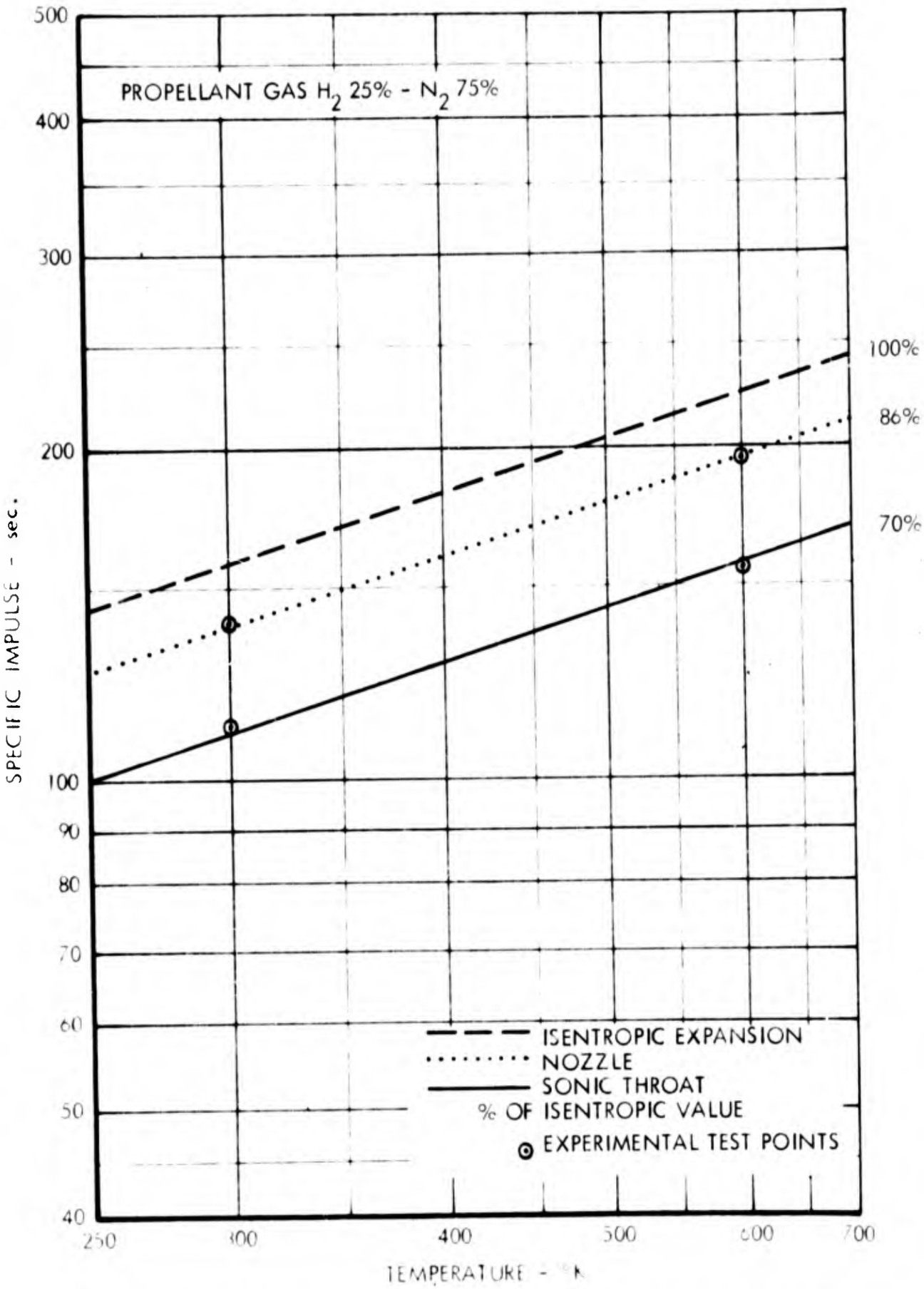

Figure 32. Experimental Results With Simple Throat and With Nozzle Using a Mixture of N_2 and H_2

full expansion is less when there are fewer degrees of freedom, and consequently the thermal and viscous losses are lower. However, there is also less to be gained by using a divergent nozzle with monatomic gas because the simple throat efficiency is already relatively high. The behavior of ammonia with the simple throat or with the nozzle has not been fully explained and should be studied further. An annular nozzle was also tested during this study, and performance is compared with results obtained with conventional nozzles and simple throats in Table 6 . The annular nozzle was found to have a slightly lower efficiency than the conventional nozzle for nearly all of the propellants used in the tests.. The test techniques used appear to offer a sensitive method for comparing the efficiency obtainable with various nozzle geometries. Further studies of this type could be valuable for developing improved nozzle configurations for practical thrustor designs.

TABLE 6

EXPERIMENTAL COMPARISON AT 300°K OF VARIOUS GEOMETRIES VERSUS THEORETICAL VALUES

Propellant	Cylindrical Throat		Nozzle		Annular Nozzle		Theoretical Value
	Isp	%	Isp	%	Isp	%	
H_2	210	70	244	81	244	81	300
He	146	81	160	88	152	84	180
NH_3	71	64	100	91	95	86	110
N_2	55	67	69	84	66	81	81
O_2	53	70	66	88	61	81	75
A	45	79	51	89	48	84	57

3.2 Tests With Arc Heating

From the preceding section it can be seen that operation with resistance heating is limited in practice to temperatures of about 3000°K. It should be possible, by using interchangeable heaters and very short operating times to extend the maximum operating temperature a few hundred degrees. A more substantial extension (to about 5000°K) can be obtained in principle by using molten refractory metals for the heating elements as described in Section 2.2.3. Effort on the development of this type of thrustor was initiated during the present program. Although tentative, results appear to be promising enough to warrant a substantial development effort in the future. In any event, there is a definite limit in temperature above which it is necessary to use arc heating. In the transition region near the limiting temperature, arc heating does not look particularly attractive. This is because the power required to maintain enough ionization of the gas for the operation of an arc is a substantial fraction of the total and cannot be recovered in the nozzle. However, as the operating temperature is further increased a regime is reached in which the input power increases more rapidly than the ionization and dissociation losses, and at higher temperatures arc heating begins to look attractive.

During earlier programs (see reports on Contracts AF 49(638)-54 and AF 49(638)-766) a large amount of work was done using arc heaters in the intermediate temperature range. The maximum specific impulse obtained during this period was 2100 seconds (tests run in 1960). Since a large

amount of work has already been done in this region, the largest portion of the present investigation was concentrated on the more attractive high temperature regime.

3.2.1 Measurements at Moderate Temperatures

A small number of tests were conducted to illustrate the performance obtainable with arc jets in the intermediate temperature range. Tables 7 and 8 compare performance obtained with the resistance heated thrustor to that obtained with an arc heated thrustor running on ammonia. The arc tests cover a range of specific impulses just above those obtainable with resistance heated thrustors. Notice that although the electrical to gas power efficiency (η^{eg}) changes in a rather uniform manner for the two sets of data, the gas to kinetic efficiency (η^{gk}) drops abruptly when the change is made from resistance heating to arc heating. This indicates that a large fraction of the energy imported to the gas by the arc (presumably ionization and dissociation energy) is not recovered in the nozzle. The figures show a reduction in overall efficiency as the specific impulse is increased in the low temperature end of the arc range, and an increase in overall efficiency in the high specific impulse end of the range. The data shown in Table 8 therefore brackets the intermediate temperature range which is too high for resistance heater operation and too low for arc heater operation with good efficiency.

TABLE 7

EFFICIENCY OF NON-IONIZED AMMONIA

WITHOUT RECOVERY OF RADIATION LOSSES

Isp	Mass Flow	Input kw	$\eta^{eg}\%$	$\eta^{gk}\%$	Btu/lb x 1000
106	1000	0.6	95	90	0.27
139	1000	1.6	85	80	0.58
200	1000	4.0	85	55	1.40
345	1000	10.0	80	60	3.50
400	1000	20.0	54	70	4.60
425	1000	24.0	50	72	5.10

TABLE 8

EFFICIENCY OF IONIZED AMMONIA AT

VARIOUS ISP WITH ARC HEATER

Isp	Mass Flow	Input kw	$\eta^{eg}\%$	$\eta^{gk}\%$	Btu/lb x 1000
500	100	8	60	27	20
900	100	29	49	27	60
1500	50	72	30	26	185
2100	50	92	36	32	285
2320	50	100	40	34	344

3.2.2 Operation at High Temperature and High Ionization

The first indication that operation at much higher specific impulses might be feasible was obtained during an earlier program (about 1960) and is reproduced herein as Table 9. This set of data (which was run entirely on hydrogen) shows the interesting result that the gas to kinetic efficiency (η^{gk}) increases as the propellant flow rate (and the arc chamber pressure) is reduced. The effect is masked by an opposite trend in η^{eg}, unless the two efficiency components are separated. It became evident from this data that some mechanism for improving nozzle efficiency came into effect as the arc chamber pressure was reduced; and that if a means could be found to substantially reduce thermal losses to the wall (improved η^{eg}), large improvements in overall efficiency might be possible at high specific impulses by going to low arc chamber pressures.

Table 10 shows results of the first tests conducted during this program to investigate this possibility. A configuration with a short nozzle and low arc chamber pressure was used, and a range of specific impulses from 2600 to 5150 seconds was obtained. The electric to gas efficiency (η^{eg}) is seen to remain relatively high over the entire range while the gas to kinetic efficiency (η^{gk}) increases steadily with increasing specific impulse. These results (obtained in August 1963) were encouraging enough that the general approach was pursued further during the remainder of the program.

The next set of data is shown in Table 11. This test, which was also run in 1963, shows similar results to those given in Table 10, but the test was

TABLE 9

OLD DATA SHOWING EFFECT OF MASS FLOW AND PRESSURE ON EFFICIENCY
Specific Impulse Range 500 - 2000 Seconds Using Hydrogen

Isp	Mass Flow mg/sec H_2	Pressure mm Hg	Input kw	Efficiency η^{eg}%	Efficiency η^{gk}%	Btu/lb x 1000
500	200	105	15	78	21	24
515	250	112	17	78	26	24
500	400	190	42	80	14	38
1000	50	54	20	52	24	90
1000	100	86	27	73	24	85
1000	200	150	68	81	14	120
1000	250	192	117	81	13	163
1000	400	240	165	87	12	155
1500	25	62	32	40	22	200
1540	50	85	45	55	23	214
1530	100	160	80	71	19	247
1500	200	200	148	81	18	260
2000	25	65	47	42	25	336
2000	50	95	70	59	23	364
2000	100	160	127	73	20	400

TABLE 10

FIRST HIGH SPECIFIC IMPULSE RESULTS WITH WATER-COOLED ELECTROTHERMAL PLASMA GENERATOR USING HYDROGEN PROPELLANT

August 1963

Isp sec	Input kw	Gas kw	η^{eg}%	η^{gk}%	η^{ek}%	Stagnation Enthalpy Btu/lb
2600	59	37	65	21	14	634000
2800	63	42	66	22	15	720000
3080	71	51	68	22	15	875000
3440	78	54	69	26	18	925000
3720	85	59	70	28	19	1015000
4070	97	70	72	28	21	1205000
4200	103	71	70	29	20	1220000
4600	115	83	72	30	21	1425000
4870	131	84	64	33	21	1440000
5150	136	86	64	37	24	1479000

Mass Flow = 0.025 gm/sec

TABLE 11

EXPERIMENTAL TEST RESULTS OBTAINED WITH A WATER-COOLED ELECTROTHERMAL PLASMA GENERATOR USING HYDROGEN PROPELLANT

December 1963

Isp Sec	KW Input	KW Gas	Thrust Grams	$\eta^{eg}\%$	$\eta^{gk}\%$	$\eta^{ek}\%$	Stagnation Enthalpy Cal/gm
3080	71	51	77	68	22	15	486000
3440	78	54	86	69	26	18	514000
3720	85	59	93	70	28	19	564000
4070	97	70	102	72	28	21	670000
4200	103	71	105	70	29	20	678000
4600	115	83	115	72	30	21	791000
4870	131	84	122	64	33	21	800000
5150	136	86	129	63	37	24	822000
6900	178	120	172	68	46	32	1142000
7200	190	128	180	68	49	33	1217000
8000	204	140	200	69	56	38	1333000
9000	224	155	225	68	62	43	1477000
10000	260	176	250	68	67	46	1680000

Mass Flow H_2 = 0.025 gm/sec

continued to higher specific impulses. η^{gk} is seen to increase continuously over the complete range. Since η^{eg} is nearly constant over the complete range, the overall efficiency (η^{ek}) also increases over the range. The overall efficiency was found to be 46 percent at a specific impulse of 10,000 seconds. Figure 33 shows the typical appearance of the exhaust plasma at gradually increased jet power and specific impulse.

The stagnation temperature corresponding to 10,000 seconds is very high. Now, if one assumes that kinetic pressure forces are entirely responsible for the acceleration of the flow, it implies that static temperatures exist in the arc of the same order of magnitude. Since we know that temperatures on the electrode surfaces are not much over 3000°K, there must be very large temperature gradients in the arc. This raises the question of whether such high temperatures and large temperature gradients actually exist in the arc or if magnetic forces are contributing to the acceleration of the flow. The existence of such forces would permit lower static temperatures for the same stagnation temperature in the expanded flow.

In the region of the arc, where the flow is heated and accelerated, the gas is a good electrical conductor. Thus, magnetic forces could be significant in the acceleration of the flow if the magnetic pressure is comparable to the gas kinetic pressure. The highest specific impulses have been obtained at currents of over 3000 amps with the chamber pressure under 0.10 atm. The self-magnetic field corresponding to 3000 amps and to the estimated arc diameter gives a magnetic pressure $B^2/2\mu_0$ comparable to 0.10 atm. It should be noted that the presence of large magnetic forces do not necessarily imply that these forces are effective in accelerating the flow.

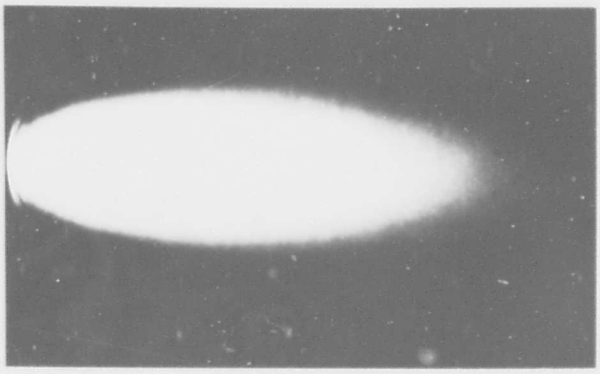

Isp = 3000 Sec - 50 KW

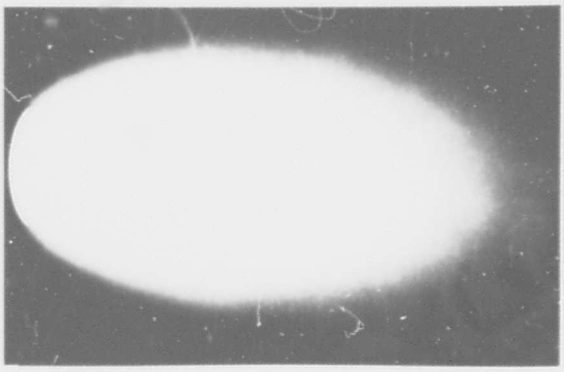

Isp = 4000 Sec - 70 KW

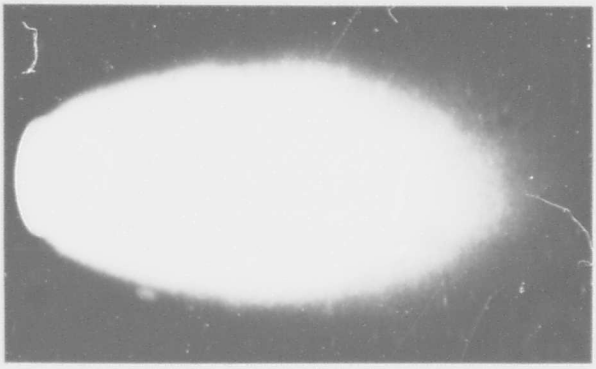

Isp = 5000 Sec - 90 KW

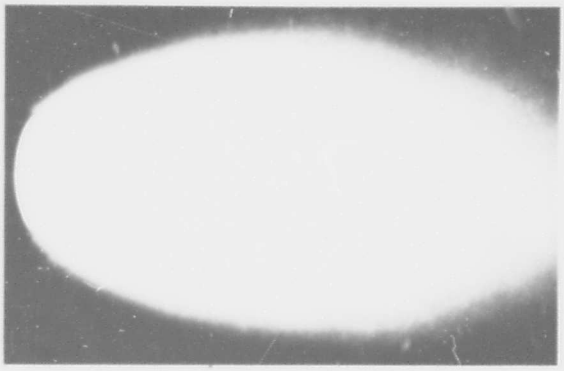

Isp = 6000 Sec - 110 KW

Isp = 7000 Sec - 127 KW

Isp = 8000 Sec - 142 KW

Figure 33. Hydrogen Jet Exhaust at Different Specific Impulses and Power Levels

Magnetic forces may be important in determining the structure of the arc as in the confinement of a current filament by its self-magnetic field. The steady-state solution of the macroscopic equations of a self-pinched, fully ionized, infinite cylindrical plasma shows that

$$2 N k T = I^2 \qquad (1)$$

where N is the number density of electrons and ions per unit length along the axis of the plasma cylinder, T is the mean temperature of electrons and ions, I is the total current, and k is Boltzmann's constant.* To obtain the result (1), it is assumed that the temperature in the plasma is constant and that the plasma is confined within a finite cross section. Dividing (1) by the cross sectional area A gives

$$2 p = I^2/A \qquad (2)$$

where $p = N k T/A$ can be interpreted as an average pressure of the plasma.**From (2) we see that, if the current is kept constant, a decrease in the average kinetic pressure in a self-pinched plasma results in an increased area. Rough observations on the arc have shown that its diameter increases as the arc chamber pressure is reduced. This qualitative agreement of the dependence of arc diameter on pressure does not imply that magnetic forces determine the arc diameter, since the diameter of the positive column of an arc discharge also increases as pressure is decreased when magnetic forces are not dominant.

---

*We are using cgs electromagnetic units.

**L. Spitzer, "Physics of Fully Ionized Gases," (Interscience Publishers, New York, 1962), 2nd ed., p. 109.

Tests have been conducted on the variation of the arc chamber pressure at constant mass flow in dependence of the value of the arc current. The pressure has been measured before the throat as illustrated in Figure 34. Increasing the arc current starting from 500 amperes the pressure in the arc chamber increases linearly until a current of about 1800 amperes is reached. At this point, an increase in the arc current results in a decrease in the arc chamber pressure. At very high currents a decrease of over 20 percent has been measured. This particular behavior can be explained with the well-known self-pinching effect of the arc current near the tip of the cathode. To further analyze this phenomena, a special cathode was constructed with a very small orifice at the center of the tip to have the possibility of measuring the pressure at that point at the same time the arc chamber pressure was measured. The results are illustrated in Figure 35 and are self-explanatory. The pressure of the arc chamber is P_1 while the pressure at the cathode tip is P_2. Increasing the arc current, both P_1 and P_2 increase until a value of about 1800 to 2000 amperes is reached. At this point P_1 begins to decrease while P_2 continues to increase. The ratio P_2/P_1 is also shown.

It is evident that a diagnostic method based on a pressure survey with the use of microprobes located all around the arc (and not only in the electrodes but in points spatially distributed in the arc chamber, throat and outside jet) can give important suggestions for the tentative explanation of the various accelerating mechanisms. This is one of the scopes of our future work.

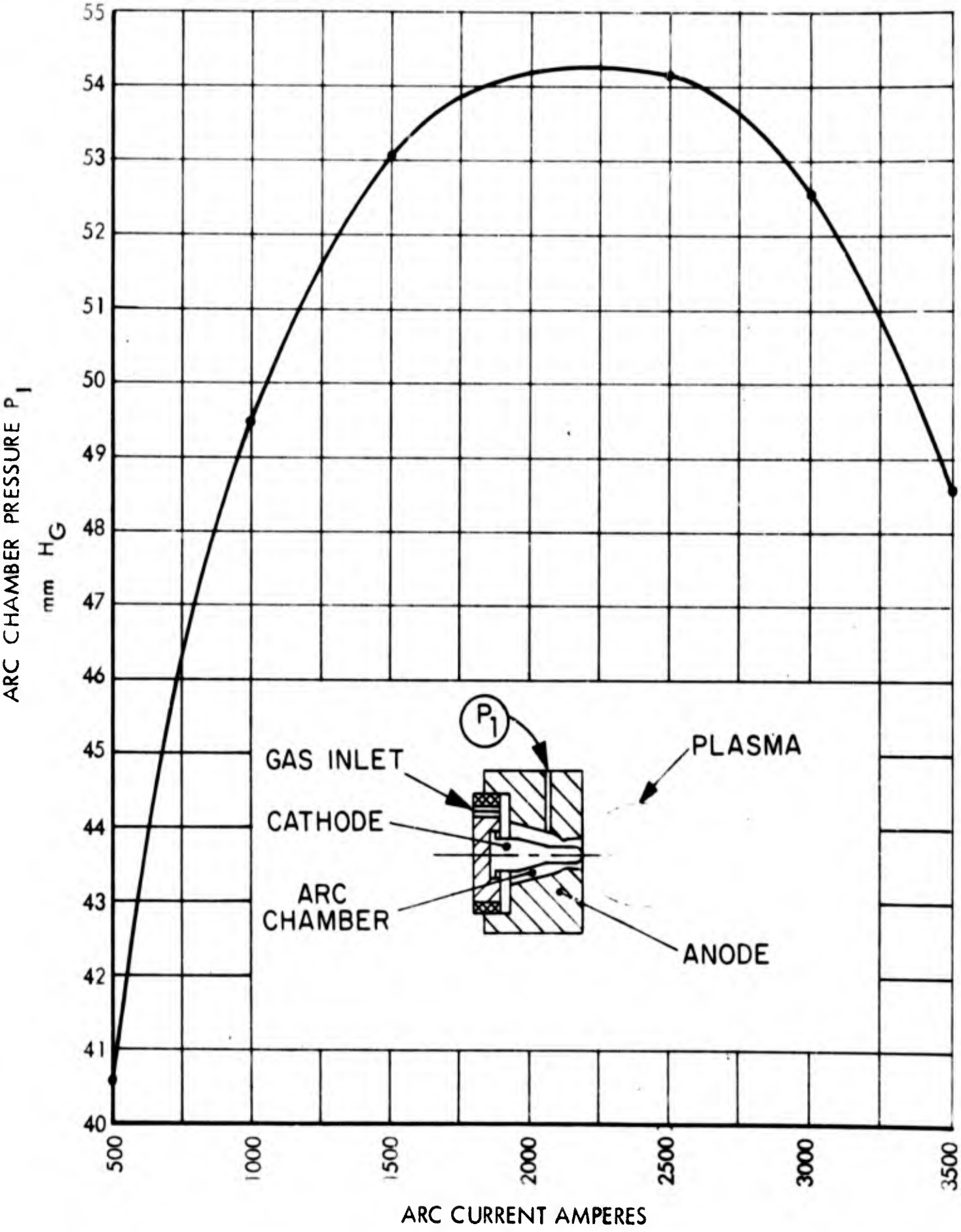

Figure 34. Variation of Arc Chamber Pressure With Increasing Current

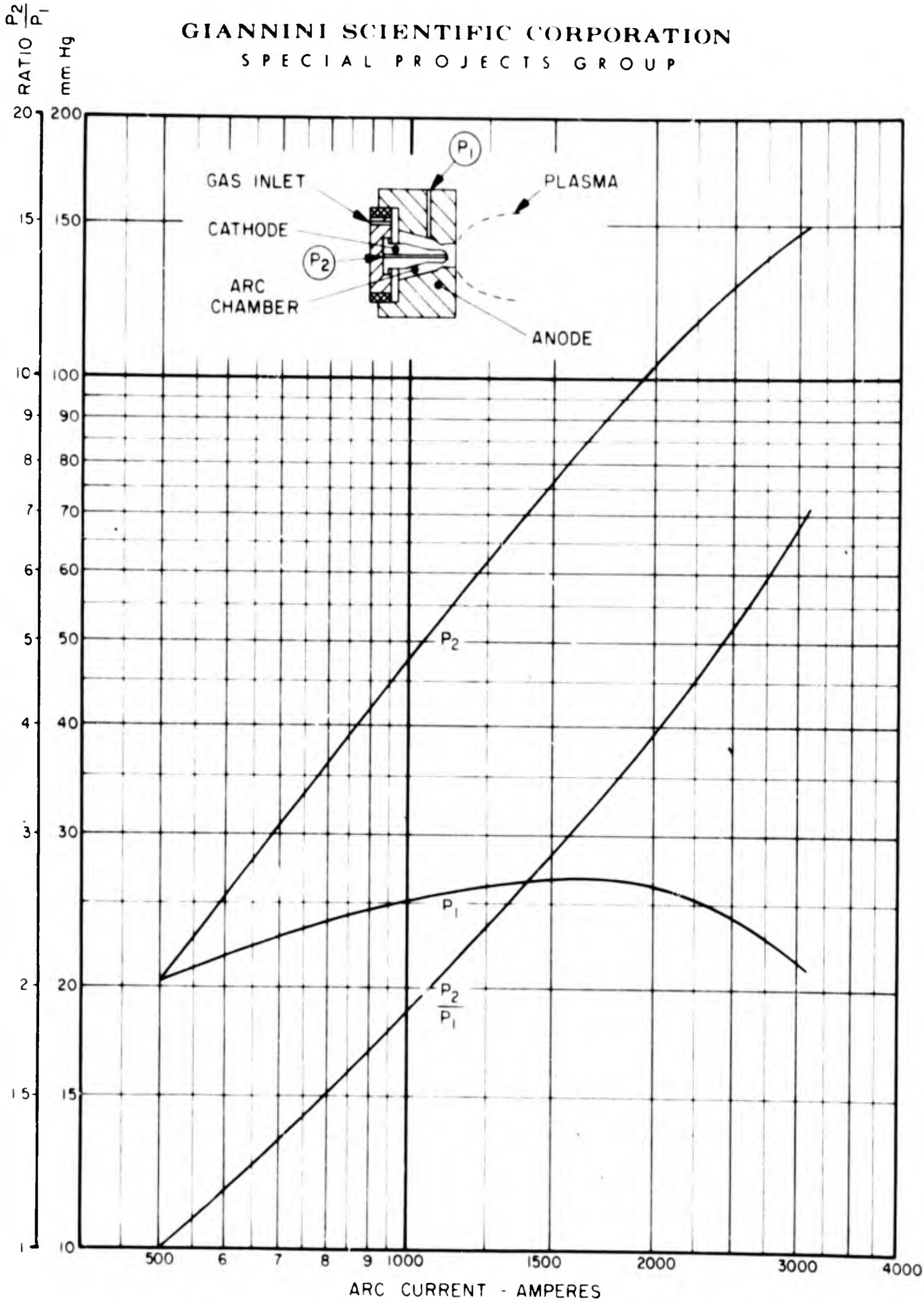

Figure 35. Variation of Pressure of Arc Chamber and Cathode Tip With Increasing Current

The effects of a superimposed axial magnetic field using hydrogen as a propellant at gradually reduced chamber pressure has also been studied. The use of a small axial magnetic field was suggested by the erosion of the anode when operated for relatively long periods of time. Because of the high current density the arc termination at the anode showed up at preferred fixed points and these simularities produced localized erosion with consequent reduction of the electrode life. The axial magnetic field which impressed a rotation to the arc termination at the anode surface eliminated the inconvenience. To simplify the practical solution a water-cooled induction coil of a few turns was connected in series with the arc and located at the end of the anode. This solution was not final because the intensity of the axial magnetic field is changing with the arc current, and has been substituted with a separately fed power supply. In the range of arc currents tested and with the various coils tested, the intensity of the axial magnetic field has been between 100 and 12,000 gauss (see Figures 11 and 12). The use of an external magnetic field, mainly applied to rotate the arc, resulted in reduction of electrode erosion which became negligible even after extended test periods. Table 12 shows typical test results at various specific impulse ranges and different external magnetic field strengths. A series of tests were run at gradually decreasing mass flow rates using hydrogen as the propellant. Specifically, mass flow rates of 50, 25, 12.5 and 6.25 milligrams of H_2 per second have been tested at various levels of specific impulse. The results of these tests are tabulated in Table 13. It is easy to see at a glance that the efficiency is drastically increasing as

TABLE 12

EXPERIMENTAL TEST RESULTS OBTAINED WITH A WATER-COOLED ELECTROTHERMAL GENERATOR WITH EXTERNALLY APPLIED MAGNETIC FIELD

Mass Flow grams	Thrust grams	Isp sec	Field gauss	Press. mm Hg	Input kw	Gas kw	Efficiencies η^{eg}%	η^{gk}%	η^{ek}%
0.025	77	3080	1500	38	62	31	50	36	18
0.025	120	5000	2000	36	104	62	59	44	26
0.025	147	5900	2000	26	122	77	63	54	34
0.013	137	10000	3500	14	162	90	55	74	41

TABLE 13

VARIATION OF EFFICIENCY WITH DECREASING PROPELLANT MASS FLOW

Mass Flow	Thrust	Isp	Arc Chamber	Input	Gas	Theoret-ical	Theoretical 100% Frozen Flow	Efficiency	
mg/sec	grams	sec	Pmm Ab	kw	kw	kw	kw	η^{eg}%	η^{gk}%
50.00	50	1000	24.0	39.7	16.5	2.4	5.85	41.5	14.5
50.00	50	1000	24.0	43.5	18.3	2.4	5.85	42.0	13.0
50.00	50	1000	23.3	42.0	17.0	2.4	5.85	40.0	14.0
25.00	50	2000	16.4	55.6	24.0	4.8	11.50	43.0	23.0
25.00	50	2000	16.5	57.0	26.0	4.8	11.50	45.0	18.0
25.00	50	2000	16.4	58.0	25.0	4.8	11.50	46.0	19.0
12.50	50	4000	11.1	52.0	22.0	9.6	28.40	42.0	43.0
12.50	50	4000	11.2	54.0	23.0	9.6	28.40	43.0	41.0
12.50	50	4000	11.1	50.0	21.0	9.6	28.40	42.0	45.0
6.25	50	8000	7.3	45.0	22.0	19.2	28.10	49.0	87.0
6.25	50	8000	7.5	46.0	21.5	19.2	28.10	47.0	90.0
6.25	50	8000	7.6	44.8	21.0	19.2	28.10	47.0	91.0

soon as relatively low mass flows are used. This effect becomes predominant when mass flows under 5 milligrams per second are reached, indicating that some parasitic error not yet identified exists in the thrust measurement. The eventual error in thrust reading is not important at high flow rates, but becomes more and more important at very low propellant flow rates. For this reason a gradual decrease of the hydrogen mass flow was attempted at flow rates under 1 milligram per second. It was noted that by decreasing the hydrogen mass flow a bluish center core appeared in the arc jet, sometimes erratic, but often very stable and bright (see Figure 36). The bluish brightness increased continuously with a decrease in the hydrogen mass flow (see Figure 37). During these experiments it was noted that to avoid the extinguishing of the arc at very low mass flow rates, the cathode temperature had to be higher than a certain minimum. The possibility of increasing the cathode temperature through a separate heater has proven very useful. Stable operation at gradually lower and lower mass flow rates was achieved without difficulty as soon as enough experience had been gained through a relatively long series of preliminary experiments. During one particularly stable condition of operation at extremely low mass flow rates it was noted that a further decrease in the mass flow apparently did not produce any effect in the arc appearance and behavior. For this reason the gas was shut off completely and the jet continued to operate with stability for a long time. The appearance of the jet is illustrated in Figure 38 and its color is essentially blue-violet. After checking for the possibility of gas leaks it was concluded that the arc was operating mainly with electrode

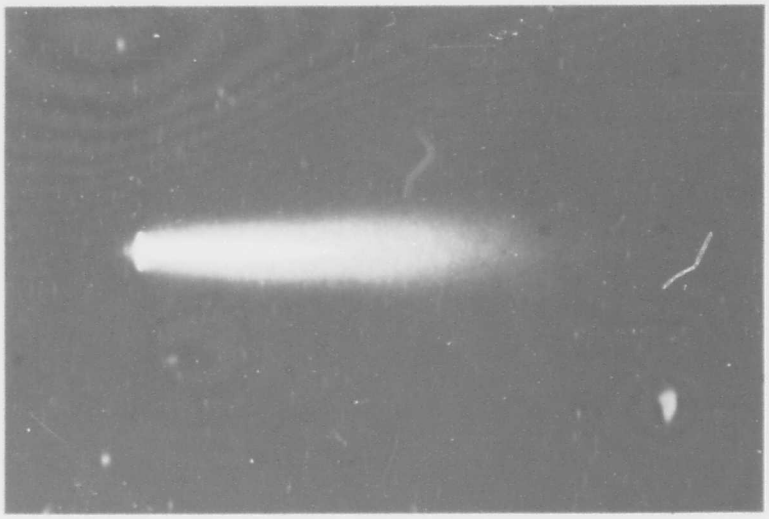

Figure 36. Arc Exhaust With Hydrogen Mass Flow Rate of 1.0 Mg/sec

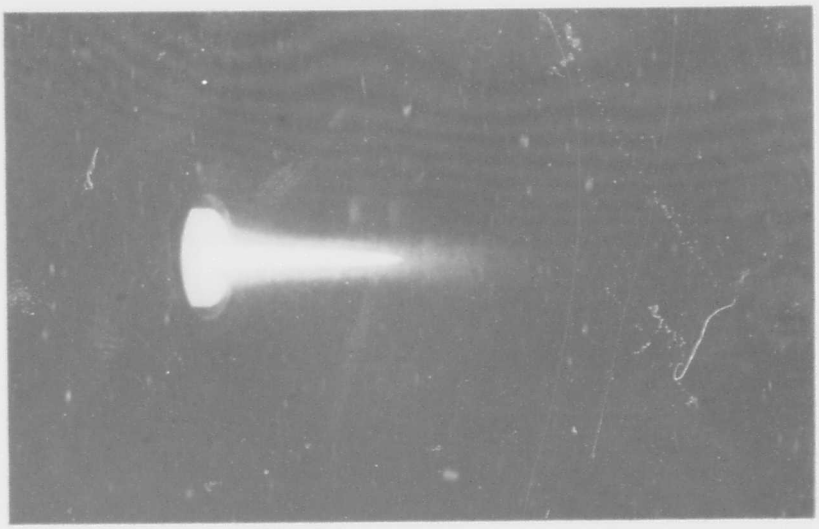

Figure 37. Arc Exhaust With Hydrogen Mass Flow Rate of 0.25 Mg/sec

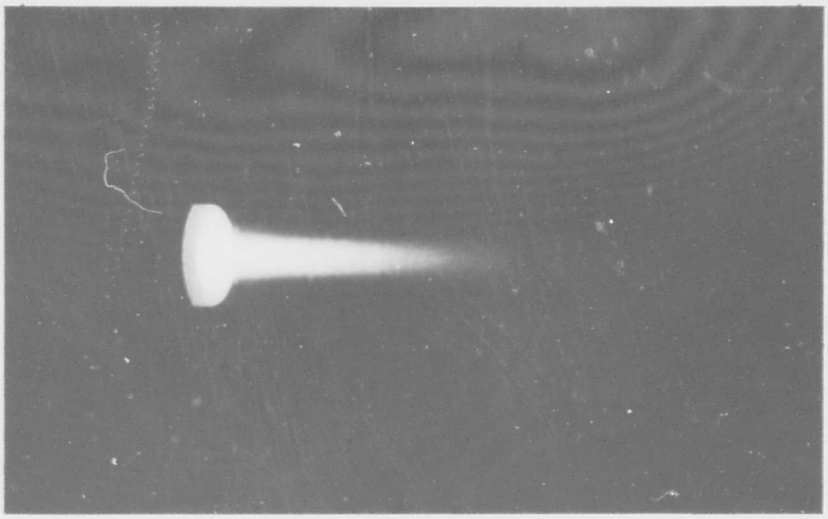

Figure 38. Arc Exhaust With No Hydrogen Flow

vapors, and this was confirmed by the weight losses of the same electrodes (mainly cathode) during accurately determined periods of time and by appreciable deposit of the electrode material on the vacuum chamber where the tests have been conducted. Substantial amounts of thrust have been measured during this type of operation. This unexpected thrust contribution can explain (under certain limits) the abnormal increase in efficiency measured when the mass flow was reduced below certain values. The relatively high values of this thrust (higher than the amount that can be calculated conventionally from the pure contribution of the measured mass loss of the electrodes) however, seem to confirm that other thrust contributions (parasitic) might be present in this type of operation. From a visual observation the jet can be schematically represented as in Figure 39 where the central core is a thin long well-directed bluish jet and the dotted lines represent estimated return paths of the arc current.

Numerous tests have been conducted with this type of plasma generator without external propellant injection and with power inputs ranging from 20 to 120 kw. Mass flow contribution has been carefully calibrated by weighing the electrodes before and after each test run. Table 14 shows a typical performance obtained during these tests. It must be noted that in this table the specific impulse value is not indicated because the factors contributing to the measured thrust are not completely known. With the assumption that the thrust measured is produced only by electrode vapors, the calculated specific impulse from the electrode weight losses would lead to very high values. These values, however, will naturally decrease if there is a mass flow participation of other constituents or if other parasitic thrust producing effects are present.

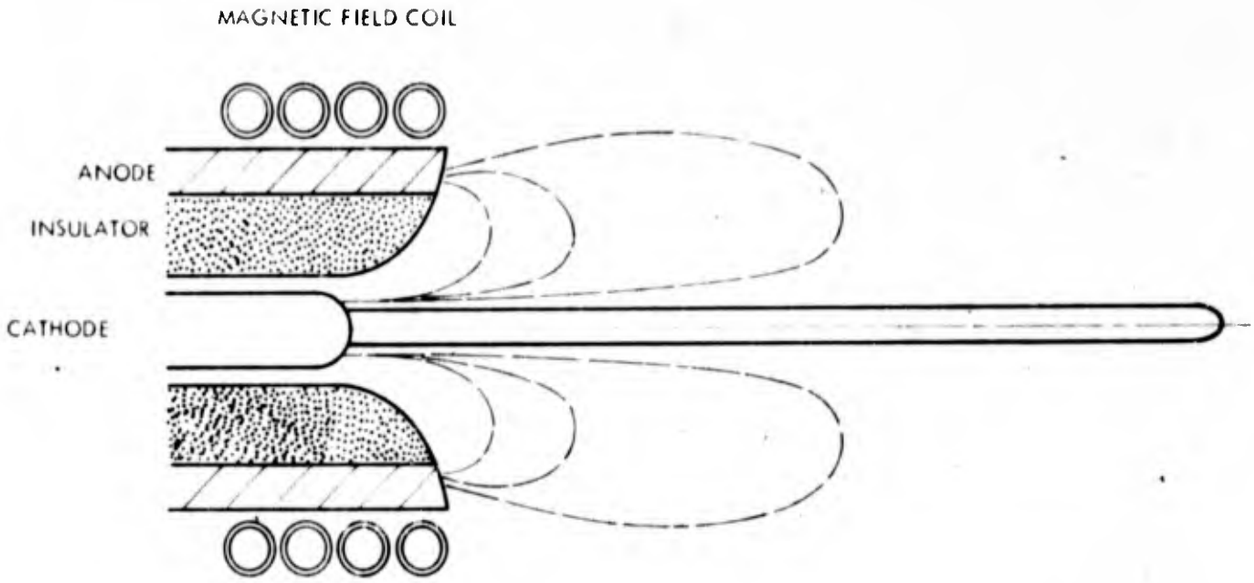

Figure 39. Schematic of Arc Generator for Low or No Propellant Throughput

TABLE 14

PERFORMANCE DATA OBTAINED WITH PLASMA GENERATOR OPERATING WITHOUT PROPELLANT THROUGHPUT

Propellant	Mass Flow mg/sec	Thrust grams	Field gauss	Press. mm Hg	Arc volts	Arc amps	Input kw	Gas kw	Efficiencies η^{eg}%	η^{gk}%	η^{ek}%
W	10.0	50	2500	3.0	60	1000	60.0	15.0	25	80	20

During the last part of the work, the suspected presence of anomalies was continuously getting more concrete in form. For this reason a plan of long range quantitative and qualitative experiments with the scope of explaining these anomalies has been prepared. While most of these newly planned tests will constitute the nucleus of future work, some have been initiated and some results have already been obtained.

A project of wide proportion has been initiated with the scope of correlating all the parameters involved in the operation of arc accelerators between the lowest and highest attainable specific impulses. The characteristic of this program is to keep constant one basic parameter at a time, while all the others are varied in succession. Basic parameters can be, for example, the mass flow, the specific impulse, the power input, the power in the gas, etc. Thus, it is possible to keep the mass flow constant over a wide range of specific impulse and measure for each Isp level the values of all the other parameters involved. Or it is possible to keep constant the power input and cover the same range of Isp recording the variation of all the other parameters. The same thing can be done keeping constant the voltage, the current, the magnetic field, etc. To reduce the exceptionally high number of tests that a program of this dimension involves, it has been decided that the variable parameters will double in value at any change. A series of measurements at specific impulses of 500, 1000, 2000, 4000, 8000, etc., with mass flows of 10, 20, etc. mg/sec and with externally applied magnetic fields of 1000, 2000, 4000, 8000, etc. gauss has already been initiated with promising results. Figure 40 shows the effect of an

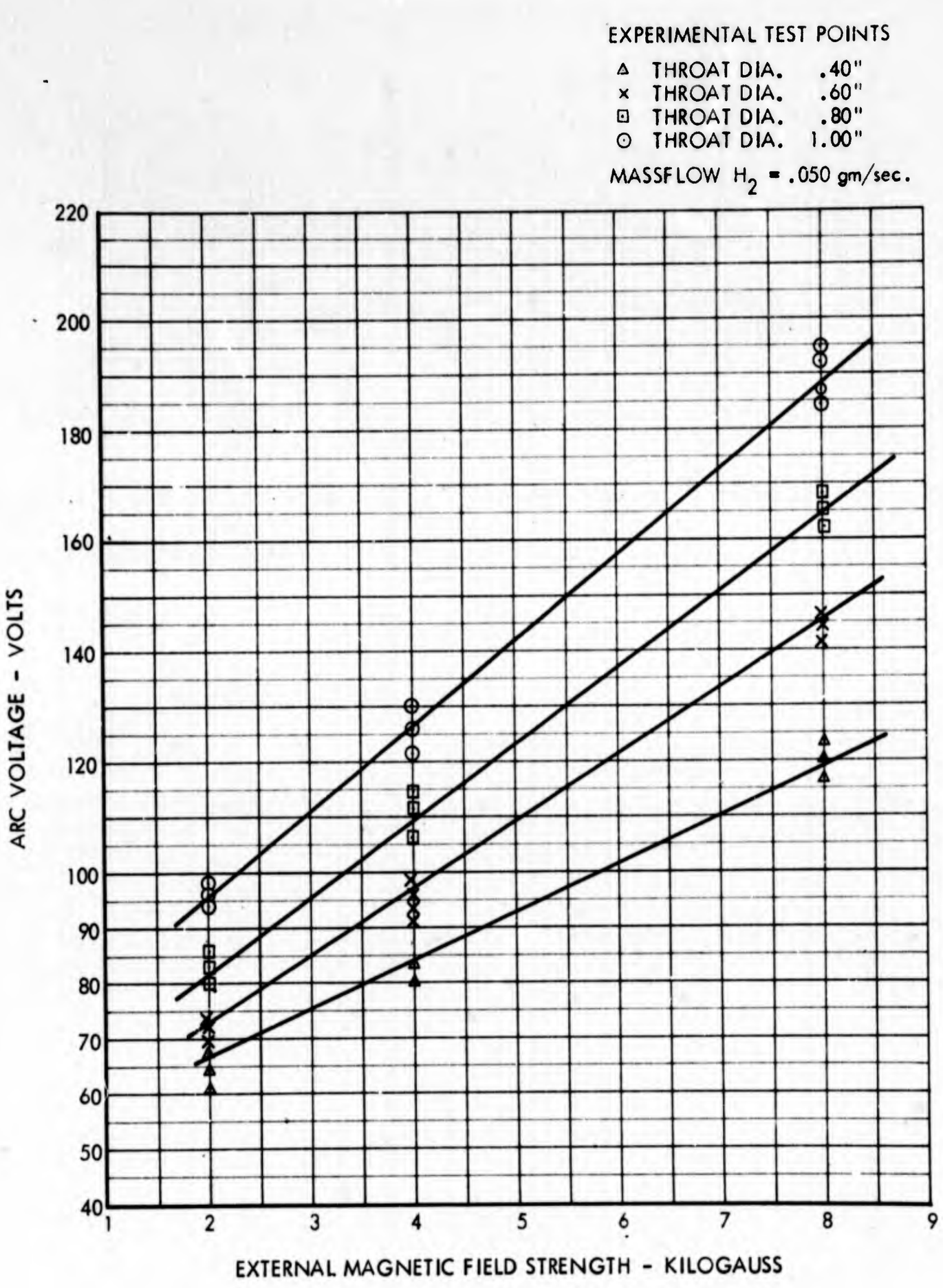

Figure 40. Arc Voltage Versus External Magnetic Field Strength With Four Throat Diameters and Isp 2000 Seconds

external magnetic field on the operating voltage at 2000 seconds Isp with various throat diameters. The variation of voltage is very pronounced. It is evident that the same data obtained for various specific impulses, mass flows, etc., can give important information for future explanation of the operating properties of this type of plasma accelerator. Figure 41 shows that the variation of the arc chamber pressure as a function of magnetic field is relatively small at Isp 2000 seconds and a mass flow of 50 mg/sec. The extension of this information to a wide field of Isp, mass flows, etc., can also be useful in the interpretation of practical results. Figure 42 shows that the efficiency of energy transfer between electric input and power in the propellant (η^{eg}) is practically independent from the value of the magnetic field and of the throat diameter. The same independence is the case for the efficiency of momentum transfer in the jet (η^{gk}). Extending this information to lower and higher specific impulse levels will be useful for the interpretation of test results.

An example of the practical use of the wide operating data survey is given by Table 15 which covers a thrust range from Isp 1000 to 16,000 seconds with a mass flow range from 50 to 3.1 mg/sec. A constant external magnetic field of 5000 gauss has been used during this series of tests (Table 13 on page 118 is similar but with a variable magnetic field applied through a coil in series with the arc current). Anomalies in the operation of the accelerator were especially noticeable at the mass flow rate of 3.1 mg/sec because the gas to kinetic efficiency was impossibly high (about 140 percent). In this case it is evident that to bring this efficiency back into reasonable

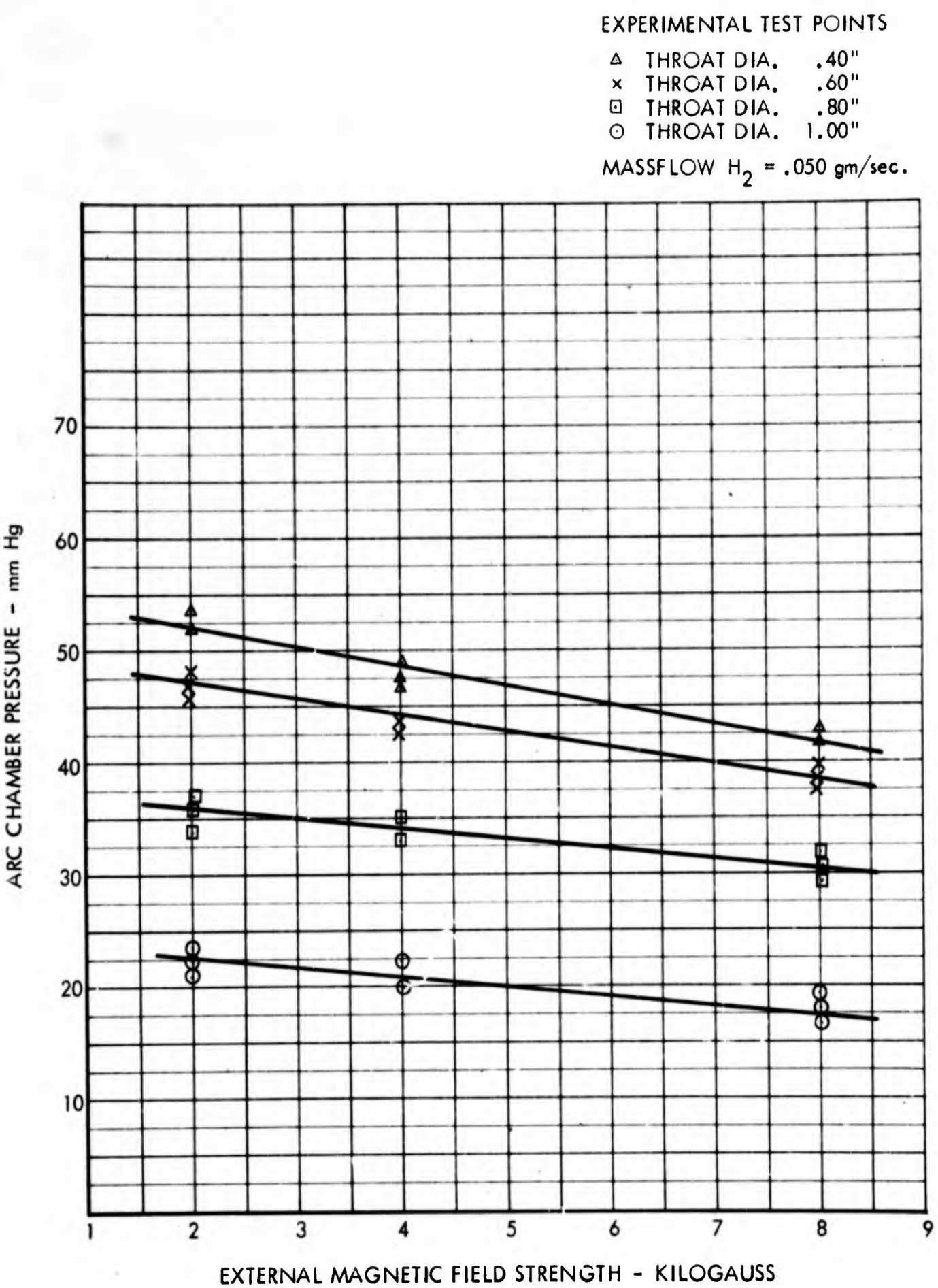

Figure 41. Arc Chamber Pressure Versus External Magnetic Field Strength With Four Throat Diameters and Isp 2000 Seconds

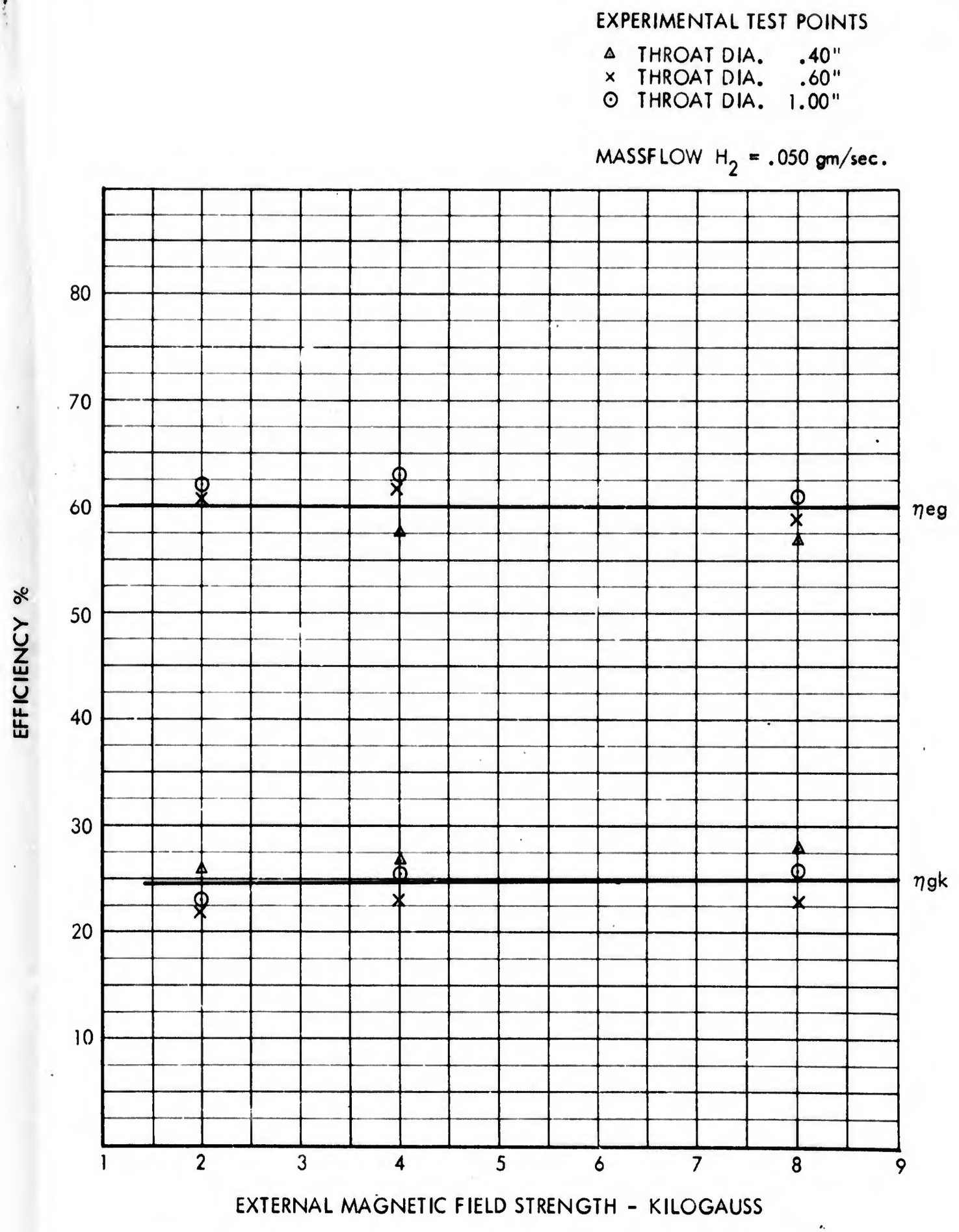

Figure 42. Efficiency Versus External Magnetic Field Strength With Three Throat Diameters and Isp 2000 Seconds

TABLE 15

VARIATION OF EFFICIENCY AT DIFFERENT MASS FLOW AND ISP USING H_2

Mass Flow mg/sec	Thrust grams	Isp sec	Field gauss	Press. mm	Input kw	Gas kw	Efficiencies η^{eg}%	η^{gk}%	η^{ek}%
50.0	50	1000	5000	24.0	32.0	20.0	62.5	12.0	7.5
50.0	50	1000	5000	24.0	32.5	20.0	61.5	12.0	7.4
50.0	50	1000	5000	23.0	33.0	20.5	62.2	11.7	7.3
25.0	50	2000	5000	17.0	47.0	28.0	60.0	17.1	10.0
25.0	50	2000	5000	16.0	46.0	27.2	59.0	17.6	10.0
25.0	50	2000	5000	18.0	45.0	29.3	61.0	16.4	10.0
12.5	50	4000	5000	12.0	50.0	28.5	57.0	33.7	19.2
12.5	50	4000	5000	12.0	52.0	29.2	56.0	32.8	18.4
12.5	50	4000	5000	12.0	51.0	29.5	58.0	32.5	18.8
6.2	50	8000	5000	9.0	49.0	26.0	53.0	74.0	39.2
6.2	50	8000	5000	8.0	50.0	27.0	54.0	71.2	38.4
6.2	50	8000	5000	9.0	53.0	27.8	52.0	69.0	36.2
3.1	50	16000	5000	6.0	54.0	27.5	51.0	139.5	71.0
3.1	50	16000	5000	6.1	53.0	28.7	49.5	134.0	72.4
3.1	50	16000	5000	6.2	55.0	29.2	53.0	131.5	69.9

limits, part of the thrust measured (50 grams) must be attributed to parasitic effects. Approximate values of the error involved can be easily computed from a series of tests of this kind and the value of the real thrust and specific impulse obtained. It must be considered that the exact separation of the various efficiencies as indicated in Table 15 is not simple because some portion of power can be by-passed from one system to the other altering the final results. To avoid or minimize this, special precautions must be taken.

While exact quantitative measurements are the final goal and basic scope of this work, it is our opinion that a substantial amount of information can be obtained from purely qualitative analysis and test. Figures 43 and 44, for example, indicate an approximate reproduction of what can be seen in the vacuum chamber when the arc is operated with various values of external magnetic field strength. Figure 45 is photographic evidence of similar patterns at different magnetic fields and using different propellants, and clearly demonstrates its possibilities in the interpretation and diagnosis of the results. The use of movie cameras (of the normal, fast, or high-speed variety) has been very important in this type of work, and a large amount of this material has been accumulated for future interpretation. The necessity of evaluating for diagnostic reasons the region extending outside the plasma accelerator makes particularly attractive any photographic methods available. For example, the so-called "bombardment" effect (illustrated in Figure 46) has been discovered visually and to date the only method of recording its characteristics is photographic. Fast and

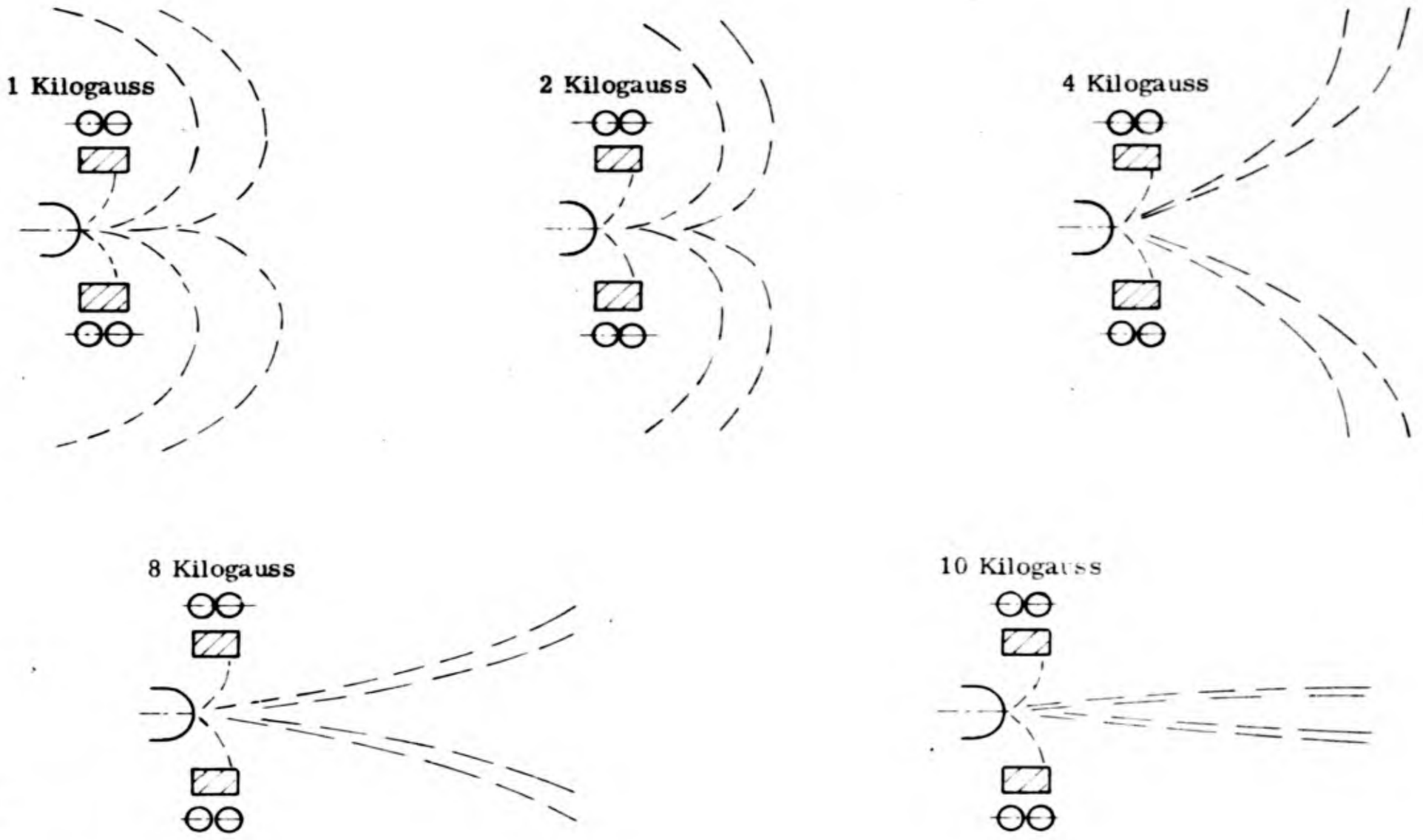

Figure 43. Visual Jet Patterns at Various External Magnetic Fields

Figure 44. Patterns of Axial and Radial Arc Discharges

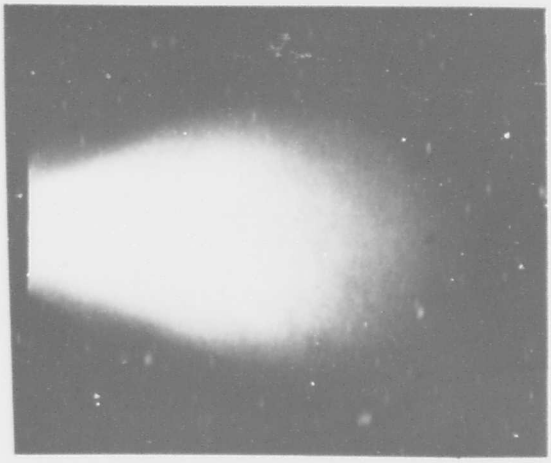

Hydrogen 5000 gauss

Lithium 10,000 gauss

Hydrogen 10,000 gauss

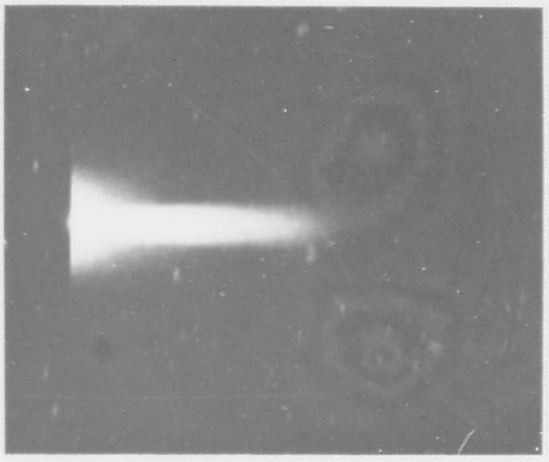

Tungsten 5000 gauss

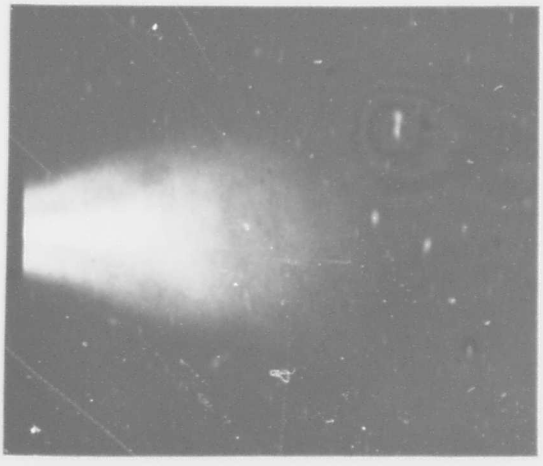

Deuterium 6000 gauss

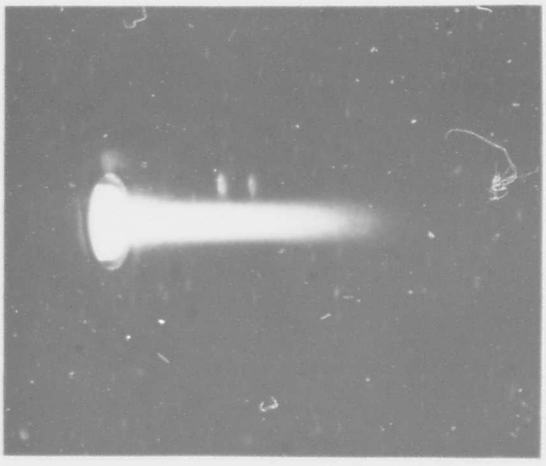

Tungsten 8000 gauss

Figure 45. Visible Portion of Various Arc Exhausts Using Different Propellants and External Magnetic Fields

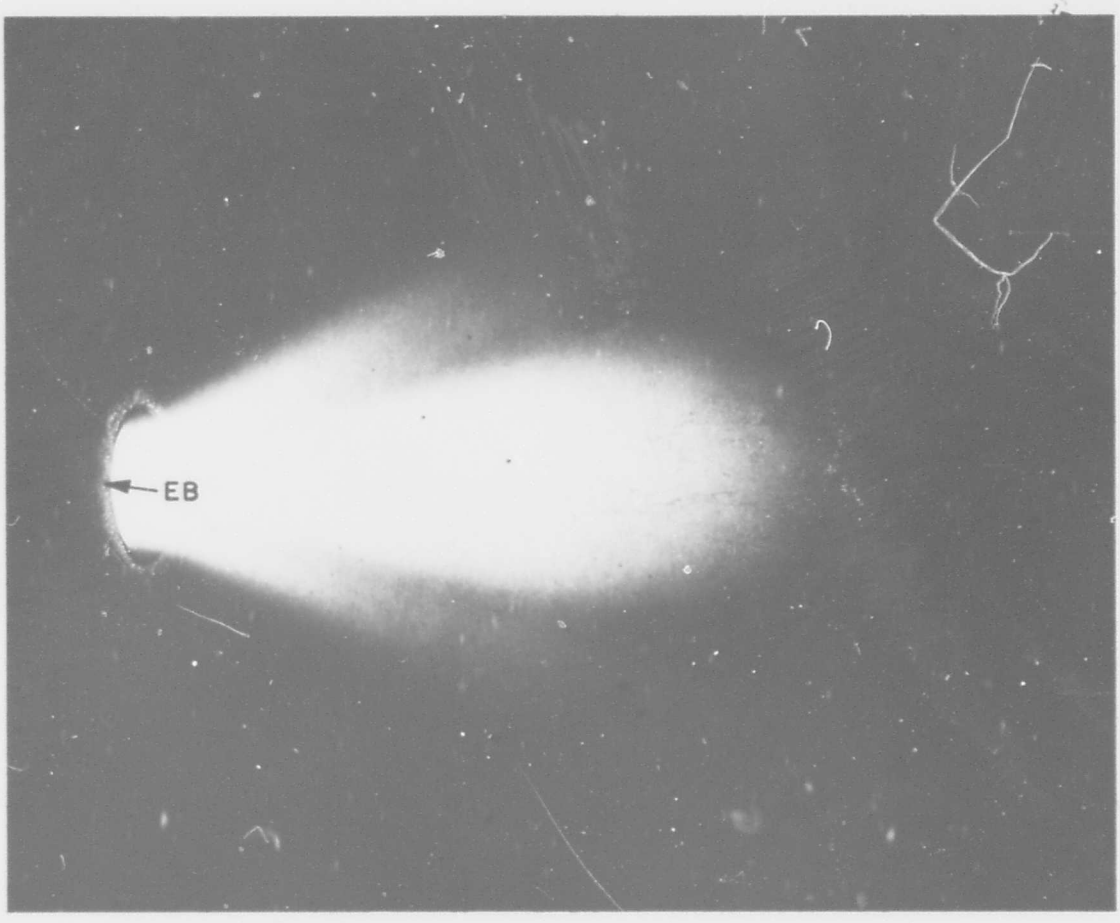

EB indicates circular area of electron bombardment on anode

Figure 46. Visual Patterns of Hydrogen Exhaust at Strong Externally Applied Magnetic Field

high-speed films of this phenomenon will certainly be very useful for the explanation of its behavior. It is evident that together with the visual pattern of the event to be studied, other characteristic parameters deserve equal or even more attention. For this reason it was recently decided to use quantitative and qualitative methods recording simultaneously both the photographic pattern and the reading of the various measuring instruments. This method already used in the early experiments (see report 3QS070-766 under Contract AF 49(638)-766) has been substantially improved and will permit integrating the data from the instruments with precision pictures of the event in future tests.

4.0 INTERPRETATION OF EXPERIMENTAL RESULTS

The work carried out under this contract divides naturally into three phases: (1) The low temperature studies with resistance heating using a variety of propellants; (2) the study of high temperature, high specific impulse, arc-heated plasma jets with hydrogen propellant; and (3) the discovery and preliminary investigation of the tungsten electrode vapor arc jet. The discussion here is a summary of the interpretation of the results obtained in these investigations.

With the exception of ammonia, the theoretical understanding of the low temperature specific impulse measurements for the various propellants used is relatively good. Some aspects of the low temperature studies with ammonia, that are related to dissociation and recombination processes, remain obscure. In the high temperature regime, there is some qualitative theoretical understanding of the performance of the arc-heated plasma jet and electrode vapor arc jet, but most of the experimental results lack adequate quantitative theoretical interpretation. In particular, the measured thrust power to gas power efficiency exceeds the frozen flow efficiency for low mass flow, low thrust operation and the causes of this condition are presently not known. Possible sources of this discrepancy are considered.

4.1 Low Temperature Thermal Acceleration

Measurements of specific impulse have been made with a variety of propellants over a range of 300 to about 2800°K. The gases were resistively heated in such a way that thermal equilibrium was obtained. For the gases used, essentially no ionization occurs in this temperature range and the theory of the continuum nozzle flow of a real gas is applicable. The theory for these low temperature nozzle flows is relatively simple if the gas is nonreacting, i.e., if it does not dissociate or recombine. When dissociation and recombination take place, the theory becomes more complicated and it is difficult to relate theory and experiment.

Argon, nitrogen, helium, hydrogen and mixtures of these gases have been tested over a temperature range of 300 to 1200°K. In this range there is no dissociation if the gases are in thermal equilibrium. For ammonia this is not the case, and the onset of dissociation takes place at about 600°K. Specific impulse measurements with NH_3 were continued up to temperatures of about 2800°K and some interesting results have been obtained. The nondissociating gases will be discussed first and then the experimental results with NH_3 will be considered separately.

According to one-dimensional isentropic flow theory, a fully expanded perfect gas flow of stagnation temperature T_o will produce a specific impulse of

$$I_{sp} = \frac{1}{g}\sqrt{\frac{2\gamma R T_o}{(\gamma - 1) M}} \qquad (1)$$

where M is the molecular weight of the gas, γ is the ratio of specific heats, g is the gravitational acceleration, and R is the universal gas constant. The specific heat of the gas is given by $c_p = \gamma R/(\gamma - 1) M$. If there is no diverging nozzle but only a throat, the specific impulse is given by

$$I^*_{sp} = \frac{1}{g}\sqrt{\frac{2(\gamma + 1) R T_o}{\gamma M}} \quad . \tag{2}$$

The ratio of these two specific impulses is

$$\frac{I^*_{sp}}{I_{sp}} = \sqrt{\frac{\gamma^2 - 1}{\gamma^2}} \quad . \tag{3}$$

This ratio represents the maximum gain in specific impulse that can be achieved by using a nozzle. For monatomic gases this gain is 20 percent; for diatomic gases it is 30 percent. For molecules of more complex structure (more degrees of freedom) the maximum increase in specific impulse through the use of a diverging nozzle becomes larger.

Specific impulse as a function of stagnation temperature without a nozzle has been measured and the results are shown in Figure 23. The solid lines are the theoretical curves calculated from Equation (2) and as can be seen, the agreement between theory and experiment is very close. Simple nozzles have been used to increase the specific impulse. The results of these tests are shown in Figures 26-32. The measured specific impulses are bounded above by the maximum possible I_{sp}, given by Equation (1), as they should

be. These measurements show that the recovery of kinetic energy from thermal energy by use of a diverging nozzle is more important for gases with more complex structure (high-γ gases), which is in qualitative agreement with Equation (3).

These low temperature tests with and without nozzle were carried out partly in anticipation of the work with the high temperature, arc-heated plasma jet. These tests and the theory indicated that in practice, for monatomic gases, it would be difficult to increase the specific impulse by more than 10 or 15 percent through use of a nozzle. Consideration of the fact that heat losses to the nozzle walls would compete with this gain, indicated that very short nozzles would be best for a high temperature fully dissociated plasma jet flow. This has proved to be the case for the high temperature, high specific impulse hydrogen arc jet.

As can be seen in Figures 24 and 25, the measured specific impulse for ammonia begins to deviate from the theoretical value at about 600°K. In view of the agreement between the measured and theoretical values of specific impulse for the other gases, these measurements show that NH_3 begins to dissociate at 600°K. The data shows that the specific impulse continues to rise faster than the theoretical curve for no dissociation, and finally crosses the specific impulse for a frozen flow of composition $N_2 + 3H_2$. This suggests that a large fraction of the gas has dissociated into monatomic nitrogen and hydrogen. However, power balance calculations indicate there is insufficient power into the gas to dissociate a large

fraction of the ammonia into monatomic hydrogen and nitrogen with the dissociation energy remaining frozen in the flow. There is thus a problem in explaining the measured specific impulse passing through the $N_2 + 3H_2$ curve in Figure 25. The measurements of thrust and mass flow ($\sim$ 1 gm/sec) are quite accurate in these experiments, the accuracy being substantiated by the agreement between theory and experiment for the nonreacting gases. Since the accuracy of the specific impulse measurements has nothing to do with whether the gas is dissociating or not, we think that the explanation must be in the measurement of temperature. The temperature of the gas has been measured before the throat (for example see Figure 1). If the gas at the point of measurement was appreciably dissociated into N and H and if recombination into H_2 and N_2 takes place before leaving the throat then the measured temperature would not give the correct stagnation temperature of the flow at the exit plane of the throat. This would cause the measured temperature to be lower than the stagnation temperature and consequentially shift the experimental points to higher temperatures. This should be considered as a very tentative explanation. It would be desirable to make some direct measurements to establish the properties of the NH_3 flow. The question of the fraction of NH_3 dissociated could be settled by a chemical analysis of the exhaust jet, since once NH_3 is dissociated it will not recombine at moderately low temperature and pressure. A measurement of power into the flow and power in the stagnated exhaust flow would then immediately yield the power used in the dissociation reaction.

Recombination of N and H in the accelerated subsonic part of the flow, as implied in the discussion above, is an interesting possibility since it would permit lower static temperatures in the electrothermal heater for equal power in the exhaust flow.

Measurements of the specific impulse of NH_3 for resistive heating and an expansion nozzle have been made in the range between 100 and 425 seconds. These results are given in Table 7. The gas power measurements were uncertain in these tests. Nevertheless, we make a qualitative observation keeping this uncertainty in mind. The gas to kinetic energy efficiency for the higher specific impulses indicate that the gas is not fully dissociated and that there cannot be large amounts of monatomic hydrogen and nitrogen in the flow. Because of the uncertainty of the gas power measurements here, and the temperature measurements in the NH_3 tests discussed above, additional tests would be required to definitely establish the performance characteristics and dissociation processes in NH_3 in these thermal accelerators.

It should also be noted that for ammonia, 94 percent of the fully expanded isentropic impulse is obtained for the cold flows (see Figure 28). This represents a significantly larger expansion efficiency than found for the other gases. This cooperative behavior of NH_3 is presently not understood.

4.2 High Temperature Arc Jets

Very high specific impulses have been obtained by adding power to a gas flow by means of an arc discharge. Arc jet performance tests have been made with both hydrogen and ammonia as propellants. The tests with arc-heated NH_3 ranged from 500 to 2320 seconds. For H_2 the specific impulses recorded were from 3000 to 10,000 seconds. It is at these very high specific impulses that self-induced magnetic effects can become important. Externally applied magnetic fields have also been utilized to increase arc jet performance. Whenever the magnetic pressure of either the self-induced magnetic field or an externally applied field is comparable to the gas pressure in a strongly ionized gas flow, magnetic effects will very likely be important in some aspect of the flow. There is no general agreement as to how the magnetic forces affect the arc jet performance. We will consider these questions after a discussion of some of the specific impulse measurements.

Specific impulse and efficiency measurements for arc-heated ammonia have been reported in Table 8 . A plot of the measured gas to kinetic energy efficiency is shown in Figure 47. It is instructive to compare the efficiency at 500 seconds with the efficiency of the resistively heated thermal accelerator at 400 seconds. The relatively low arc jet efficiency at 500 seconds suggests that the arc jet flow is ionized and dissociated well in excess of thermal equilibrium values. This would not be surprising, since the condition where electron "temperatures" are significantly greater than

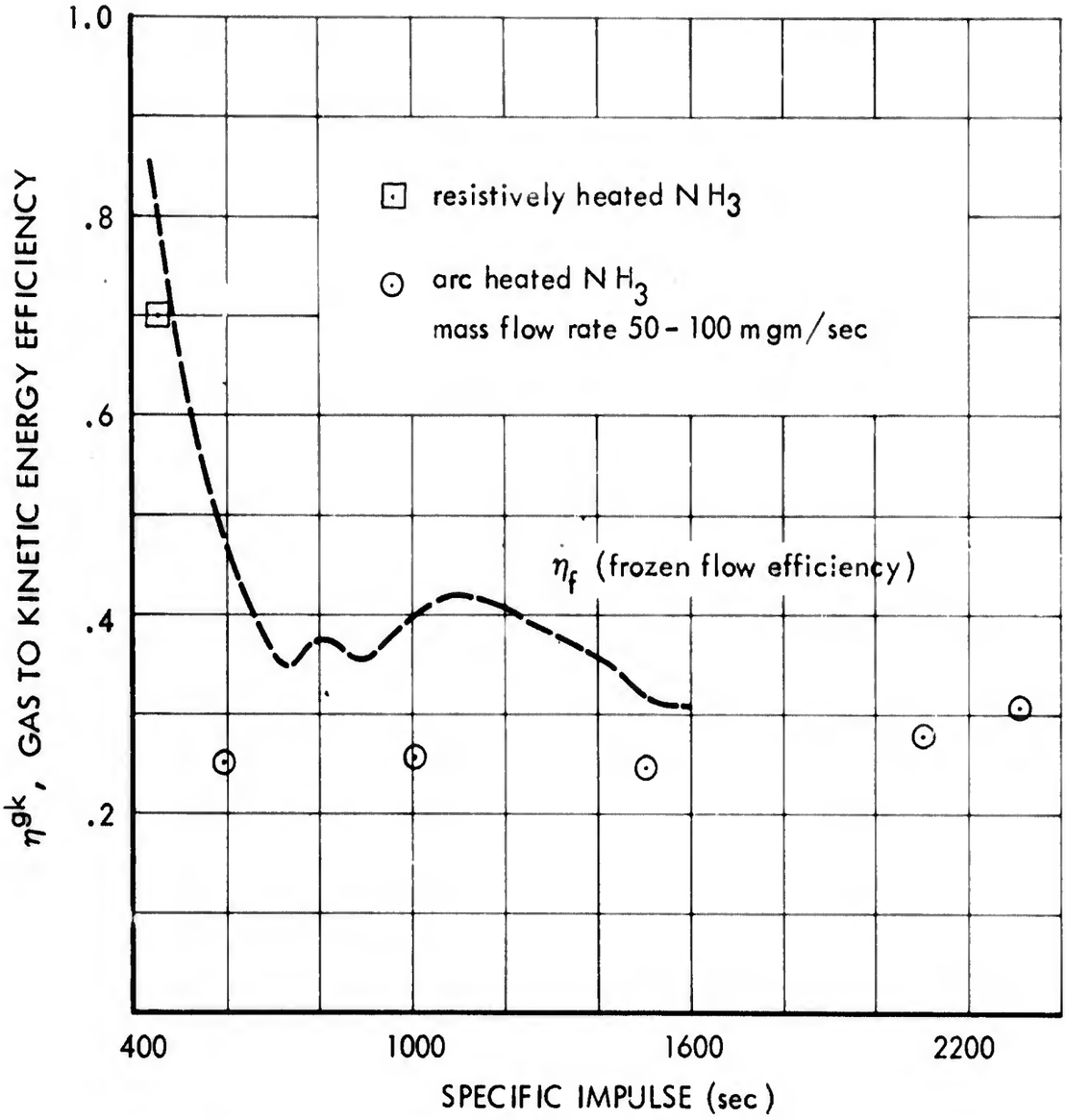

Figure 47. Comparison of Measured Specific Impulse With Frozen Flow Efficiency for NH_3 Propellant

the heavy particle "temperatures" often exists in arcs. This nonequilibrium state arises from the electrons acquiring energy directly by acceleration in the electric field of the arc, while the heavy particles are heated by energy-exchange collisions with the electrons. The magnitude of the temperature differences between the electrons and heavy particles will depend on the collision relaxation time for energy exchange. In Figure 47 it can be seen that as the specific impulse increases, the efficiency follows the frozen flow efficiency more closely, which could mean that a thermal equilibrium degree of dissociation and ionization is more nearly obtained at the higher specific impulses. This is plausible since as the specific impulse increases the degree of ionization increases and for a strongly ionized gas the electron-ion collision cross section determines the energy relaxation time. Since the Coulomb cross section is generally more than an order of magnitude larger than the electron-neutral cross sections, provided the temperature is not too high, the energy exchange relaxation times could be much less in a strongly ionized gas and hence the departure from thermal equilibrium (before expansion) of the strongly ionized flow could be much less than for a weakly ionized flow.

Specific impulse for hydrogen propellant as a function of stagnation enthalpy is shown in Figure 48. The experimental points are shown together with two theoretical curves. The upper curve gives the specific impulse for frozen flow efficiency, which is obtained by assuming that the thermal equilibrium dissociation and ionization fraction is determined by the static temperature equal to the stagnation temperature of the flow, and no

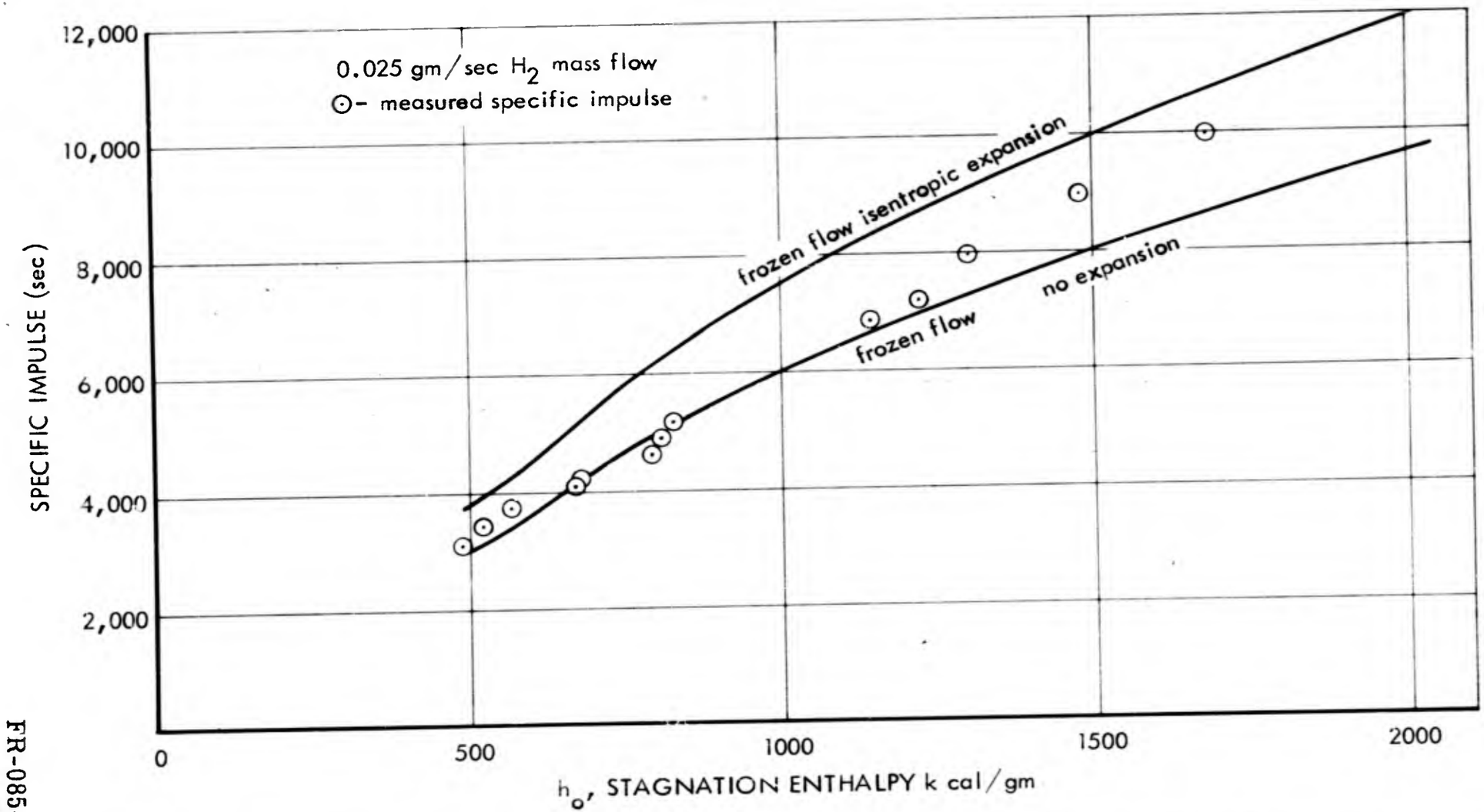

Figure 48. Comparison of Measured Specific Impulse With Theoretical Frozen Flow Specific Impulse for Complete Isentropic Expansion and No Expansion

recombination occurs. The specific impulse is then given by

$$I_{sp} = \frac{1}{g}\sqrt{2\,\eta_f\,h_o} \quad . \tag{4}$$

where η_f is the frozen flow efficiency, h_o is the stagnation enthalpy of the gas. The lower curve gives the theoretical specific impulse obtained by assuming, as above, that the ionization and dissociation fraction are determined by the static temperature equal to the stagnation temperature of the flow, but that there is no expansion (no magnetic or metal nozzle). In this case, the specific impulse for a one-dimensional flow is

$$I^*_{sp} = \frac{1}{g}\sqrt{\frac{\gamma^2 - 1}{\gamma^2}\;2\,\eta_f\,h_o} \quad , \tag{5}$$

where γ is the ratio of the specific heats corresponding to the frozen composition of the flow. For a fully dissociated gas $\gamma = 5/3$ and remains unchanged by ionization. For high specific impulses where dissociation is probably complete we may take γ constant. The approach here, for the high specific impulse, parallels that for the cold flows. That is, we are trying to establish sensible upper and lower bounds on the specific impulse. Equations (4) and (5) are analogous to (2) and (3) for the case of cold flow, and as before the ratio of the "minimum" to "maximum" specific impulse is $(\gamma^2 - 1)/\gamma^2$, where now, however, γ will always have the value for a monatomic gas. Stagnation enthalpy is now used rather than temperature as a variable and the additional complexity introduced because of the reacting flow is accounted for by the factor η_f which represents the fraction of the gas power used for dissociation and ionization.

The measured gas to kinetic energy efficiency is defined by

$$\eta^{gk} = \frac{g^2 I_{sp}^2}{2 h_o} \tag{6}$$

In our measurements, as is usually the case, specific impulse is a derived quantity, being calculated from $I_{sp} = F/\dot{m}$ where the thrust F and the mean weight flow rate $\dot{m}$ are measured directly.* For isentropic expansion to zero pressure and no recovery of dissociation or ionization energy by recombination, the gas to kinetic energy efficiency is just the frozen flow efficiency, as expressed by Equation (4). For no expansion (no nozzle) the theoretical gas to kinetic energy efficiency is defined by

$$\eta_f^* = \frac{g^2 I_{sp}^{*2}}{2 h_o} \tag{7}$$

where I_{sp}^* is given by Equation (5). We have plotted η_f and η_f^* in Figure 49 with the measured gas to kinetic energy efficiency η^{gk}. The dashed curve is a fit of the data obtained by assigning a constant value for the expansion, or nozzle efficiency. The dashed curve is given by

$$\eta^{gk} = \eta_n \, \eta_f \, . \tag{8}$$

where the expansion efficiency has been taken to be 0.8. This relatively high expansion efficiency is a little surprising when one recalls that the highest expansion efficiency obtained for the cold flows with monatomic gases were also about 0.8 and the nozzles here were not designed more carefully than for the cold flow (see Figures 26-32). (The expansion efficiency

*At times in the text instead of "mean weight flow rate" we use the common but less precise terminology of "mass flow."

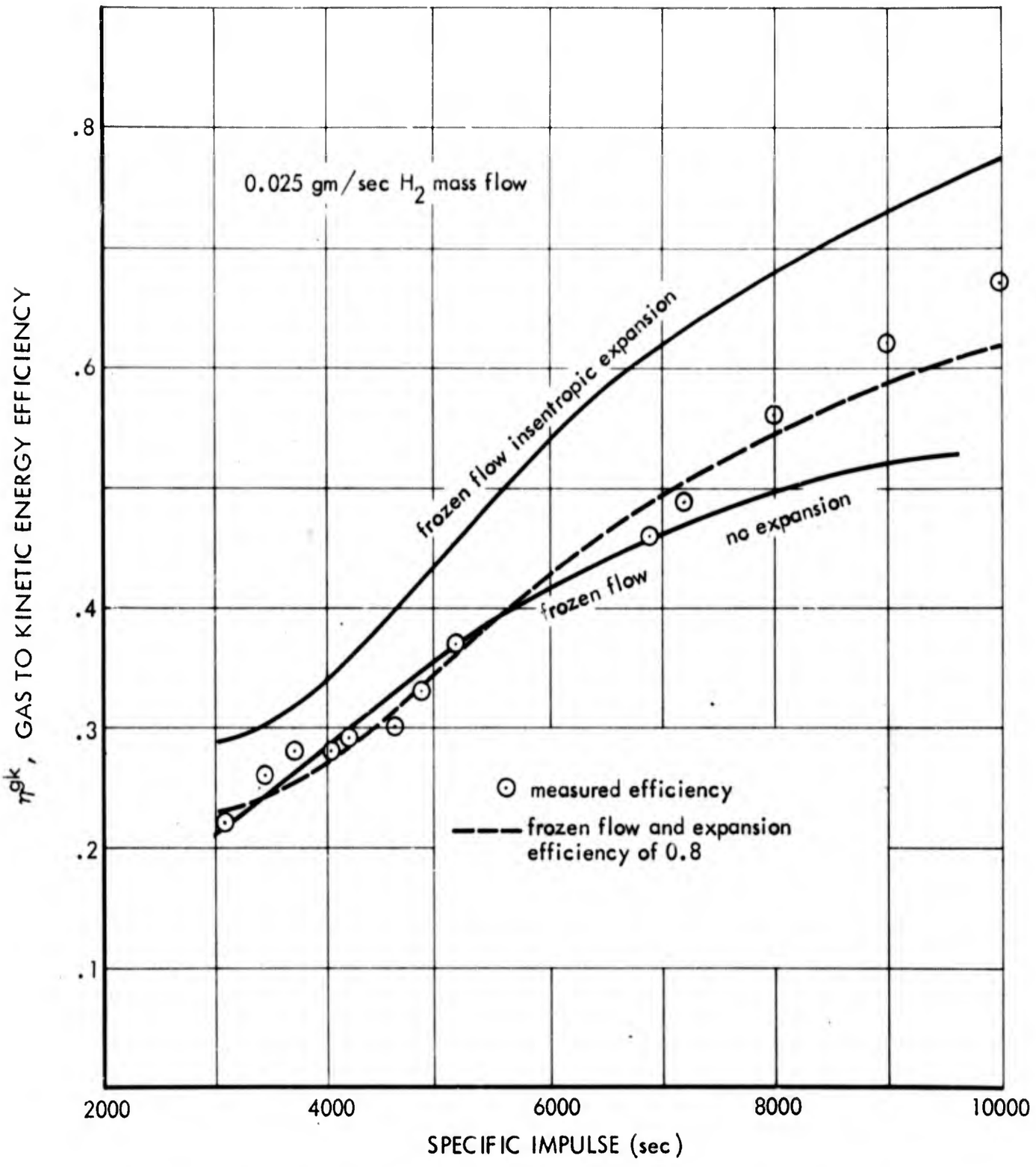

Figure 49. Comparison of Measured Gas to Kinetic Energy Efficiency With Frozen Flow Efficiency and Efficiency for Frozen Flow With No Expansion

corresponding to η_n is obtained by taking the square of the ratio of the measured specific impulse to the maximum theoretical impulse.) We note that an external magnetic field was not employed in these experiments.

In Table 13 we show data that has been obtained for H_2. Figure 50 here shows a plot of the gas to kinetic energy efficiencies given in Table 13. These tests with H_2 were performed at a constant thrust of 50 grams and variable mass flows ranging from 50 down to 6.25 m gm. The frozen flow efficiency is shown for comparison in the same figure, and it is seen that at specific impulses of 4000 and 8000 seconds the gas to kinetic energy efficiency is greater than the frozen flow efficiency by a substantial amount. This was the first strong indication that there were extraneous effects contributing to high performance at low mass flow, low thrust and high specific impulse operation. This was demonstrated more dramatically later when the arc was operated stably without any through flowing propellant at all, which gives, by the usual rules of calculation, an infinite specific impulse and an infinite efficiency. Before discussing these high H_2 efficiencies further, let us consider the electrode vapor arc.

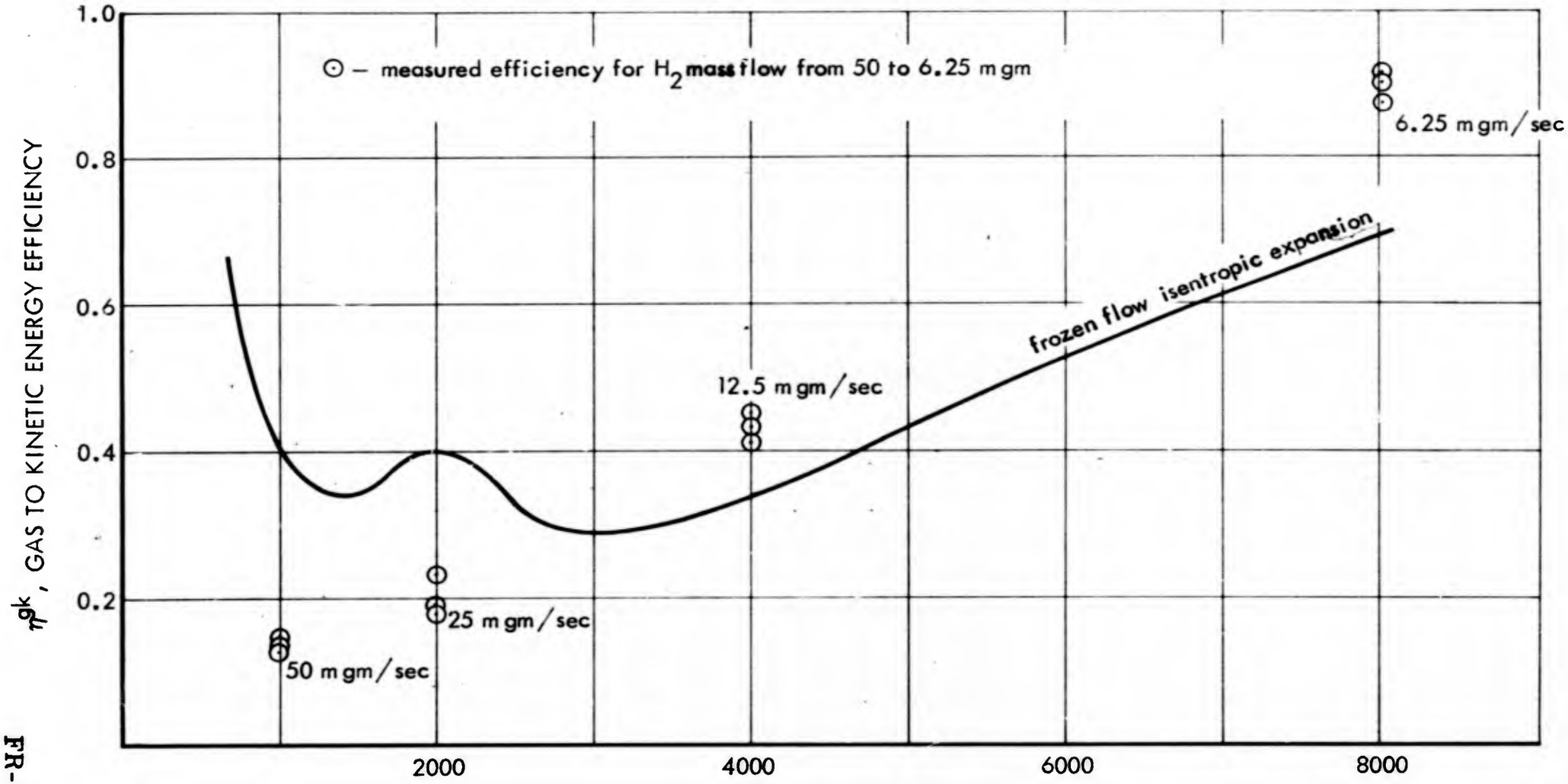

Figure 50. Comparison of Measured Efficiency With Frozen Flow Efficiency

4.3 Th Electrode Vapor Arc

The initial discovery that an arc jet can operate stably without any propellant flow in the usual sense has been described in the Eighth Semi-annual Report. Visual observation of a central core emanating from the cathode, erosion of the electrodes, and also evidence of a large amount of electrode material (tungsten) being deposited on the tank walls indicate that vaporization and ejection of the electrode material plays a prominent role in the operation of the arc. It is also possible that entrainment, ionization, heating, and acceleration of ambient gas can have a significant effect on the performance in the no mass flow operation. Spectroscopic measurements of the radiation from the arc jet plume have been made for very low mass flow and no mass flow. These measurements have established that vaporized and ionized electrode material are an intrinsic part of the jet plume. Some physical characteristics of the jet plume inferred from these measurements are discussed below.

By mass flow rate we shall always mean the measured mass flow entering through the arc jet chamber and leaving by the metal and magnetic nozzle. An analysis of the spectrum of the radiation at different axial distances from the exit plane of the anode has been made. The observations were made looking perpendicular to the axis of symmetry of the coaxial configuration at the anode exit plane, and at about eight inches, one foot, and two feet from the anode.

At eight inches from the anode for a mass flow of 0.5 mgm/sec, the line spectrum of hydrogen and the band spectra of N_2^+ and N_2 and OH were

detected. No emission from tungsten was observed. When the mass flow was reduced to 0.15 mgm/sec the many line spectrum of tungsten was clearly identified in addition to emission from H, N_2^+, N_2 and OH similar to that of the larger mass flow. The emission from ionized tungsten (W II) was much more intense than from neutral tungsten (W I). This shows that at eight inches from the anode the tungsten part of the flow is strongly ionized.

For no mass flow at eight inches from the anode the emission from W II increases by about a factor of seven from the 0.15 mgm/sec flow. The spectrum of N_2^+ and N_2 did not change and the OH emission decreased in intensity. At the exit plane of the anode for no mass flow, the line radiation was found to be entirely due to neutral tungsten, no emission from W II or other particles was detected. This implies a relatively low electron temperature and degree of ionization near the exit plane of the anode. The larger degree of ionization at eight inches indicates a much higher electron temperature there. We may then infer that in a zone extending from the exit plane of the anode to eight inches downstream from the anode there is a large amount of energy added to the flow.

The spectrum at about one foot from the anode was dominated by emission from N_2^+ and OH. The emission from W I and W II was not seen. The nature of the band spectrum of N_2^+ indicated a lower electron temperature than at eight inches. There still could be electric currents and ohmic heating in this region of the flow, but cooling by expansion and

interaction of the electrons with the cold ambient particles evidently dominates, causing the decrease in electron temperature.

Observation of the plume at about two feet from the anode, near the boundary of the outer luminous plume showed only emission from N_2^+ and the characteristics of the spectrum indicated a lower temperature than at one foot from the anode.

On the basis of the above results we obtain the following crude picture of the arc jet plume for no mass flow conditions. At the exit plane the arc consists of a tungsten plasma. The degree of ionization and electron temperature in this region are relatively low. The electron temperature and the degree of ionization of the tungsten component of the plasma increases with increasing distance from the anode. At eight inches the tungsten is fully ionized. In some region less than a foot from the anode the electron temperature begins to decrease and continues to decrease to the outer boundary of the luminous region which is about two feet from the anode. The fraction of ambient particles in the flow increases with increasing distance from the anode. At eight inches, in addition to W I and W II, the spectrum of the radiation showed significant emission from N_2^+, N_2 and OH. We do not know the relative amounts of these particles in the flow. This is a region of energy addition, so if the mass fraction of ambient particles is comparable to the mass of tungsten in the flow then an accurate evaluation of thrustor performance probably will have to account for this entrained fraction of the flow.

4.4 Discussion of Parasitic Effects

The fact that η^{gk} exceeds the frozen flow efficiency (see Figure 50 and Table 13) requires explanation. Either there are parasitic effects that have not been accounted for or else the frozen flow efficiency is not a valid upper limit. Recombination in an expanding part of the flow could increase this theoretical upper limit, but it is generally accepted that recombination does not affect the efficiency in low density arc jet flows and we have not re-examined this question for the special conditions of these measurements.

It is possible to think of an analytical model of an arc jet flow with no recombination that gives a higher upper limit. For example, if the highest static temperature in a flow is less than the stagnation temperature, the equilibrium dissociation and ionization fraction should be calculated using the static temperature rather than the stagnation temperature. To obtain an idea of the change in efficiency caused by a condition of this kind we assume a one-dimensional nozzle flow where all the energy is added in the subsonic part of the flow, that the highest static temperature is reached at the sonic point and the chemical composition of the flow freezes at the sonic point. The "frozen flow efficiency" calculated from this model for the energy addition, though higher, still lies substantially below the measured efficiency at 8000 seconds. Other possible effects that could contribute to the relatively high η^{gk} efficiency are an electrostatic and magnetic interaction between thrustor and tank and interaction of the ambient gas with the jet.

A correction of about 13 grams, or 25 percent of the measured thrust is required to bring the η^{gk} efficiency below the frozen flow efficiency curve shown in Figure 50. If the thrustor and the tank should both acquire charge distributions, an electrostatic force between the tank and thrustor will be produced. This force is of the order $4 \pi \epsilon v^2$ or less, where ϵ is the inductive capacity of the gas and v is the voltage difference between thrustor and tank. For a voltage of 100 volts, the force will be several orders of magnitude too small to be of any consequence.

The possibility of tank currents causing a magnetic interaction between tank and thrustor which could produce torque and thrust or perhaps affect stability or other arc characteristics has not been thoroughly investigated. We have made some very rough calculations that indicate that a magnetic force between tank and thrustor will be negligible for tank currents of 100 amperes or less (no external magnetic field).

Interaction of the jet with the ambient gas is another possible source of discrepancy. If ambient particles are entrained and actually contribute to the force on the thrustor, then this fraction of the mass should be counted when computing the specific impulse and efficiency. A correction of 3.5 m gm/sec would bring the measured efficiency below the frozen flow efficiency in Figure 50. Corrections of 3.5 m gm/sec to the mass flow of 25 m gm/sec would cause changes of about 10 percent in the measured specific impulse shown in Figure 49. A correction of a few m gm/sec to the mass flow of 6.25 m gm/sec (see Figure 48 at 8000 sec), however, produces a large change in specific impulse and efficiency.

We consider here some of the elementary aspects of the interaction of the ambient gas with a high temperature jet. At present we do not know if this interaction has a significant effect on the arc jet performance in these experiments. The possibility of such an interaction being important arises from the current pattern of the arc extending outside the metal surfaces of the thrustor. The tendency for the currents to flow outside the arc is partly due to the self magnetic field being strongest on the concave side of a bend in a current carrying conductor. This effect leads to what is known as the kink instability in the confinement of stationary plasmas. In a coaxial electrode geometry this magnetic force tends to blow the arc downstream. In the arc jet we have the balance of inertial, pressure and magnetic forces on the arc that permits a stable current pattern. The exterior currents and self-field make it possible to create a high pressure region outside the thrustor by ohmic heating and partial confinement by the self-field. This high pressure region outside the thrustor, under some conditions, may be felt as a pressure force at the thrustor surfaces. In such a situation, if ambient particles are heated, contribute to the pressure, and are then ejected, they should be counted as propellant flow. After the jet has expanded to ambient pressure it may still be hot and mixing of the jet with ambient particles may continue but the performance of the thrustor will be indifferent to this interaction once the jet reaches ambient pressure.

5.0 DISCUSSION OF FUTURE STUDIES

5.1 Future Experimental Work

During the past years the study of the various influences affecting the efficiency in plasma propulsion under various environmental conditions resulted in obtaining interesting results not only in the discrimination between the various losses, but also in determining new operating conditions.

The most difficult task in this analysis proved to be the discrimination of the various losses. These have tentatively been grouped in three main categories until future work permits widening the classification. The first category, known as eg (electric to gas), refers to the losses encountered in the transfer of the electrical input energy to the propellant and proved to be the most important and the most likely to permit rapid progress toward higher efficiencies. The second category, known as gk (gas to kinetic), refers to the losses encountered in concentrating the energy transferred to the propellant in a single direction. The third category, known as M (miscellaneous), refers to losses that are not referred to in the two preceding categories or are not yet discriminated. For each category it has been found that various factors influence the total losses. During the past work many factors have been identified. A tentative grouping of the various factors found to date is presented in Table 16. The losses are grouped in four great divisions, i.e.; losses relative to the propellant, electrodes, arc, and jet proper. In each division the factors affecting the losses are numbered progressively. For each one of them a symbol is given indicating

TABLE 16

FACTORS AFFECTING THE EFFICIENCY IN PLASMA ACCELERATION

Propellant	η^{eg}	η^{gk}	η^{M}	Arc	η^{eg}	η^{gk}	η^{M}
1 Composition	+	+	+	16 Geometry	●	●	○
2 Flow	●	○		17 Power Form	○	○	○
3 Pressure	+	+	○	18 Voltage	●	○	●
4 Dissociation		●	○	19 Current	+	+	+
5 Ionization		●	●	20 Self-magnetic Fields	+	+	+
6 Recombination	○	●	●	21 Ext. Magnetic Fields	+	+	+
7 Radiation	●			22 HF Oscillations	○	○	○
Electrodes				Jet			
8 Geometry	●	●	○	23 Radiation	○		
9 Material	●		○	24 Electron Bombardment	+	○	+
10 I^2R Losses	○			25 Self-magnetic Fields		○	●
11 Evaporation	○	+	+	26 Ext. Magnetic Fields		+	+
12 Thermionic Emiss.	○	+	+	27 Ext. Electrostatic Fields		+	○
13 Self-magnetic Fields	●	●	●	28 Discharge to Tank		+	+
14 Ext. Magnetic Fields	●		●	29 Recirculation in Tank		+	+
15 Radiation	●			30 Geometry of Tank		+	+

Estimated research effort required. Intensive + Strong ● Moderate ○

the estimated amount of research effort for each category of losses (eg, gk, M) in relation to the actual state-of-the-art. The future work must be concentrated on the analysis of the factors that require an intensive research effort, as estimated in Table 16, particularly the propellant composition and pressure (1 and 3), the evaporation and thermionic emission of the electrodes (11 and 12), the current and self and external magnetic field in the arc (19, 20, and 21), the electron bombardment returning from the plasma jet (24), the effects of magnetic and electrostatic fields on the plasma jet (26 and 27), the eventual parasitic effects introduced by the proximity of the tank containing the jet and by the imperfect vacuum existing in it (28, 29, and 30).

Most of the work has been conducted to date using hydrogen as a propellant. For specific impulses of the order of 10,000 seconds and higher, hydrogen is one of the best propellants available because as soon as it is fully ionized, and this is obtained at the lowest temperature compared to any other propellant, perfect gas conditions are attained and very high efficiency can be obtained. For lower values of specific impulses hydrogen is not so interesting because the frozen flow losses reach extremely high levels. In this range lithium, sodium, potassium, calcium, titanium, etc., seem promising, especially if the ionization level is kept as low as possible. The recently proved possibility to partly operate the arc with electrode materials suggests the use of compounded electrodes containing mixtures of materials capable of being operated at the necessary temperatures with the minimum frozen flow losses. Porous tungsten electrodes with injections of lithium

or potassium can also be interesting combinations, especially if the ratio of the various components is so chosen as to permit the continuous operation with uniformly consumable electrodes. The use of propellants of this kind in this analysis has another important advantage - to permit their condensation before the pumping stages are reached. This simplifies the problem of very high vacuum operation at relatively high mass flow rates. The future work will analyze the behavior of the most promising propellants of this type and especially the various influences acting on the overall efficiency of each of them. Important problems are to be solved to obtain reproducible results in this field.

It has been proven that the evaporation and thermionic emission of the electrodes might have important influences in the operation of plasma jets, especially when very low mass flows are used. In the operation with mostly electrode material as mention before, these phenomena are becoming very important and basic. For this reason a complete analysis of the relative effects of evaporation and thermionic emission of the electrodes under high and very high vacuum is considered very important.

During the past work it has been found that by increasing the intensity of the externally applied magnetic field and the throat diameter, the arc current was reduced considerably and the arc voltage proportionally increased. This effect limits the magneto-dynamic action in acceleration, and for this reason the benefit of increasing the magnetic field is eliminated. It is our opinion that a complete analysis of the phenomena is necessary to obtain

stable operation at the highest possible arc current and at the highest possible intensity of the magnetic field. To solve the problem it seems necessary to study unconventional geometries for the electrode configuration. This variation in geometry has been, until now, very difficult because of the gaseous nature of the propellants used. The eventual use of solid and evaporating propellants that recent experiments seem to anticipate should permit the use of a relatively simple geometry without the usual feeding difficulties. For this reason, during the future work an analysis of the acceleration obtainable with evaporating electrodes under very strong magnetic fields will be attempted and the relative operating conditions, stabilities, and losses determined experimentally in a wide range of environmental conditions.

It has been proven during the past work that the plasma jet emerging from the anode under a relatively strong axial magnetic field is sometimes very far from complete neutrality (see Figure 44 in Section 3.2). It has also been proven that excess electrons present in the propellant stream return on the anode surface (note the small luminosity around the anode throat (EB) of Figure 44). These returning electrons impacting on the anode produce dangerous effects such as melting and evaporation in a manner very similar to that obtained in electron beam welding and melting processes. This behavior is often a limiting factor in the operation of plasma thrustors and reduces their operating life. A study of this phenomenon is necessary to obtain sufficient information for its elimination. Complete neutralization of the emerging plasma jet or reduction of the velocity of returning electrons

or other solutions are necessary to avoid the important malfunctions originated by electron bombardment, especially in the very high vacuum of space where the returning paths can assume relatively large dimensions.

It is well-known that an axial magnetic field can shape a plasma jet as a substitute for a mechanical nozzle. The effect of this "magnetic" nozzle on the overall efficiency is not yet well known and for this reason an analysis on the subject appears necessary. The incomplete neutrality of the jet suggests that some interaction can be obtained with purely electrostatic means and for this reason a study along this line is also considered useful. Magnetic field intensities to cover 12 kilogauss will be used while the electrostatic field strength will not exceed a few kilovolts. These tests will be conducted mostly with a well-known propellant (like hydrogen, for example) but the effects on other propellants (especially heavier ones) will also be studied. By using electrostatic fields the effects of the electron bombardment mentioned in the preceding paragraph might be modified.

During the last work period it has been proven that when the mass flow rate is extremely low the values of thrust measured are higher than expected and calculated. Various explanations to take care of this error have been suggested, but to date no practical confirmation has been obtained. Because of the imperfect vacuum existing in the test chamber the hypothesis of a residual gas entrainment and relative recirculation has been suggested as an explanation of the excess values of thrust measured. It is felt that the recent state-of-the-art requires new testing facilities capable of handling

the new problems encountered. Figure 51 schematically illustrates a test tank of large dimensions, nonmagnetic, and with insulated walls. As reported before, when great dimensions of the test vacuum chambers are economically impossible, the use of chambers made of insulating materials becomes essential. During future work an economical solution for a completely insulated, very high vacuum tank must be attempted.

It seems necessary to consider seriously what could happen if arc thrustor devices would be used in space. Figure 52 is a hypothetical schematic of an arc discharge as it may occur even in a huge vacuum chamber. It is not unlikely to think that the entire spacecraft could be surrounded by belts of ionized particles extending eventually for miles and causing problems to communications and other equipment. A real simulation of space operation is therefore very important.

Spectroscopic examination of the residual gases present in the testing chamber will be essential in any future work. The immediate objective of the spectroscopic analysis is to determine the plasma composition along different lines of sight (at right angels to the arc axis). As a next step, quantitative evaluation of emission spectra along selected lines of sight will be executed. This will hopefully yield atom densities in selected regions of the arc jet plasma. This analysis will also be useful in the determination of the materials present in the arc jet during its operation without feeding external propellant. During the past operation in these conditions a substantial amount of electrode material has been found in the jet stream but its localization along its various zones has not been completed. For

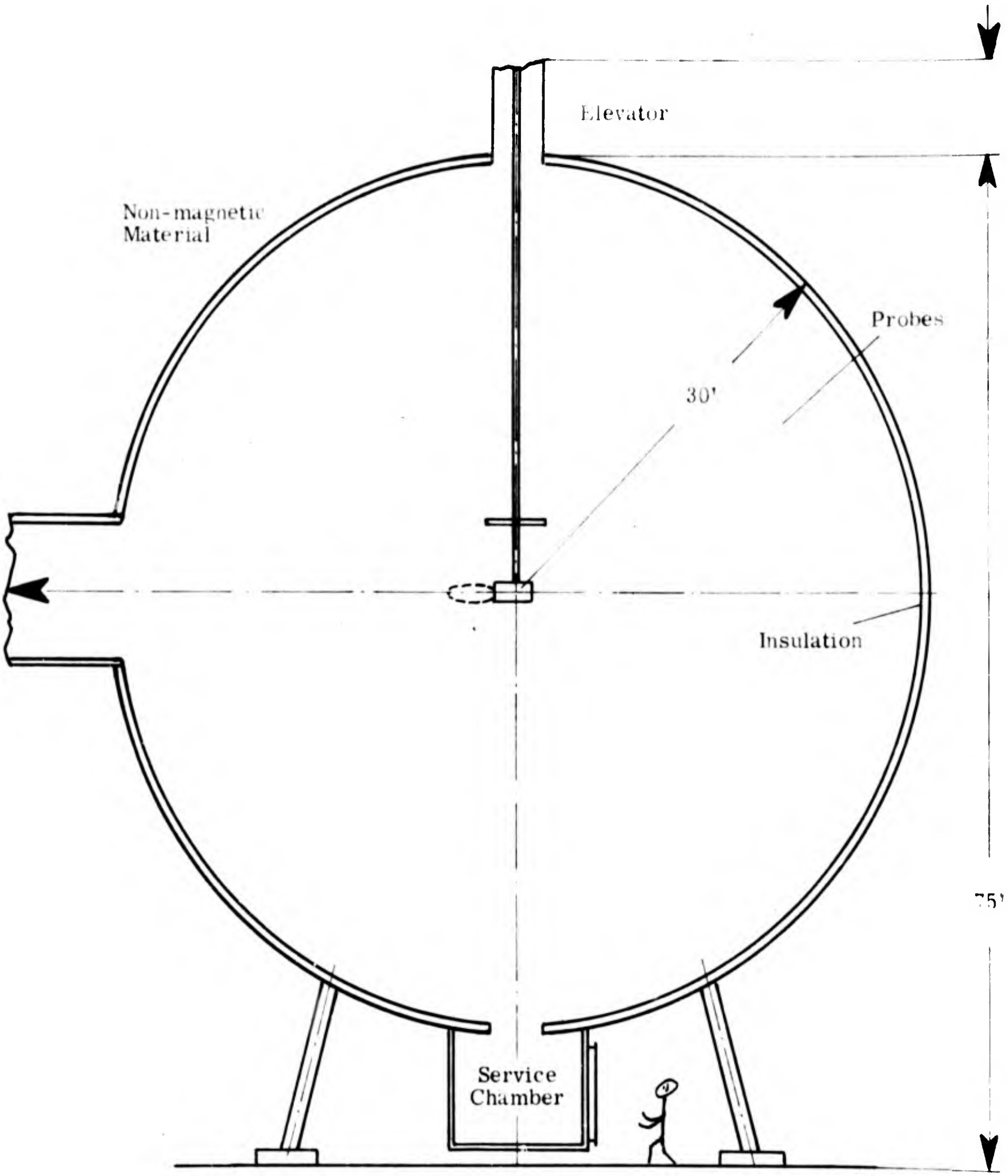

Figure 51. Proposed Vacuum Chamber for Simulation of Space Conditions for Testing With High Specific Impulse Arc Jets

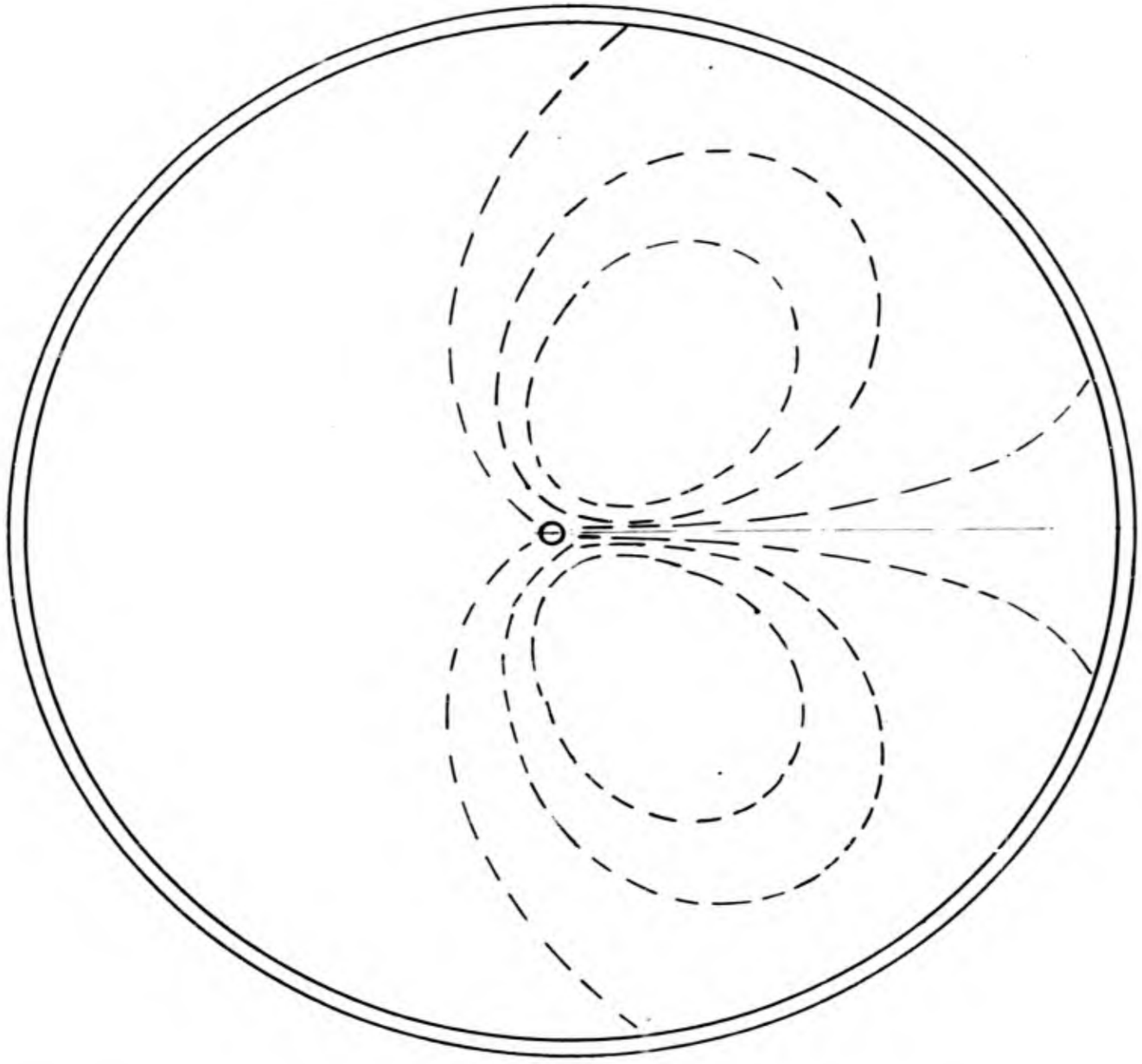

Figure 52. Estimated Patterns of Nonequilibrium Arc Exhaust in Large Space Simulation Chamber

this reason a quantitative spectroscopic analysis seems necessary at various distances from the jet axis and possibly in a relatively large zone around the plasma jet. Precision determination of the various materials constituting the jet will be of great help in determining the cause of parasitic thrust.

5.2 Future Analytical Work

Measured gas to thrust power conversion efficiency has been compared with frozen flow efficiency for complete expansion and no expansion (see Figures 48 and 49). This comparison shows that the theoretical efficiencies do indeed provide upper and lower bounds on the efficiency. If one takes these theoretical limits as a guide, it is clear what gains can in principle be made in gas to thrust power efficiency. It is probable that gains of about 10 to 15 percent can be achieved by employing a magnetic nozzle. Increases significantly greater than this will probably be difficult to obtain. The motivation for employing a magnetic field would then be to achieve a 10 to 15 percent increase in gas to thrust power efficiency and to increase stability and lifetime by the rotational action of the magnetic field on the plasma.

Further increases in overall efficiency must come from improvement of the electrical to gas power efficiency and by a choice of propellant with optimum frozen flow efficiency in the desired range of specific impulse. The energy transfer to the anode is the largest single component of the thermal

losses. It is likely that a thorough understanding of the energy transfer processes in the neighborhood of the anode would greatly facilitate a reduction in thermal losses. A simple analytical model for the energy transfer processes from plasma to anode is needed.

A significant result of the present studies was the experimental indication that under certain conditions large nonuniformities and departures from thermal equilibrium existed in the plasma. That is, when measured gas to thrust power efficiency shows no inclination to follow the frozen flow efficiency we attribute this to ionization in excess of thermal equilibrium (before expansion) and to nonuniformities in the flow. These nonequilibrium effects can be quite large as can be seen in Figures 47 and 50. The conditions required to approximate thermal equilibrium and uniformity need to be studied. The facotrs affecting electrical to gas power conversion and gas to thrust power need not be independent, and an increase of one may take place at the expense of the other (e.g., see Table 9). A theoretical investigation of the simultaneous optimization of the η^{eg} and η^{gk} efficiencies would be helpful.

The anomalies presented by the experiments at very low mass flows warrant further investigation. These anomolous effects are thought to be caused by air entrainment or perhaps magnetic effects. Methods by which the effects of air entrainment can be measured or calculated need to be studied. This study would require an investigation of the region of the arc exterior to the electrodes. Such a study is not only important to the problem of air

entrainment but is also relevant to understanding the factors affecting efficiency. In particular the tendency for electrons to return to the anode along magnetic field lines in the outer periphery of the jet is of interest in view of the possible importance to the energy transfer to the anode.

5.3 PAPERS GIVEN

"Thermally Accelerated Plasma Jets." Paper presented by Adriano C. Ducati at the 5th AFOSR Contractors' Meeting, Hollywood Roosevelt Hotel, Hollywood, California, March 1962.

"Thermal Accelerated Plasma Jets." Paper presented by A. C. Ducati at the 6th AFOSR Contractors' Meeting, Northwestern University; Evanston, Illinois; 15 March 1963.

"Efficiency in Thermal Acceleration." Paper presented by Adriano C. Ducati at the 7th AFOSR Contractors' Meeting, Hotel Sheraton, Philadelphia, Penn., March 1964

"High Specific Impulse Thermo-Ionic Acceleration." AIAA paper No. 64-668 presented by Adriano C. Ducati at the 4th AIAA Electric Propulsion Conference in Philadelphia, Pa. on 31 August 1964.

"Recent Progress in High Specific Impulse Thermo-Ionic Acceleration." AIAA Paper No. 64-96 presented by Adriano C. Ducati at the 2nd Aerospace Sciences Meeting in New York, N. Y. in January 1965.

"Factors Affecting the Efficiency in Thermal Acceleration." Paper presented bv Adriano C. Ducati at the 8th AFOSR Contractors' Meeting, Sportsman's Lodge, Los Angeles, California, April 1965.

Unclassified
Security Classification

DOCUMENT CONTROL DATA - R&D
(Security classification of title, body of abstract and indexing annotation must be entered when the overall report is classified)

1. ORIGINATING ACTIVITY (Corporate author)
Giannini Scientific Corporation
Santa Ana, California

2a. REPORT SECURITY CLASSIFICATION
Unclassified

2b. GROUP

3. REPORT TITLE
STUDY OF THE FACTORS AFFECTING THE EFFICIENCY IN THERMAL ACCELERATION OF PROPELLANTS

4. DESCRIPTIVE NOTES (Type of report and inclusive dates)
Final Technical Report, May 1962 through April 1965

5. AUTHOR(S) (Last name, first name, initial)
Ducati, Adriano C. (PZ)

6. REPORT DATE	7a. TOTAL NO. OF PAGES	7b. NO. OF REFS
August 1965	~~171~~ 199	6

8a. CONTRACT OR GRANT NO.	9a. ORIGINATOR'S REPORT NUMBER(S)
AF 49(638)-1161	FR-085-1161
b. PROJECT NO. 9751-01	
c.	9b. OTHER REPORT NO(S) (Any other numbers that may be assigned this report) AFOSR 66-0495
d.	

10. AVAILABILITY/LIMITATION NOTICES
[illegible] of this document is unlimited

11. SUPPLEMENTARY NOTES	12. SPONSORING MILITARY ACTIVITY
	Air Force Office of Scientific Research Washington DC 20333

13. ABSTRACT This report describes the experimental and analytical work conducted to study the various influences affecting the operating characteristics of electrothermal accelerators. A summary of the initial state-of-the-art is given together with the basic results obtained. A survey of the testing facilities, including vacuum systems, resistance heaters, and liquid metal heaters is given. Arc heaters are discussed with and without the application of external magnetic fields, and with gradually reduced propellant injection. Instruments for the measurement of thrust, mass flow, power, pressure, temperature, magnetic field, etc., are illustrated, together with suggestions for future developments. The experimental work conducted with hydrogen, helium, ammonia, nitrogen, oxygen, and argon at temperatures ranging from 300°K to 3000°K is described. Conical and annular nozzles are compared with simple cylindrical throats, and the experimental and analytical expressions relative to their behavior are included. Outlined are the development of low pressure arc heaters and the experiments which led, for the first time, to the attainment of specific impulse levels of over 10,000 seconds using hydrogen. Performance comparisons between resistance and arc heating and associated anomalies using ammonia are also discussed. The behavior of self-magnetic fields in the arc heater is explained, together with the effects of externally applied magnetic fields ranging from 500 to 12,000 gauss. Included are operation at low mass flow rates and the development of arc heaters working without propellant throughput using electrode vapors or residual ambient gas as the working fluid. Anomalies discovered during experimentation with extremely low mass flow rates are postulated and methods for their identification are suggested.

DD FORM 1 JAN 64 1473

Unclassified
Security Classification

14. KEY WORDS	LINK A		LINK B		LINK C	
	ROLE	WT	ROLE	WT	ROLE	WT
electrothermal accelerators plasma arc jet propulsion resistojet liquid metal heaters high specific impulse metal vapor propellants anomalies						

INSTRUCTIONS

1. ORIGINATING ACTIVITY: Enter the name and address of the contractor, subcontractor, grantee, Department of Defense activity or other organization *(corporate author)* issuing the report.

2*a*. REPORT SECURITY CLASSIFICATION: Enter the overall security classification of the report. Indicate whether "Restricted Data" is included. Marking is to be in accordance with appropriate security regulations.

2*b*. GROUP: Automatic downgrading is specified in DoD Directive 5200.10 and Armed Forces Industrial Manual. Enter the group number. Also, when applicable, show that optional markings have been used for Group 3 and Group 4 as authorized.

3. REPORT TITLE: Enter the complete report title in all capital letters. Titles in all cases should be unclassified. If a meaningful title cannot be selected without classification, show title classification in all capitals in parenthesis immediately following the title.

4. DESCRIPTIVE NOTES: If appropriate, enter the type of report, e.g., interim, progress, summary, annual, or final. Give the inclusive dates when a specific reporting period is covered.

5. AUTHOR(S): Enter the name(s) of author(s) as shown on or in the report. Enter last name, first name, middle initial. If military, show rank and branch of service. The name of the principal author is an absolute minimum requirement.

6. REPORT DATE: Enter the date of the report as day, month, year; or month, year. If more than one date appears on the report, use date of publication.

7*a*. TOTAL NUMBER OF PAGES: The total page count should follow normal pagination procedures, i.e., enter the number of pages containing information.

7*b*. NUMBER OF REFERENCES: Enter the total number of references cited in the report.

8*a*. CONTRACT OR GRANT NUMBER: If appropriate, enter the applicable number of the contract or grant under which the report was written.

8*b*, 8*c*, & 8*d*. PROJECT NUMBER: Enter the appropriate military department identification, such as project number, subproject number, system numbers, task number, etc.

9*a*. ORIGINATOR'S REPORT NUMBER(S): Enter the official report number by which the document will be identified and controlled by the originating activity. This number must be unique to this report.

9*b*. OTHER REPORT NUMBER(S): If the report has been assigned any other report numbers *(either by the originator or by the sponsor)*, also enter this number(s).

10. AVAILABILITY/LIMITATION NOTICES: Enter any limitations on further dissemination of the report, other than those imposed by security classification, using standard statements such as:

(1) "Qualified requesters may obtain copies of this report from DDC."

(2) "Foreign announcement and dissemination of this report by DDC is not authorized."

(3) "U. S. Government agencies may obtain copies of this report directly from DDC. Other qualified DDC users shall request through _____."

(4) "U. S. military agencies may obtain copies of this report directly from DDC. Other qualified users shall request through _____."

(5) "All distribution of this report is controlled. Qualified DDC users shall request through _____."

If the report has been furnished to the Office of Technical Services, Department of Commerce, for sale to the public, indicate this fact and enter the price, if known.

11. SUPPLEMENTARY NOTES: Use for additional explanatory notes.

12. SPONSORING MILITARY ACTIVITY: Enter the name of the departmental project office or laboratory sponsoring *(paying for)* the research and development. Include address.

13. ABSTRACT: Enter an abstract giving a brief and factual summary of the document indicative of the report, even though it may also appear elsewhere in the body of the technical report. If additional space is required, a continuation sheet shall be attached.

It is highly desirable that the abstract of classified reports be unclassified. Each paragraph of the abstract shall end with an indication of the military security classification of the information in the paragraph, represented as *(TS)*, *(S)*, *(C)*, or *(U)*.

There is no limitation on the length of the abstract. However, the suggested length is from 150 to 225 words.

14. KEY WORDS: Key words are technically meaningful terms or short phrases that characterize a report and may be used as index entries for cataloging the report. Key words must be selected so that no security classification is required. Identifiers, such as equipment model designation, trade name, military project code name, geographic location, may be used as key words but will be followed by an indication of technical context. The assignment of links, rules, and weights is optional.

GPO 886-551